PlantMod

exploring the physiology of plant canopies

Ian R Johnson

Published by IMJ Software
PO Box 182
Dorrigo
NSW 2453
Australia
www.imj.com.au

Originally published April 2010

This version published September 2013

Citation:

Johnson IR (2013). PlantMod: exploring the physiology of plant canopies. IMJ Software, Dorrigo, NSW, Australia. www.imj.com.au/software/plantmod.

Preface

PlantMod is an interactive program for exploring photosynthesis and respiration by plants and canopies, canopy transpiration, canopy temperature, and the canopy energy balance in response to environmental conditions. The models are based on published models, with a complete description presented here.

PlantMod was originally published in 1991, with version 2.1 being released in 1994. These early versions were published by Greenhat Software. Since that time there has been a hiatus owing to my involvement in other major projects, particularly the development of pasture simulation models. However, PlantMod 2.1 remains popular with a number of users and it was always my intention to do an update. This new version is a complete reworking of the models and rewrite of the code and documentation, since there have been advances in the general theory of the underlying physiology and obvious advances in computer software technology.

The underlying objective in developing PlantMod has been to make the models readily accessible. Few teachers, students, or researchers have the time or skills to develop computer simulation models, yet they do have the background knowledge of the physiology and how these systems function. Hopefully, PlantMod will give them ready access to the myriad of complex physiological interactions that occur in plant canopies. One consequence of making the models easily accessible is that it becomes quite simple to explore their behaviour for a wide range of physiological parameters and environmental conditions. This can expose limitations and weaknesses in the models and that can only be seen as a good thing as it highlights areas that require refinement. Consequently, while the models in PlantMod do seem robust and versatile, there will always be room for improvement. I welcome feedback and comments about the models.

There are three aspects to the PlantMod package: the computer program, designed to run under Microsoft® Windows™, the interactive Help file which gives a general overview of the program and models, and this document which provides a full mathematical description of the models, including the necessary background mathematics, physics and chemistry.

I would like to acknowledge my friend, colleague and in many ways mentor, John Thornley, with whom I have been collaborating with for 30 years, and who has had a major influence on the way I approach plant, crop and pasture modelling. I am also grateful to Bruce Bugbee and Jonathan Franz for their comments on PlantMod and many interesting discussions relating to plant and crop physiology.

Finally, I welcome any questions or comments about PlantMod, and can be contacted via the 'Help, About' menu item in the program.

Ian Johnson (Melbourne, Vic, August 2011)

Contents

1 Introduction 1

1.1 Overview 1

1.2 Plant and crop modelling 1

1.2.1 Hierarchical systems 1

1.2.2 Types of models 2

1.3 Background mathematical functions 3

1.3.1 Rectangular hyperbola 3

1.3.2 Non-rectangular hyperbola 5

1.3.3 Switch functions 7

1.3.4 CO_2 response function 8

1.3.5 Temperature response functions 9

1.4 Plant composition components 13

1.5 Atmospheric composition 14

1.5.1 CO_2 concentration 16

1.5.2 Water vapour 17

1.6 Stomatal conductance and resistance 18

1.6.1 Flux of CO_2 20

1.6.2 Flux of water vapour 21

1.6.3 Which units to use? 22

1.6.4 Environmental effects on stomatal conductance 23

1.7 Final comments 25

1.8 References 26

2 Radiation 27

2.1 Introduction 27

2.2 Black body radiation 27

2.3 Non-black body and gray body radiation 29

2.4 Radiation energy for photosynthesis: PAR and PPF 29

2.5 Radiation units and terminology 29

2.6 Canopy light interception and attenuation 30

2.6.1 Mean PPF 30

2.6.2 Direct and diffuse PPF 31

2.6.3 Ground cover 33

2.7 Clear-sky solar radiation and daylength 33

2.8 Net radiation 38

2.8.1 Incoming shortwave radiation 39

2.8.2 Outgoing longwave radiation 39

2.8.3 Isothermal net radiation 41

2.8.4 Net radiation balance 43
2.9 Final comments 44
2.10 Variables and parameters 44
2.11 References 47

3 Leaf photosynthesis and respiration 48

3.1 Introduction 48
3.1.1 C_3 and C_4 photosynthesis 49
3.2 Leaf photosynthesis 51
3.2.1 Light response 52
3.2.2 Leaf photosynthetic response to temperature, CO_2 and enzyme concentration 53
3.3 Leaf respiration 60
3.4 Illustrations 61
3.5 Final comments 62
3.6 Variables and parameters 63
3.7 References 64

4 Canopy photosynthesis 66

4.1 Introduction 66
4.2 Photosynthetic enzyme distribution through the canopy 67
4.3 Instantaneous canopy gross photosynthesis 70
4.4 Daily canopy gross photosynthesis 71
4.5 Canopy structure and carbon partitioning 72
4.6 Daily canopy respiration rate 73
4.6.1 Growth respiration 74
4.6.2 Maintenance respiration 75
4.7 Daily growth rate and net canopy photosynthesis 76
4.8 Optimized plant enzyme content 77
4.9 Non-optimum plant enzyme distribution 81
4.10 Further illustrations 82
4.10.1 General model behaviour 82
4.10.2 C_4 canopies 85
4.11 Final comments 86
4.12 Variables and parameters 87
4.13 References 89

5 Canopy transpiration, temperature and energy budget 91

5.1 Introduction 91
5.2 Transpiration 91
5.2.1 Instantaneous transpiration 92
5.2.2 Daily transpiration 95

5.2.3 Summary of climate inputs 95
5.3 Temperature 96
5.4 Energy components 97
5.4.1 Latent heat flux 97
5.4.2 Sensible heat flux 97
5.4.3 Absorbed solar radiation 97
5.4.4 Absorbed longwave radiation 97
5.4.5 Emitted longwave radiation 98
5.4.6 Net outgoing longwave radiation 98
5.4.7 Net radiation balance 98
5.5 Canopy conductances 98
5.5.1 Canopy height 99
5.5.2 Canopy conductance 99
5.5.3 Boundary layer conductance 100
5.6 Illustrations 102
5.7 Final comments 106
5.8 Variables and parameters 106
5.9 References 109

1 Introduction

1.1 Overview

Carbon and water are the basic building blocks of life. The photosynthetic reaction combines atmospheric carbon dioxide with water to produce carbohydrate and emit oxygen and this is the fundamental source of life on the planet. Although water is a key component, virtually all of the water taken up by the plant is lost as transpiration to the atmosphere. Thus, while the study of photosynthesis addresses the assimilation of sugars from atmospheric carbon dioxide and water, the analysis of water use focuses on transpiration. The study of canopy photosynthesis and transpiration therefore lies at the heart of our understanding of the growth of crops and pastures, and their interaction with the environment.

PlantMod is an interactive program for exploring carbon assimilation (photosynthesis and respiration) by plants and canopies, canopy water use (transpiration), canopy temperature, and the canopy energy balance in response to environmental conditions. The program is designed for experienced and inexperienced modellers and requires only basic computer skills. The models are based on published models, but a complete description is presented here. In this Introduction, a general overview of plant and crop modelling is presented and then some background topics are discussed, which are required in the later chapters. Further discussion can be found in Thornley and Johnson (2000) and Thornley and France (2007).

1.2 Plant and crop modelling

In recent years, models have become an integral component of the plant and crop sciences. They have a wide variety of uses in many aspects of agricultural management, such as irrigation scheduling and pasture management. Equally so, they also play an important role in plant and crop research: for example, models have helped identify the growth and maintenance components of plant respiration. This interest in modelling has had many benefits and has provided a means of integrating concepts from many different branches of science.

When constructing models it is important that model design meets the objectives of the project. It is therefore important to consider the different types of model and how these relate to each other. The main model types used in PlantMod are *mechanistic* and *empirical*, as discussed in Section 1.2.2 below. Before proceeding, it is worth noting that it is unlikely that one model of a particular process will suit all likely modelling objectives.

1.2.1 Hierarchical systems

Plant biology, and biology in general, has many organizational levels. In physics and chemistry there is a clear distinction between moving from atomic and molecular behaviour to that of liquids and solids, in biology there are several levels that can be considered. This range of different levels gives rise to the great diversity of the biological world. A typical hierarchical scheme for the plant sciences is:

…	…
…	landscape
$i+1$	crop or pasture
i	plant
$i-1$	organs
…	tissues
…	cells
…	organelles
…	macromolecules
…	molecules and atoms

PlantMod focuses on processes primarily at levels $i+1$, i, $i-1$.

The principal features of this hierarchical system are:

1. Each level has its own language. For example, crop yield has little meaning at the cell level.
2. Each level is an integration of items at lower levels, so that the response of the system at one level can be related to responses at lower levels. For example, canopy photosynthesis is calculated in terms of the sum of the photosynthesis of the leaves in the plants that make up the canopy.

Other features of this system are discussed in Thornley and Johnson (2000) and Thornley and France (2007).

1.2.2 Types of models

Models can be divided into several categories, with perhaps the most widely used being mechanistic and empirical, deterministic and stochastic. The difference between deterministic and stochastic models is that deterministic models predict a precise value for a variable of the system, whereas stochastic models also involve statistical variation. Both have their value, but in PlantMod the statistical features of the behaviour of the system are not considered.

Empirical models

Empirical models do not involve details of the underlying scientific basis of the system, but are curves that are used to describe patterns of behaviour or to summarize sets of data. An example of empirical modelling is the use of growth functions to describe crop dry weight during the growth period. Generally, an empirical model describes the response of the system at a single level in the hierarchical structure mentioned in the previous section.

Although empirical models are usually curves that can be fitted to experimental data, and that display the general expected characteristics of the response, they are much more useful if the curves have readily interpreted parameters. For example, the temperature response functions discussed in Section 1.3.5 below are used to describe the influence of temperature on various processes in PlantMod. These response functions are empirical but are formulated with minimum, optimum and maximum temperature parameters for the processes, which makes them simple to apply. Another example of an empirical model is the description of the influence of environmental conditions on stomatal conductance. The method discussed in Section 1.6.4 below is based on the widely used approach of Ball *et al.* (1987) which defines the influence of light, relative humidity and CO_2 concentration on stomatal conductance. There is no underlying physiological basis for these equations, but they display the observed characteristics of the responses, have readily interpreted

parameters, and provide a robust way of incorporating these effects in the model of canopy transpiration.

Mechanistic models

Mechanistic models are constructed from descriptions of the underlying processes involved in the system being studied, and these descriptions are quite often empirical (or semi-empirical). They generally operate between two or three levels in the hierarchical structure discussed in the previous Section. For example, canopy gross photosynthesis can be defined in terms of an equation describing single leaf photosynthesis in response to light and another describing light attenuation through the canopy. Ideally, each of these sub-models will have parameters that have some biophysical interpretation, but they may not be founded on detailed mechanisms.

The complexity of mechanistic models will increase as the range of processes used to build that model increases, or if greater detail is used to describe these processes. Again, using canopy photosynthesis as an example, the light within the canopy can be treated as homogeneous or allowance can be made for direct sunlight and diffuse radiation (both these scenarios are explored in PlantMod). The complexity at which a model is developed is therefore subject to some degree of choice. The greater the detail, the more complex the model. It is important that the complexity of the model suits the objectives of the system being investigated and this means that there is generally no single model of a biological process that suits all purposes.

The distinction between mechanistic and empirical models is not always clear. For example, the equation used to describe single leaf gross photosynthesis in PlantMod, the *non-rectangular hyperbola* which is discussed in detail later, can be derived from a very simple model of leaf photosynthesis. However, the underlying model contains such broad assumptions that it does not really encapsulate the biochemical details of leaf photosynthesis. In this case, we can regard the equation as semi-empirical, recognising that it has the desired behaviour but with a limited biophysical basis.

1.3 Background mathematical functions

Some background calculations are now presented. These are used in the later model descriptions.

1.3.1 Rectangular hyperbola

The simple rectangular hyperbola (RH) can be derived from basic concepts of enzyme kinetics. It is generally presented in one of two forms:

$$y = \frac{\alpha x y_m}{\alpha x + y_m} \tag{1.1}$$

or

$$y = y_m \frac{x}{x + K} \tag{1.2}$$

although the symbol v for the speed of the reaction, and S for substrate concentration are often used instead of x and y. In both equations, y_m is the asymptotic value of y as $x \to \infty$; with eqn (1.1), α is the initial slope of the curve, while for eqn (1.2) y takes half its maximum value when $x = K$, that is $y(x = K) = y_m/2$. These two forms of the RH are mathematically equivalent and it is readily shown that

$$K = \frac{y_m}{\alpha} \tag{1.3}$$

The rectangular hyperbola of the form (1.2) is often referred to as the Michaelis-Menten equation due to their early application of this equation to enzyme kinetics in 1913.

The form of the equation that is used depends on the particular application – sometimes it is convenient to prescribe the initial slope of the response, α, while in other cases the value of x for half-maximal response, K, is more convenient.

The equation is referred to as a *rectangular hyperbola* since it has two asymptotes that are at right angles to each other. These are:

$$y = y_m \tag{1.4}$$

and

$$x = \frac{-y_m}{\alpha} \quad \text{or} \quad x = -K \tag{1.5}$$

In practice, only positive values of x are used. The RH is illustrated in Fig. 1.1.

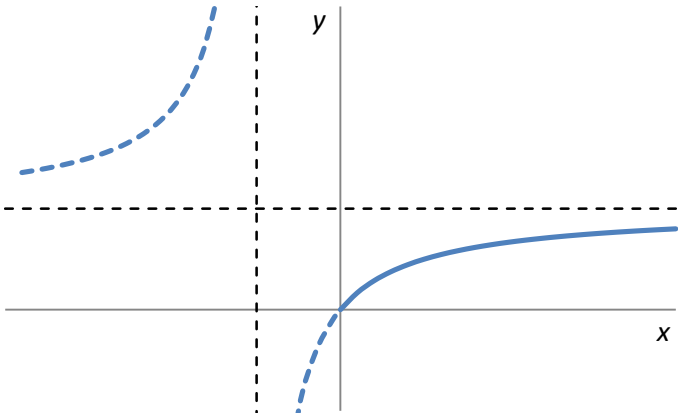

Figure 1.1: Rectangular hyperbola (blue lines), eqn (1.1) or (1.2), and the asymptotes given by eqns (1.4) and (1.5) (black dashed lines). The solid blue line is the part of the equation that is generally used in biological models.

The RH is also shown in Fig. 1.2 where now only the part of the curve that is biologically meaningful is shown, along with the key equation parameters. While the RH is a simple curve to work with, and the parameters have biological meaning, it is limited in that it generally approaches the asymptote quite slowly. The more general non-rectangular hyperbola that is discussed in the next section overcomes this limitation.

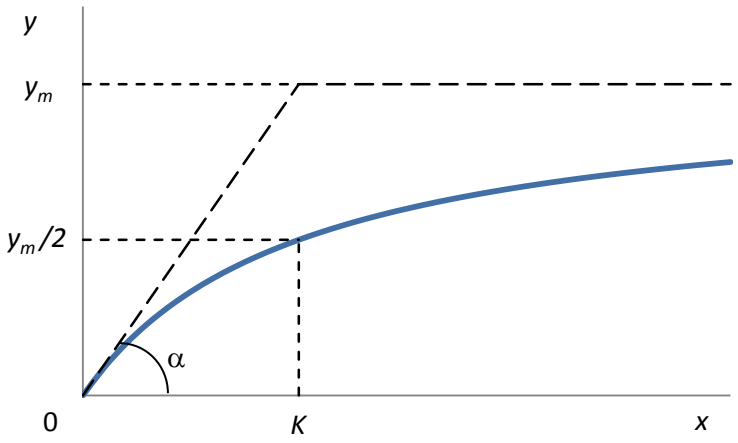

Figure 1.2: Rectangular hyperbola (blue line) with the key parameters as indicated. See text for details.

1.3.2 Non-rectangular hyperbola

The non-rectangular hyperbola (NRH) is a useful generic equation that is widely used to describe the leaf photosynthetic response to irradiance (see Chapter 3). It will also be used here for the CO_2 response. Mathematically, it is a modification of the rectangular hyperbola (RH) discussed in the previous section that has an extra parameter and where the asymptotes are now not perpendicular to each other. An overview of the equation is given here and for more detail, see Thornley and Johnson (2000) or Thornley and France (2007). Adding a quadratic equation to the RH, the NRH equation can be written

$$\theta y^2 - (\alpha x + y_m) y + \alpha x y_m = 0 \tag{1.6}$$

For $\theta = 0$ it reduces to the RH, eqn (1.1).

The solutions to eqn (1.6) are

$$y = \frac{1}{2\theta}\left[\alpha x + y_m \pm \left\{(\alpha x + y_m)^2 - 4\alpha\theta y_m x\right\}^{1/2}\right] \tag{1.7}$$

Note that for this equation to have two real solutions, it is necessary that

$$4\alpha\theta y_m x \le (\alpha x + y_m)^2 \tag{1.8}$$

for all values of x. For $x \ge 0$ this requires

$$\theta \le \frac{(\alpha x + y_m)^2}{4\alpha y_m x} \tag{1.9}$$

It is easy to show that the right-hand side of this equation takes its minimum value of 1 when $\alpha x = y_m$, so that the required constraint is

$$\theta \le 1 \tag{1.10}$$

Before looking at these solutions given by (1.7), note that eqn (1.6) can be factorized to give

$$(y - y_m)\left[\theta y - \left\{\alpha x + y_m(1-\theta)\right\}\right] = y_m^2(1-\theta) \tag{1.11}$$

from which it can be seen that there are two asymptotes at

$$y = y_m \quad \text{and} \quad y = \frac{\alpha x + y_m(1-\theta)}{\theta} \tag{1.12}$$

The solutions to eqn (1.6) as given by (1.7), along with the asymptotes (1.11) are illustrated in Fig. 1.3. Note that in biological models, and all the present applications, the lower solution in (1.7) is used, with $x \geq 0$: this is illustrated with the solid line in Fig. 1.3

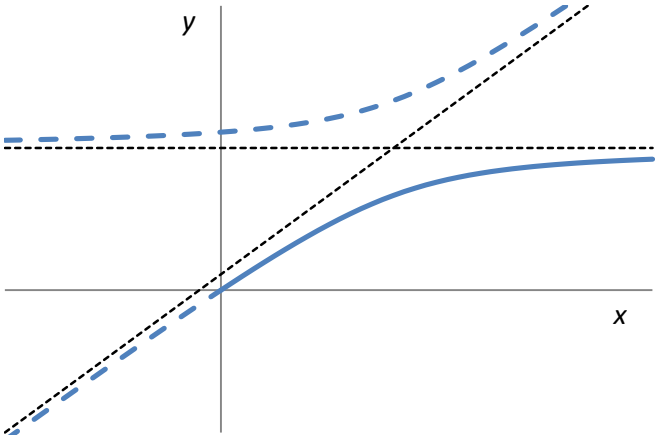

Figure 1.3: Non-rectangular hyperbola (blue lines), eqns (1.6) and (1.7), and the asymptotes given by eqns (1.12) (black dashed lines). The solid blue line is the part of the equation that is generally used in biological models.

Now consider the behaviour of this equation for the biologically appropriate situation for $x \geq 0$. The three parameters are α, θ, y_m. As mentioned above, y_m is the asymptote, so that

$$y(x \to \infty) \to y_m \tag{1.13}$$

It can be shown that α is the initial slope of the curve, which means that

$$y(x \to 0) \to \alpha x \tag{1.14}$$

The third parameter, θ, controls the curvature of the response function. As seen above, for $\theta = 0$, the equation reduces to the simpler rectangular hyperbola. For $\theta = 1$ it becomes two straight lines:

$$y = \begin{cases} \alpha x, & x \leq y_m/\alpha \\ y_{m,} & x > y_m/\alpha \end{cases} \tag{1.15}$$

The general solution is

$$y = \frac{1}{2\theta}\left[\alpha x + y_m - \left\{(\alpha x + y_m)^2 - 4\alpha\theta y_m x\right\}^{1/2}\right] \tag{1.16}$$

As mentioned earlier, the constraint $\theta \leq 1$ must apply (eqn (1.10)) and, while solutions do exist for negative values of θ, it is convenient to define a family of curves between the rectangular hyperbola and the two straight lines given by eqn (1.15) and so the constraint (1.10) is extended to

$$0 \leq \theta \leq 1 \tag{1.17}$$

and this is applied through the analysis.

The non-rectangular hyperbola is illustrated in Fig. 1.4 for a range of θ values. This is a powerful, versatile equation that is easy to work with. The three parameters each control the key aspects of the response: the initial slope, curvature and asymptote. This is the form of the equation that is used to describe the light response for leaf gross photosynthesis. It is also used in the CO_2 response function.

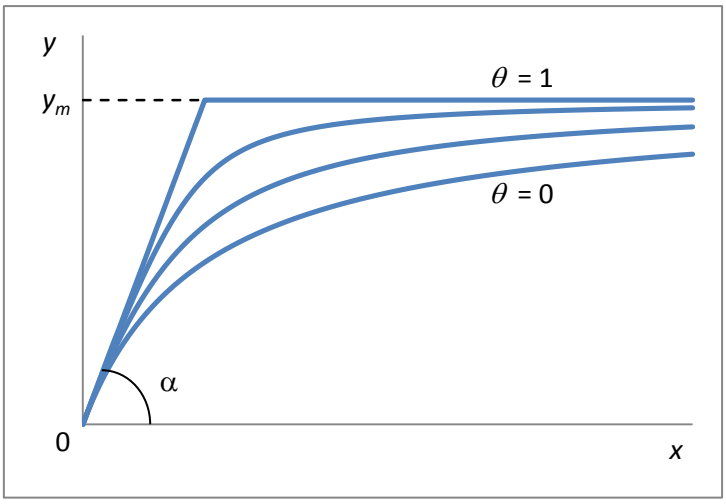

Figure 1.4: Non-rectangular hyperbola, eqn (1.16) for θ increasing from 0 (lower line,) to 1 (upper line). The initial slope is α and the asymptote is y_m.

1.3.3 Switch functions

It is sometimes useful to have expressions to define 'switch-on' or 'switch-off' behaviour. Simple equations for this are

$$y_{on} = y_m \frac{x^n}{x^n + K^n} \tag{1.18}$$

which is quite similar to the rectangular hyperbola, and

$$y_{off} = y_m \frac{K^n}{x^n + K^n} \tag{1.19}$$

Both of these equations, which are illustrated in Fig. 1.5, take the value $y_m/2$ when $x = K$.

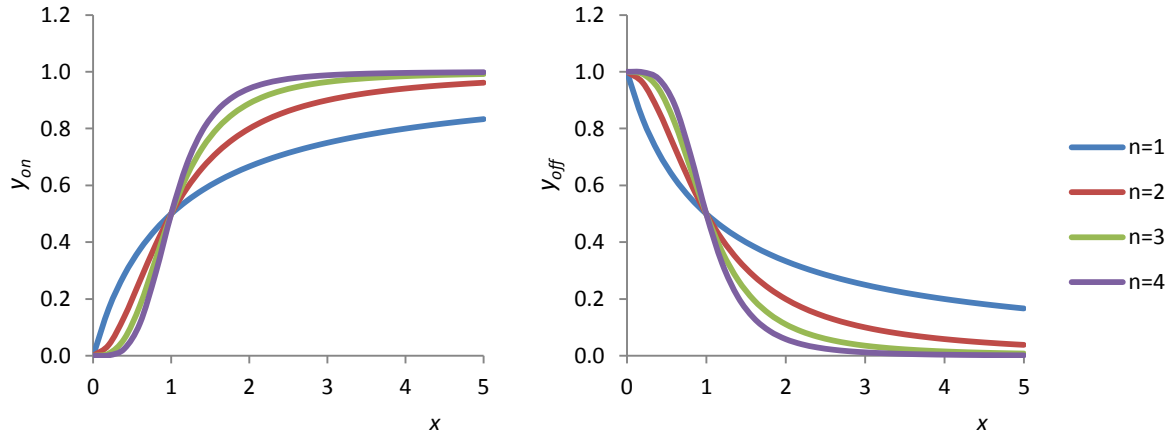

Figure 1.5: 'Switch-on' (left) and 'switch-off' (right) functions given by eqns (1.18) and (1.19), with $y_m = 1$, $K = 1$ and n as indicated

These functions are not actually used in PlantMod, but are presented here as simple extensions of the rectangular hyperbola that may be of use in other modelling exercises.

1.3.4 CO_2 response function

The NRH will be used in the treatment of the photosynthetic response to CO_2. However, it is convenient to re-cast the equation. First consider the general equation given by

$$f_C(C)=\frac{1}{2\phi}\left[\beta C+f_{C,m}-\left\{\left(\beta C+f_{C,m}\right)^2-4\phi\beta f_{C,m}C\right\}^{1/2}\right] \tag{1.20}$$

which is of the form eqn (1.16), where C is atmospheric CO_2 concentration, β is the initial slope, ϕ $(0\le\phi\le 1)$ the curvature and $f_{C,m}$ the asymptote.

In order to assist with parameterisation, the function is constrained to take the value unity at ambient CO_2 and λ at double ambient, so that

$$\left.\begin{aligned} f_C(C=C_{amb})&=1\\ f_C(C=2C_{amb})&=\lambda\end{aligned}\right\} \tag{1.21}$$

which are the values at ambient and double ambient CO_2 concentration, where C_{amb} is the ambient atmospheric CO_2 concentration, taken to be $C_{amb}=380\ \mu\text{mol mol}^{-1}$, eqn (1.70) below.

For example, consider this equation as used for leaf gross photosynthesis at saturating irradiance. If $\lambda=1.5$ and $f_{C,m}=2$ then the photosynthetic rate increases by 50% when CO_2 is double ambient, and is increased by 100% at saturating CO_2. It is now necessary to calculate the appropriate values of β and ϕ in eqn (1.20) in order to satisfy (1.21). After some algebra, it can be shown that

$$\phi=\frac{f_{C,m}\left[\lambda\left(f_{C,m}-1\right)-2\left(f_{C,m}-\lambda\right)\right]}{\lambda^2\left(f_{C,m}-1\right)-2\left(f_{C,m}-\lambda\right)} \tag{1.22}$$

and

$$\beta=\frac{\lambda\left(f_{C,m}-\phi\lambda\right)}{2C_{amb}\left(f_{C,m}-\lambda\right)} \tag{1.23}$$

so that β and ϕ are evaluated in terms of λ and $f_{C,m}$. Care must be taken to ensure that values for λ and $f_{C,m}$ are selected such that $0\le\phi\le 1$ and $\beta>0$. To do so, note that

$$\phi=1 \text{ when } f_{C,m}=\lambda;\ \text{and } \phi=0 \text{ when } f_{C,m}=\lambda/(2-\lambda) \tag{1.24}$$

Since $\lambda>1$, it then follows that the required constraint is

$$f_{C,m}\le\frac{\lambda}{2-\lambda} \tag{1.25}$$

This is checked in the program. Note that with the default values

$$\lambda=1.5,\quad f_{C,m}=2 \tag{1.26}$$

it follows that

$$\beta=0.0032,\quad \phi=0.8 \tag{1.27}$$

The function is illustrated in Fig. 1.6 where ambient, double ambient, and the asymptote are also shown.

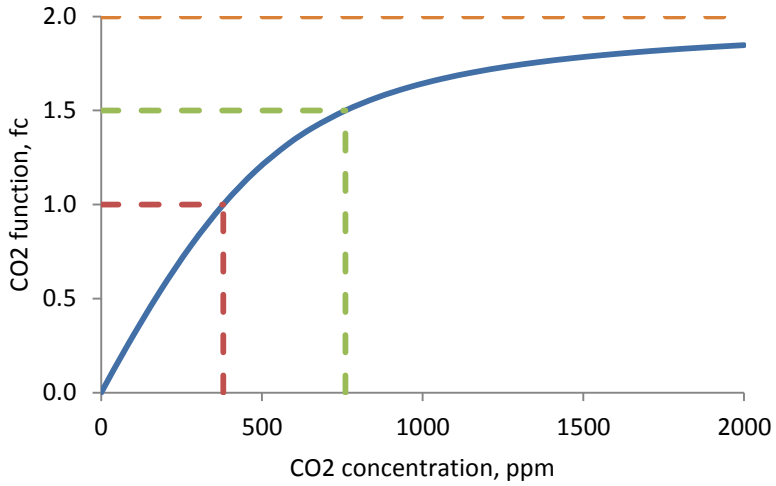

Figure 1.6: Generic CO_2 response function f_C, eqn (1.20), subject to (1.21), (1.22), (1.23) with C_{amb} = 380ppm, $f_C(C = C_{amb})$ = 1, $f_C(C = 2C_{amb})$ = 1.5, $f_C(C \to \infty)$ = 2.

1.3.5 Temperature response functions

Two forms of temperature response are used in the model – either with or without a temperature optimum. For more details see Johnson and Thornley (1985), Thornley and Johnson (2000), Thornley and France (2007).

Temperature response without an optimum

The simplest equation to use is the so-called Q_{10}, which is given by

$$k = k_r Q_{10}^{(T-T_r)/10} \tag{1.28}$$

where k is the reaction rate, T is temperature, T_r is a reference temperature, taken to be

$$T_r = 20°\text{C} \tag{1.29}$$

k_r is the value of k at the reference temperature T_r, and Q_{10} is the temperature coefficient. According to this equation,

$$\frac{k(T+10)}{k(T)} = Q_{10} \tag{1.30}$$

for all values of T, so that the reaction rate increases by a factor Q_{10} for every 10°C increase in temperature. Q_{10} is typically of order 1.5 to 2 for most practical applications.

An alternative equation that is sometimes used is the Arrhenius equation, which is defined by

$$k = Ae^{-E_a/RT} \tag{1.31}$$

where A is a rate parameter with the same dimensions as k, E_a (J mol^{-1}) is the *activation energy*, T (K) is the absolute temperature, and $R = 8.3145$ J K^{-1} mol^{-1} is the gas constant. A derivation of eqn (1.31) can be found in Johnson and Thornley (1985) or Thornley and Johnson (2000).

It is convenient to normalize (1.31) so that it takes a reference value at the reference temperature T_r, which requires

$$A = k_r e^{E_a/293.15R} \tag{1.32}$$

where the factor 293.15 is 20°C converted to absolute degrees (K). Equation (1.31) is now written

$$k = k_r \exp\left[\frac{E_a}{R}\left(\frac{1}{T_r} - \frac{1}{T}\right)\right] \tag{1.33}$$

so that

$$k = k_r \left(T = T_r\right) \tag{1.34}$$

In practice, the activation energy, E_a is treated as an empirical parameter to fit to data. This can be compared to the Q_{10} equation, eqn (1.28), by using the fact that they both take the value k_r at the reference temperature, T_r, and then equating them at 30°C to give

$$E_a = 8.3145 \times \frac{293.15 \times 303.15}{10} \ln\left(Q_{10}\right) = 74{,}130 \ln\left(Q_{10}\right) \tag{1.35}$$

With typical values of 1.5 and 2 for Q_{10}, the corresponding E_a values are

$$\begin{aligned} Q_{10} &= 1.5; \quad E_a = 29{,}960 \text{ J mol}^{-1} \\ Q_{10} &= 2; \quad E_a = 51{,}216 \text{ J mol}^{-1} \end{aligned} \tag{1.36}$$

The Q_{10} and Arrhenius equations are illustrated in Fig. 1.7 for these parameter values. It can be seen that the responses are virtually identical over a practical temperature range.

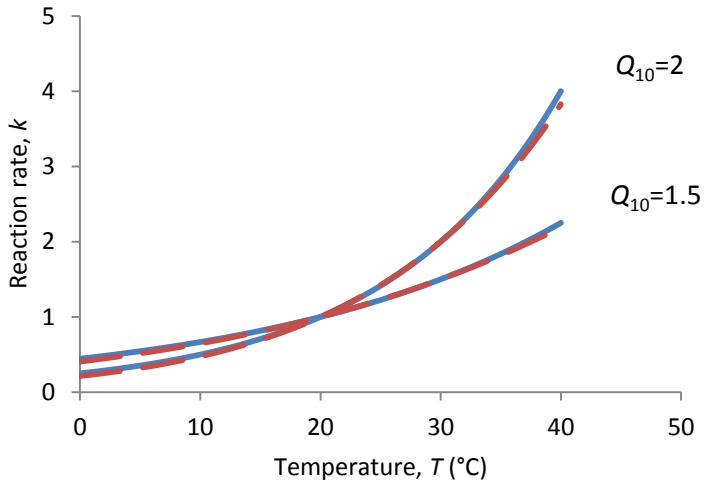

Figure 1.7. Q_{10} equation, blue lines, and Arrhenius equation, dashed red lines, for the Q_{10} values as indicated and activation energies given by eqn (1.36). The two equations give virtually identical responses.

Given the close similarity between the two equations, the choice here is to use the Q_{10} approach since the Q_{10} parameter is intuitive to work with and is simple to relate to data. Furthermore, the Arrhenius equation is based on a single chemical reaction, whereas processes such as plant respiration involve sequences of many reactions which may have different individual energy characteristics.

Temperature response with an optimum

Temperature responses with a temperature optimum are more complex to deal with than those without that were considered above. The scheme for the Arrhenius equation can be generalized to generate a response function that has a maximum, and the resulting equation is

$$k = \frac{A\exp\left(-E_a/RT\right)}{1+\exp\left(\Delta S/R - \Delta H/RT\right)} \tag{1.37}$$

where, again, A is a rate constant, E_a (J mol^{-1}) is the activation energy, T (K) is the absolute temperature, and R is the gas constant. The additional parameters are ΔS (J K^{-1} mol^{-1}) which is an entropy term, and ΔH (J mol^{-1}) which is an enthalpy term. A derivation of eqn (1.37) is given in Johnson and Thornley (1985) or Thornley and Johnson (2000). Equation (1.37) is illustrated in Fig. 1.8.

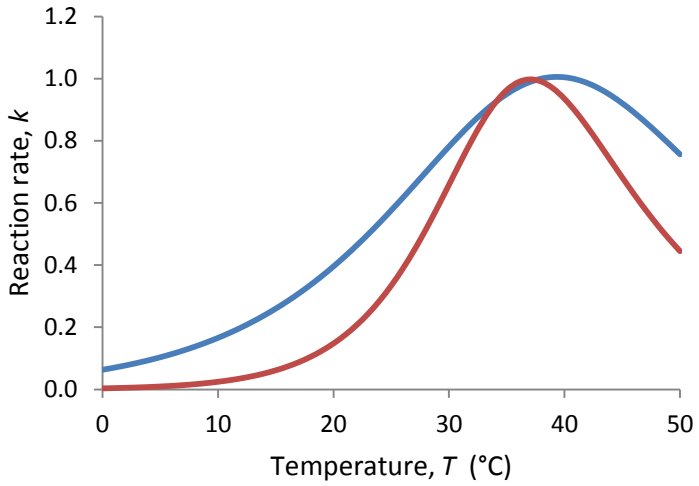

Figure 1.8: Temperature response function, eqn (1.37).
Blue line: $A = 5.33 \times 10^{10}$, $E_a/R = 7.5 \times 10^3$ K, $\Delta S/R = 48$, $\Delta H/R = 1.5 \times 10^4$ K.
Red line: $A = 2.5 \times 10^{10}$, $E_a/R = 1.5 \times 10^3$ K, $\Delta S/R = 81$, $\Delta H/R = 2.5 \times 10^4$ K

While parameter values can be selected in eqn (1.37) to describe temperature responses, it is quite complex to vary the parameters routinely to adjust the details of the curve. As for the Arrhenius equation discussed above, eqn (1.31), the underlying scheme that leads to eqn (1.37) involves an idealized single enzyme-substrate reaction where the enzyme can exist in either an active or inactive state. There is little theoretical justification in using this scheme for the sequence of reactions that occur in photosynthesis. It should be noted that variations to eqn (1.37) can be derived.

For the present purposes, a simpler empirical temperature response function is used. Following Thornley (1998), Thornley and France (2007), consider the temperature response function given by

$$f_T(T) = \left(\frac{T - T_{mn}}{T_r - T_{mn}}\right)^q \left(\frac{T_{mx} - T}{T_{mx} - T_r}\right) \tag{1.38}$$

where T_{mn} and T_{mx} are the minimum and maximum temperatures such that

$$f_T(T_{mn}) = f_T(T_{mx}) = 0 \tag{1.39}$$

$q \geq 1$ is a curvature parameter, and T_r is a reference temperature with

$$f_T\left(T_r\right)=1 \tag{1.40}$$

This equation has a maximum value at

$$T_{opt}=\frac{T_{mn}+qT_{mx}}{1+q} \tag{1.41}$$

from which

$$T_{mx}=\frac{\left(1+q\right)T_{opt}-T_{mn}}{q} \tag{1.42}$$

Equation (1.42) can be used in (1.38) to eliminate T_{mx}, giving

$$f_T\left(T\right)=\left(\frac{T-T_{mn}}{T_r-T_{mn}}\right)^q\left(\frac{\left(1+q\right)T_{opt}-T_{mn}-qT}{\left(1+q\right)T_{opt}-T_{mn}-qT_r}\right) \tag{1.43}$$

This equation describes the temperature response in terms of the minimum and optimum temperatures, as well as the curvature coefficient q. Alternatively, if it was more convenient, q could be derived from eqn (1.41) to give an equation in terms of the minimum, optimum and maximum temperatures. This is not presented here, and eqn (1.43) will be used.

In applying this function, the constraint

$$T_r \le T_{opt} \tag{1.44}$$

should be applied. While this is not absolutely necessary, it does ensure sensible behaviour of eqn (1.43).

The function is illustrated in Fig. 1.9.

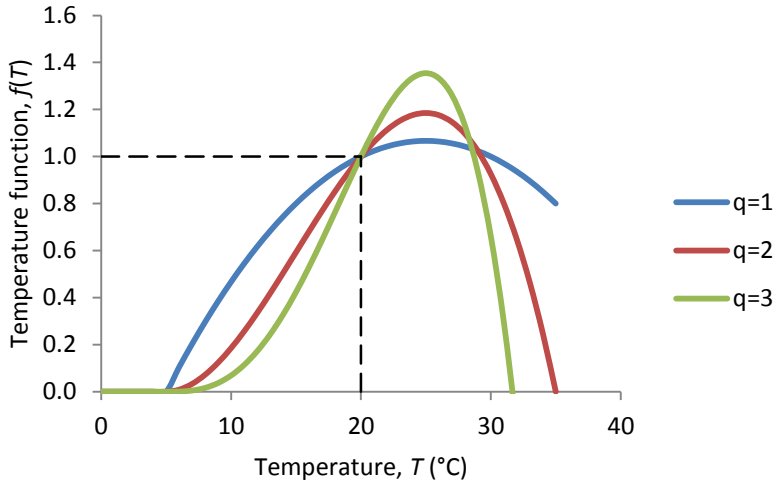

Figure 1.9. Generic temperature function, eqn (1.43). Parameters are: $T_r = 20$°C, $T_{mn} = 5$°C, $T_{opt} = 25$°C, q as indicated. Note that $f(T = T_r) = 1$.

This equation is versatile and simple to use, having easily interpreted parameter values, and will be used for temperature responses that have an optimum. It should be noted that when $q = 1$ the temperature response is symmetric around the optimum temperature. This rarely happens in biological processes and values of q in the range 2 to 3 are generally more appropriate.

1.4 Plant composition components

The theory presented here involves plant dry weight (d.wt) as well as photosynthetic rates. While the mole is the preferred unit for photosynthesis, in most plant growth experiments the units of plant dry weight are usually kg d.wt. To reconcile these units, it is assumed that the plant comprises sugars, which are mono and disaccharides, protein, and cell wall material which is primarily cellulose and hemicelluloses. Other components such as lipids are not considered here, although the analysis could be extended to include them in a straightforward way. Taking the sugars to be primarily disaccharides (sucrose, fructose), the following carbon compositions by mass are used:

$$\left.\begin{array}{ll} \text{Cell wall:} & 0.44 \text{ kg carbon } (\text{kg cell wall})^{-1} \\ \text{Protein:} & 0.48 \text{ kg carbon } (\text{kg protein})^{-1} \\ \text{Sugars:} & 0.42 \text{ kg carbon } (\text{kg sugar})^{-1} \end{array}\right\} \tag{1.45}$$

Denote the molar and dry weight fractions of plant material by

	mole	dry weight
Cell wall fraction:	f_w	F_w
Protein fraction:	f_p	F_p
Sugar fraction:	f_s	F_s

It follows that the fraction of carbon in total plant dry weight is

$$F_C = 0.44F_w + 0.48F_p + 0.42F_s \tag{1.46}$$

The conversions between mole and dry weight fractions of the individual components are:

$$\left.\begin{array}{l} f_w = F_w \times 0.44/F_C \\ f_p = F_p \times 0.48/F_C \\ f_s = F_s \times 0.42/F_C \end{array}\right\} \tag{1.47}$$

As an example, consider the plant dry weight composition to be 65% cell wall, 25% protein and 10% sugars by weight, so that

$$F_w = 0.65, \quad F_p = 0.25, \quad F_s = 0.1, \tag{1.48}$$

which gives (working to 2 significant figures)

$$F_C = 0.45, \tag{1.49}$$

and

$$f_w = 0.64, f_p = 0.27, f_s = 0.09 \tag{1.50}$$

Thus, while the mole and dry weight fractions of plant material do not vary greatly, they are, nevertheless, not identical and appropriate care should be taken.

F_C can be seen to be relatively insensitive to moderate changes in plant composition, although the carbon content of the plant components will affect the calculation of F_C.

For whole plant material,

$$1 \text{ mol C} = \frac{0.012}{F_C} \text{ kg d.wt} \tag{1.51}$$

and, using eqn (1.49), this gives

$$1 \text{ mol C} = 0.027 \text{ kg d.wt} \tag{1.52}$$

or

$$1 \text{ kg d.wt} = 37 \text{ mol C} \tag{1.53}$$

This is the conversion used here, although alternative values for F_C could readily be used. The parameter

$$\gamma = 37 \text{ mol C (kg d.wt)}^{-1} \tag{1.54}$$

will be used to convert from dry weight to mole units.

1.5 Atmospheric composition

Photosynthesis is influenced by atmospheric CO_2 concentration, while transpiration and evaporation depend on the water vapour concentration in the atmosphere. Methods for defining atmospheric gas components are now considered.

Density is defined as kg m^{-3} and concentration as mol m^{-3}. From the gas laws, the mole concentration of any gas, φ (mol m^{-3}), is given by

$$\varphi = \frac{P}{RT_K} \tag{1.55}$$

where P (Pa) is the atmospheric pressure, T_K (K) is temperature and $R = 8.314$ J K^{-1} mol^{-1} is the gas constant. Note that, while C is often used to define concentration in analysis of this type, φ is used here to allow C to be used in the treatment for CO_2. Also, the notation T_K is used to avoid confusion with T °C. The atmosphere is taken to comprise the dry air components plus water vapour, with the principal constituents of dry air (working to 2 percentage decimal places) being nitrogen (78.08%), oxygen (20.95%), argon (0.93%), and carbon dioxide (0.04%). When water vapour is included, it can account for up to around 4% of the atmosphere (although this is subject to considerable variation) and in this case the proportions of the main atmospheric constituents will decline slightly.

It is convenient to use either normal temperature and pressure (NTP) or standard temperature and pressure (STP). NTP is usually taken to be 20°C and 101.325 kPa. STP is 0°C and 101.325 kPa. Note that 101.325 kPa is the SI definition of pressure and is equivalent to 1 atmosphere (atm) which, in turn, is equivalent to 760 mm Hg and is a traditional value for atmospheric pressure at sea level. In all of the analysis here, NTP will be used, since 20°C is generally a more appropriate temperature for biological processes than 0°C, and is defined as:

$$\text{NTP: } 20°\text{C, } 101.325 \text{ kPa.} \tag{1.56}$$

Thus, at NTP

$$\varphi_{NTP} = 41.574 \text{ mol m}^{-3} \tag{1.57}$$

which is the molar concentration of any gas.

The density ρ, kg m^{-3}, is given by

$$\rho = M\varphi \tag{1.58}$$

where M (kg mol^{-1}) is the molar mass, for example 44.01×10^{-3} kg mol^{-1} for CO_2.

In practice, the components of the atmosphere, such as CO_2, O_2, or water vapour are required. Denoting the concentration of the atmosphere as φ_{atm}, eqn (1.55) can be rewritten as

$$\varphi_{atm} = \frac{P}{RT_K} \tag{1.59}$$

The partial concentration of any component of the atmosphere, φ_i (mol m^{-3}), such as CO_2 or water vapour, has concentration

$$\varphi_i = \frac{e_i}{RT_K} \tag{1.60}$$

where e_i (Pa) is the partial pressure of the gas.

The fractional concentration of gas i, c_i mol gas i (mol atmosphere)$^{-1}$, is simply

$$c_i = \frac{\varphi_i}{\varphi_{atm}} \tag{1.61}$$

so that, using (1.59)

$$\varphi_i = c_i \frac{P}{RT_K} \tag{1.62}$$

which defines the molar concentration in terms of the fractional concentration, atmospheric pressure, the gas constant and temperature. As an example, consider CO_2 at NTP, eqn (1.56), and with $c_i = 380$ μmol mol^{-1} (equivalent to 380 ppm), so that the true concentration of CO_2 is

$$\varphi_{CO_2} = 0.01580 \ \mu\text{mol m}^{-3} \tag{1.63}$$

Similarly, the partial pressure of constituent i, using (1.60) and (1.62), is

$$e_i = c_i P \tag{1.64}$$

so that the sum of the partial pressures of all the constituent gas components is equal to the atmospheric pressure.

In general, fractional concentration is independent of temperature and pressure so that, for example, the proportion of oxygen in the air at the top of Mount Everest is the same as at sea level, but the actual mole concentration will decline. Thus, if c_i is constant then eqn (1.62) implies that

$$\varphi_i \propto \frac{P}{T_K} \tag{1.65}$$

and (1.64) that

$$e_i \propto P \tag{1.66}$$

Although fractional molar concentration is generally used in models and analysis, the true mole concentration, φ_i, is arguably more appropriate for describing physiological processes as it defines the absolute number of molecules per unit volume. As an example consider humans breathing oxygen. It is common knowledge that we struggle at high altitudes. In this case, the fractional oxygen concentration is the same as at sea level but the true concentration declines substantially. Clearly, our physiology is responding to the true concentration. One possible reason why fractional

concentrations are used in plant physiology relates to the physiology of leaf photosynthesis, which is discussed in Chapter 3.

Now consider the air. Equation (1.58) gives

$$\rho_a = M_a \varphi_a \tag{1.67}$$

and for the constituent gases

$$\rho_i = M_i \varphi_i \tag{1.68}$$

For eqn (1.67) to be applied, it is necessary to derive an expression for the molar mass of air, M_a. This is generally evaluated for dry air and the standard values for the molar mass and fractional concentration are given in Table 1.1. Denoting the molar mass of dry air as $M_{a,dry}$, this is given by

$$M_{a,dry} = M_{N_2} c_{N_2} + M_{O_2} c_{N_2} + M_{Ar} c_{ar} + M_{CO_2} c_{CO_2} = 0.02895 \text{ kg mol}^{-1} \tag{1.69}$$

If water vapour is present, as is usually the case, then M_a will be slightly lower than $M_{a,dry}$, although the difference is small (around 1%).

Table 1.1: Composition of dry air. M is the molar mass and c the fractional concentration. These values are taken from Monteith and Unsworth (2008), but adjusted so that the CO_2 fractional concentration is closer to current ambient.

Gas	Nitrogen	Oxygen	Argon	CO_2
M (kg mol^{-1})	0.02801	0.03200	0.03898	0.04401
c (%)	78.08	20.95	0.93	0.04

1.5.1 CO_2 concentration

As mentioned above, atmospheric CO_2 concentration is often defined in *parts per million,* or ppm, which refers to volume parts per million, and is equivalent to μmol mol^{-1}, which is *fractional molar concentration*, or *mole fraction.* Following convention, C will be used to define CO_2 concentration in units μmol CO_2 mol air, or ppm, and the current ambient CO_2 is taken to be

$$C_{amb} = 380 \ \mu\text{mol mol}^{-1} \tag{1.70}$$

Equation (1.62) can be applied to the fractional molar concentration of CO_2, C μmol mol, to give

$$\varphi_{CO_2} = \frac{C}{10^6} \frac{P}{RT_K} \tag{1.71}$$

so that, for example, at normal temperature and pressure, eqn (1.56)

$$\varphi_{CO_2,NTP} \left(C = C_{amb} \right) = 0.01580 \text{ mol } CO_2 \text{ m}^{-3} \tag{1.72}$$

and, taking the molar mass of CO_2 to be 0.04401 kg mol^{-1} in eqn (1.68), the density is

$$\rho_{CO_2,NTP} \left(C = C_{amb} \right) 0.0006953 \text{ kg } CO_2 \text{ m}^{-3} = 0.6953 \text{ g } CO_2 \text{ m}^{-3} \tag{1.73}$$

1.5.2 Water vapour

Atmospheric water vapour content can be defined using the same approach as for CO_2 above. However, the two most common methods are to use vapour density, ρ_v kg H_2O m^{-3}, or vapour pressure, e_v kPa. Using eqns (1.67) and (1.68) with (1.59) and (1.60) gives

$$\rho_v = \rho_a \frac{M_v}{M_a}\frac{e_v}{P} \tag{1.74}$$

where subscript v refers to water vapour. Assuming M_a can be represented by $M_{a,dry}$, eqn (1.69), and taking $M_v = 0.01802$, this becomes

$$\rho_v = 0.622\rho_a \frac{e_v}{P} \tag{1.75}$$

It should be noted that in some texts the analysis leading to eqns (1.74) and (1.75) uses the density and pressure for dry air and then combines that with the water vapour, rather than the present approach which considers the total air composition including water vapour. This leads to a similar expression, but with the term $P - e_v$ in the denominator which is subsequently approximated to P (see, for example, Thornley and Johnson (2000) pp 423 and 633). With the present approach, it is necessary to assume that the molar mass of air can be represented by the value for dry air. In practice, any errors are small and eqns (1.74) and (1.75) can be used with confidence.

As the amount of water vapour in the air increases it eventually reaches saturation. The *saturation vapour pressure*, e'_v, is related to temperature and is given by Tetens formula (Campbell and Norman, 1998)

$$e'_v = 0.611\exp\left(\frac{17.5T}{T+241}\right)\text{kPa} \tag{1.76}$$

which defines e'_v in units of kPa, with T in °C. The coefficients in (1.76) differ slightly from those given by Allen *et al.* (1998), although the effect on e'_v is negligible. Equation (1.76) is illustrated in Fig. 1.10.

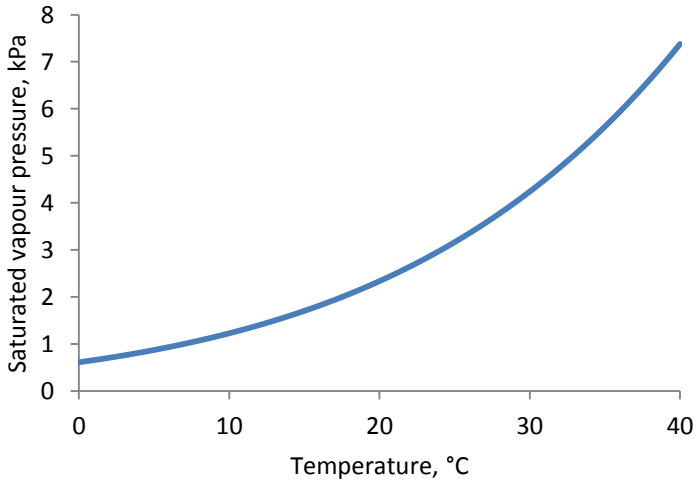

Figure 1.10: Saturated vapour pressure, e'_v, as a function of temperature.

The vapour density, ρ_v, is often referred to as the *absolute humidity*, and the ratio of the actual vapour density to saturated vapour density is the *relative humidity*, h_r, that is

$$h_r = \frac{\rho_v}{\rho_v'} = \frac{e_v}{e_v'} \tag{1.77}$$

where the prime denotes saturation and eqn (1.74) has been used to convert between pressure and density. Relative humidity cannot exceed unity and is often expressed as a percentage.

Vapour pressure deficit is widely used and is the difference between the saturated and actual vapour pressure, that is

$$\Delta e_v = e_v' - e_v \tag{1.78}$$

which, using eqn (1.77), may be written

$$\Delta e_v = e_v' \left(1 - h_r\right) \tag{1.79}$$

Relative humidity is a simple unit to work with and has appeal. However, it has limitations in terms of defining plant and canopy processes since for a given amount of water in the atmosphere it will vary substantially in response to temperature. To illustrate this point, Fig. 1.11 (left) shows the relative humidity as a function of temperature with $e_v = 0.6e_v'(T = 20°\text{C})$ so that the relative humidity at 20°C is 60%. It is quite clear that the relative humidity will vary substantially for a fixed amount of atmospheric water vapour. The corresponding vapour pressure deficit is shown in Fig. 1.11 (right) which demonstrates that the driving force for transpiration and evaporation, the vapour pressure deficit, will vary in response to temperature for a fixed vapour pressure. Equation (1.79) should be used with caution and (1.78) is preferable. In PlantMod, if relative humidity is prescribed, it will be for a specified temperature.

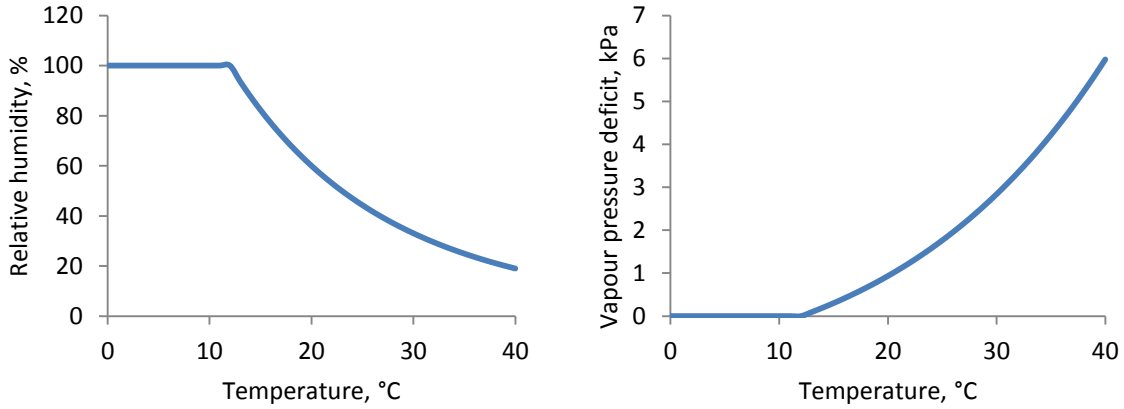

Figure 1.11: Left: relative humidity, h_r (%), as a function of temperature for vapour pressure corresponding to 60% saturation at 20°C. Thus, h_r = 60% at 20°C in this illustration. Right: the corresponding vapour pressure deficit.

1.6 Stomatal conductance and resistance

The standard approach for modelling transpiration, that is the flux of water, or photosynthesis which is the flux of CO_2, across the leaf stomata uses the process of diffusion, as described by Fick's law. This has received considerable attention in the literature – see, for example, Jones (1992), Campbell and Norman (1998), Monteith and Unsworth (2008). In its basic form as applied in plant physiology, the flux of water vapour or CO_2 is defined by

$$F = G\Delta\varphi \tag{1.80}$$

where F (mol m^{-2} s^{-1}) is the flux density, G (m s^{-1}) the conductance, and $\Delta\varphi$ (mol m^{-3}) the concentration difference. Note that density (kg m^{-3}) can be used instead of concentration and, in this case, the flux density will have units kg m^{-2} s^{-1}. G rather than g is used for conductance since g is used later for commonly used units for stomatal conductance which are considered below and in the following sections dealing specifically with the flux of CO_2 and water vapour. The units m s^{-1} for conductance are referred to here as *standard* units.

Resistance can also be used instead of conductance, where the resistance r, s m^{-1} is

$$r = \frac{1}{G} \tag{1.81}$$

which is the reciprocal of conductance. For pathways in series, such as the movement of water vapour across the stomata and then from the leaf surface to the bulk air stream, resistances are additive, whereas for pathways in parallel, conductances are additive. Thus, for two pathways in series or parallel:

$$\text{series:} \qquad r = r_1 + r_2; \quad \frac{1}{G} = \frac{1}{G_1} + \frac{1}{G_2} \tag{1.82}$$

$$\text{parallel:} \qquad \frac{1}{r} = \frac{1}{r_1} + \frac{1}{r_2}; \quad G = G_1 + G_2 \tag{1.83}$$

These equations can be extended to any number of pathways in an obvious manner.

When considering the flux density of CO_2 for photosynthesis and respiration, or water vapour for transpiration, if concentration units are used then eqn (1.80) applies directly. Thus, for CO_2, the flux density across the stomata and into the leaf, F_{CO_2}, mol CO_2 m^{-2} s^{-1}, is

$$F_{CO_2} = G_{CO_2}\left(\varphi_{CO_2,a} - \varphi_{CO_2,l}\right) \tag{1.84}$$

where subscripts a and l refer to the bulk air and internal leaf respectively. The corresponding equation for water vapour is

$$F_v = G_v\left(\varphi_{v,l} - \varphi_{v,a}\right) \tag{1.85}$$

although this is now a flux density from within the leaf to the bulk air. It must be noted in these equations that the mole concentrations in either the leaf interior or bulk air will depend on atmospheric pressure and local temperature through eqn (1.62).

Equations (1.84) and (1.85) are the basic equations describing the diffusion of CO_2 and water vapour between the leaf and the atmosphere, and are defined in terms of mole concentration, mol m^{-3}. However, fractional concentration for CO_2, as discussed above in Section 1.6.1, is often used, with units of either mol CO_2 (mol air)$^{-1}$ or, more commonly, μmol CO2 (mol air)$^{-1}$ which is ppm. Similarly, for water vapour, fractional vapour pressure is often used (Section 1.6.2), which is the ratio of the vapour pressure to atmospheric pressure. While these units have some attractive features, the benefit of using concentration units (mol m^{-3}) is that the standard physics of diffusion, dating back to Fick's work in the 19th century, can be applied directly. Two results in particular are of importance, which relate the conductance for different gases and the influence of atmospheric conditions. These are considered in turn.

For molecular diffusion of a gas through the stomata, the actual conductance depends on the molecular diffusivity of the gases which, in turn, is related to their molar masses. According to

Graham's law, the ratio of the diffusivity of two gases is proportional to the inverse of the square root of their molar masses. Thus, for water vapour and CO_2 this is $\sqrt{44/18} = 1.6$, so that the conductances for water vapour and CO_2 diffusion through the stomata are related by

$$G_v = 1.6 G_{CO_2} \tag{1.86}$$

It must be emphasised that this equation only applies to molecular diffusion. For turbulent transfer the conductances are approximately equal. When defining stomatal conductance, it is therefore essential to state whether it refers to water vapour or CO_2. Equation (1.86) gives a direct conversion between the two.

The influence of the atmospheric conditions can be incorporated by considering diffusion through a narrow pore. The details are not presented here but, according to Jones (1992, p 51),

$$G = G_0 \left(\frac{T_K}{T_{K,0}} \right)^{1.75} \frac{P_0}{P} \tag{1.87}$$

where the subscript 0 refers to a reference temperature and pressure, taken here to be NTP, eqn (1.56). According to this equation, the stomatal conductance increases in response to an increase in temperature or a decrease in atmospheric pressure. It should be noted that eqn (1.87) only includes the influence of temperature and pressure on the actual movement of the gas and so does not account for any influence on stomatal aperture.

1.6.1 Flux of CO_2

Although there is no direct consideration of the influence of stomatal conductance on photosynthesis in PlantMod, the common approach for describing this in relation to fractional CO_2 concentration is briefly considered.

Equation (1.84) defines the flux of CO_2 from the bulk air to the interior of the leaf in terms of mole CO_2 concentrations. However, fractional mole concentration, eqn (1.61), is frequently used to define the atmospheric CO_2. Using eqn (1.62) in (1.84) gives

$$F = G_{CO_2} \frac{P}{R} \left(\frac{c_a}{T_{K,a}} - \frac{c_l}{T_{K,l}} \right) \tag{1.88}$$

where subscript c_l and c_a, mol CO_2 (mol air)$^{-1}$, are the fractional CO_2 concentrations in the substomatal cavity and the bulk air stream respectively, and $T_{K,l}$ and $T_{K,a}$, K, are the leaf and air temperatures respectively. The fractional concentrations will not vary in response to temperature and pressure and, for relatively small temperature differences between the leaf and air it is reasonable to use air temperature. For example, if the air temperature increases from 15 to 20°C, which is 288 to 293 K, the change in $1/T_K$ is 1.7%. Equation (1.88) can therefore be approximated as

$$F_{CO_2} = g_{CO_2} \left(c_a - c_l \right) \tag{1.89}$$

where

$$g_{CO_2} = G_{CO_2} \frac{P}{R T_{K,a}} \text{ mol m}^{-2} \text{ s}^{-1} \tag{1.90}$$

so that g_{CO_2} has the same units as F in eqn (1.88). The standard conversion is to use normal temperature and pressure, eqn (1.56), to give

$$g_{CO_2}\left(\text{mol m}^{-2}\ \text{s}^{-1}\right)=41.6G_{CO_2}\left(\text{m s}^{-1}\right) \tag{1.91}$$

although eqn (1.90) is simple to use for other conditions. Now consider the influence of temperature and pressure on g_{CO_2}. Combining eqns (1.87) and (1.90) it is readily shown that

$$g_{CO_2}=g_{0,CO_2}\left(\frac{T_{K,l}}{T_{K,0}}\right)^{0.75} \tag{1.92}$$

where g_{0,CO_2} is the value of g_{CO_2} at NTP. Note that the derivation of this equation leads to the exponent 0.75 even though the exponent in eqn (1.87) is 1.75.

Comparing eqns (1.87) and (1.92) it can be seen that with the concentration difference that drives diffusion defined in mol m^{-3} units, the conductance is dependent on pressure and temperature, whereas with fractional concentration the conductance only depends on temperature. However, due to the influence of temperature and pressure on mole concentration, the resulting equations using either set of units are equivalent. It should be noted that for practical temperature ranges, the direct influence of temperature on the diffusion of CO_2 or water vapour is small: for example, increasing the temperature from 10 to 30°C in eqn (1.92) results in a 5% increase in g_{CO_2}.

1.6.2 Flux of water vapour

In the treatment of transpiration, it is common to use either vapour density, vapour pressure or fractional vapour pressures to define the flux of water vapour.

With vapour density, eqn (1.58) can be used in (1.85) to give

$$F^*=G_v\left(\rho_{v,l}-\rho_{v,a}\right) \tag{1.93}$$

where, again subscript v refers to water vapour, l and a are the leaf and air respectively, and now the flux density F^* has units kg water m^{-2} s^{-1}.

With vapour pressure, using eqn (1.60) in (1.85) gives

$$F_v=G_v\frac{1}{R}\left(\frac{e_{v,l}}{T_{K,l}}-\frac{e_{v,a}}{T_{K,a}}\right) \tag{1.94}$$

As for the treatment of CO_2 in the previous section, it is reasonable to use air temperature in this equation and write it as

$$F_v=g_v\left(\frac{e_l-e_a}{P}\right) \tag{1.95}$$

where, analogous to eqn (1.90), the conductance is now given by

$$g_v=G_v\frac{P}{RT_{K,a}}\ \ \text{mol m}^{-2}\ \text{s}^{-1} \tag{1.96}$$

and the conversion factor 41.6 in eqn (1.91) again applies. The influence of temperature on g_v, corresponding to eqn (1.92), is

$$g_v=g_{0,v}\left(\frac{T_{K,l}}{T_{K,0}}\right)^{0.75} \tag{1.97}$$

where $g_{0,v}$ is the value of g_v at NTP.

Note that, from eqns (1.90) and (1.96), the factor 1.6 in eqn (1.86) still applies, so that

$$g_v = 1.6 g_{CO_2} \tag{1.98}$$

An interesting application of the theory is to consider the effect of atmospheric pressure on transpiration. It is generally observed that transpiration increases in response to a decrease in atmospheric pressure (Gale, 2004; Bruce Bugbee, *pers. comm.*) but, as mentioned earlier, the fractional partial pressure, or fractional concentration, of water vapour (e_a/P) is relatively insensitive to atmospheric pressure, assuming the proportion of water vapour in the air is unaltered, eqn (1.66). As will be discussed in Chapter 5, the water vapour in the substomatal cavity is, to a very close approximation, saturated for leaves even when there is a degree of water stress. Thus, taking the vapour pressure within the leaf to be at saturation, (1.95) can be written

$$F_v = g_v \left(\frac{e'_{v,l}(T_l)}{P} - \frac{e_{v,a}}{P} \right) \tag{1.99}$$

Now, saturated vapour pressure is independent of atmospheric pressure so that decreasing P results in an increase in the first term in the brackets in this equation, while the second term is relatively unaffected. Thus, the term in brackets increases as P declines so that, even though g_v, which is given by eqn (1.97), is independent of P, the overall response is for F_v to increase as P declines. Note that the same result can, of course, be derived using the water vapour flux equation in terms of mole concentration of vapour, using eqn (1.85). The influence of atmospheric pressure on canopy transpiration is illustrated in Chapter 5 when transpiration is considered in more detail.

1.6.3 Which units to use?

The analysis presented here considers the standard physics units of m s^{-1} for stomatal conductance as well as the units of mol m^{-2} s^{-1} which are widely used, although not universally, in plant physiology. Which are preferable?

With m s^{-1} conductance is interpreted as the mean speed at which the gas moves. Resistance, which is the inverse of conductance and has units s m^{-1}, is the time taken to move a unit distance. Both of these interpretations are quite simple concepts to grasp. The added advantage of using these units is that the basic physics of diffusion, which was developed over 150 years ago, can be applied with confidence. The disadvantage is that the units for CO_2 or water vapour concentration, mol m^{-3} are less familiar to work with than ppm or fractional vapour pressure. Also, these quantities vary in response to temperature and pressure, although in practice the temperature response is small..

With mol m^{-2} s^{-1}, conductance has the same units as flux density and is interpreted as the change in flux density per unit change in fractional concentration difference for CO_2, or fractional vapour pressure for water vapour. If resistance is used, which is the reciprocal of conductance and has units m^2 s mol^{-1}, it is more difficult to ascribe a simple interpretation. The advantage of these units is that atmospheric CO_2 content is defined in fractional units – that is ppm – that are widely used and with which people are familiar. By using fractional vapour pressure, transpiration is then defined analogously to photosynthesis. The considerable advantage of using fractional concentration or pressure is that these quantities are independent of temperature and pressure.

It seems appropriate, therefore, to regard the standard units for conductance, along with true mole concentration for gases and water vapour, as the more fundamental approach to the treatment of diffusion of either CO_2 or water vapour across stomata. On the other hand, the use of fractional

concentration and pressure, in which case conductance is expressed as mol m^{-2} s^{-1} can be regarded as a derived framework that has its own advantages. In either case, the influence of temperature and pressure as described in the previous sections can be applied.

Stomatal conductance is only used in PlantMod for water vapour and, in keeping with current trends, fractional concentrations for CO_2 and water vapour will be used in the analysis, so that stomatal conductance has units mol m^{-2} s^{-1}. In the PlantMod program conductances can be displayed in either set of units. An appreciation of the traditional physics of diffusion will definitely be of benefit in the study of photosynthesis and transpiration.

1.6.4 Environmental effects on stomatal conductance

The analysis presented here has considered the effect of atmospheric pressure and temperature on stomatal conductance through the influence on the actual process of diffusion. However, responses to environment are also observed that are a direct result of climatic conditions on stomatal aperture. The symbol g_s is used for stomatal conductance which can refer to the conductance for either CO_2 or water vapour.

A concise discussion is given by Thornley and France (2007, p. 378) and, as discussed in that text, there is no clear method for incorporating the influence of environmental factors on g_s. Various empirical approaches have been proposed relating g_s to vapour deficit or relative humidity, atmospheric CO_2 concentration and either net photosynthesis or light intensity. There are challenges when working with net photosynthesis which can lead to circularity in the model – is photosynthesis affected by or affecting stomatal conductance, and *vice versa*. Some authors (for example, Blonquist Jr, *et al.*, 2009) have used such an approach successfully, although Bunce (2000) compared various approaches with mixed results.

A simple approach is used here which captures the general behaviour of models that are used, with g_s being defined by

$$g_s(J,h_r,C)=g_{s,ref}f_{g,J}(J)f_{g,h_r}(h_r)f_{g,C}(C) \tag{1.100}$$

where the f functions define the response of g_s to irradiance , J (J m^{-2} s^{-1}) (Chapter 2), relative humidity, h_r (fraction) (Section 1.5.2 above), and atmospheric CO_2 concentration, C (μmol mol^{-1}) (Section 1.5.1 above), and $g_{s,ref}$ is a reference value for g_s so that, at the reference values J_{ref}, $h_{r,ref}$, C_{ref},

$$f_{g,J}(J_{ref})=f_{g,h_r}(h_{r,ref})=f_{g,C}(C_{ref})=1 \tag{1.101}$$

The irradiance function is

$$f_{g,J}(J)=\left(\frac{J_{ref}+K_J}{J_{ref}}\right)\left(\frac{J}{J+K_J}\right) \tag{1.102}$$

where K_J, (J m^{-2} s^{-1}) is a curvature parameter. This is a rectangular hyperbola, written so that it takes the value unity at $J=J_{ref}$ as required, and increases from zero to an asymptote as J increases. The default parameter values are

$$\begin{aligned} J_{ref} &= 400 \text{ J m}^{-2} \text{ s}^{-1} \\ K_J &= 100 \text{ J m}^{-2} \text{ s}^{-1} \end{aligned} \tag{1.103}$$

The relative humidity function is

$$f_{g,h_r}(h_r)=\begin{cases} f_{g,h_r,mn}+\left(1-f_{g,h_r,mn}\right)\left(\dfrac{h_r}{h_{r,ref}}\right)^{q_{hr}}, & h_r \le h_{r,ref} \\ \dfrac{h_r}{h_{r,ref}}, & h_r > h_{r,ref} \end{cases} \tag{1.104}$$

which is a simple function that takes the value $f_{g,h_r,mn}$ when $h_r = 0$, increases to 1 when $h_r = h_{r,ref}$, and is proportional to h_r as h_r increases. A non-zero value as h_r approaches zero is required to allow the stomata to remain open in very dry air. In order to ensure that the slope of this curve is continuous at $h_r = h_{r,ref}$, the exponent q_{hr} is given by

$$q_{h_r}=\frac{1}{1-f_{g,h_r,mn}} \tag{1.105}$$

The default parameter values are

$$\begin{aligned} h_r &= 0.5\,(50\%) \\ f_{g,h_r,mn} &= 0.6 \end{aligned} \tag{1.106}$$

so that at zero relative humidity stomatal conductance is reduced to 60% of its maximum value at the reference relative humidity of 50%. Note that, with this value for $f_{g,h_r,mn}$,

$$q_{h_r}=2.5 \tag{1.107}$$

Finally, the CO_2 function is

$$f_{g,C}(C)=f_{g,C,mn}+\left(1-f_{g,C,mn}\right)\frac{C_{amb}}{\max(C,300)} \tag{1.108}$$

which takes the minimum value $f_{g,C,mn}$ at high C. According to this function, $f_{g,C}$ declines as C increases. The restriction that it does not change for C less than 300 μmol mol^{-1} is to prevent unrealistic responses at very low C, since $1/C \to \infty$ as $C \to 0$. If studies require lower C than 300 then eqn (1.108) may have to be modified. The default value for $f_{g,C,mn}$ is

$$f_{g,C,mn}=0.2 \tag{1.109}$$

which means that stomatal conductance will fall to 20% of its value at ambient CO_2 as the CO_2 concentration gets very large. C_{amb} is taken to be 380 μmol mol^{-1} (eqn (1.70)). It should be noted that at extreme CO_2 concentrations of the order 10,000 μmol mol^{-1}, stomatal conductance can actually increase (Mackowiak *et al.*, 1992). Such situations are not considered here.

Equations (1.102), (1.104), (1.108) are illustrated in Fig. 1.12 where it can be seen that they all take the value unity at the reference conditions. Stomatal conductance increases in response to increases in irradiance and relative humidity, but decreases as CO_2 increases. Note that while stomatal conductance increases in proportion to relative humidity, h_r, transpiration is also affected by h_r through its influence on the vapour pressure gradient between the evaporating surface and bulk air stream. Thus, the influence of h_r on transpiration is not solely due to the effect on stomatal conductance.

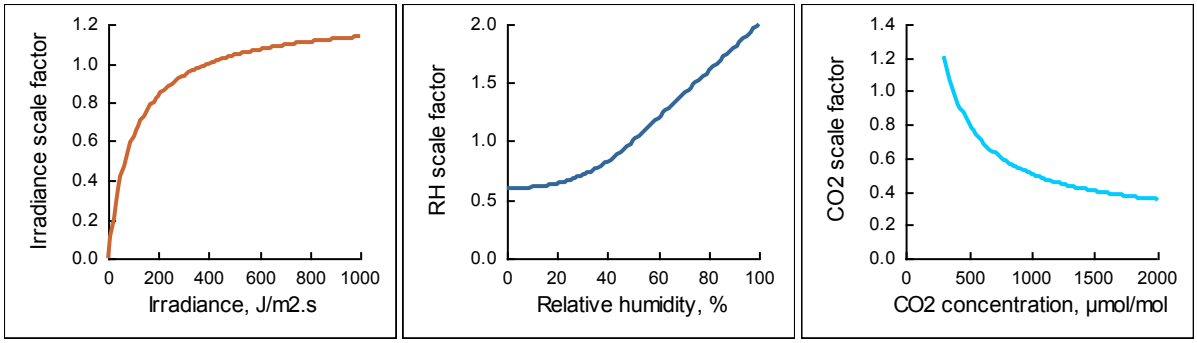

Figure 1.12: Stomatal conductance scaling functions for irradiance (left), relative humidity (centre), CO_2 (right), as given by eqns (1.102), (1.104), (1.108) respectively with parameters in eqns (1.103), (1.106), (1.109). Note the different scales. From PlantMod.

This approach for defining the direct environmental effects on stomatal conductance is similar to that proposed by Ball *et al* (1987) that has been quite widely used, but with some differences:

- The Ball *et al* equation incorporates photosynthesis rather than irradiance, although g_s is seen to respond to irradiance – see for example, Bunce, 2000, but note that Bunce uses a negative exponential curve that has very similar behaviour to the rectangular hyperbola used in eqn (1.102).
- Ball *et al* prescribed an explicit minimum value for g_s, whereas minimum values for the h_r and CO_2 responses are incorporated separately.
- Their equation has a linear response to relative humidity. The approach here is quite linear in behaviour over practical values of h_r, but with a non-zero minimum value at low h_r, which is consistent with the analysis of Blonquist *et al* (2009) (Bruce Bugbee, *pers. comm.*).

Direct effects of temperature on stomatal conductance are not included, in spite of the fact that the theory of diffusion shows as small response to temperature as discussed earlier. It is assumed that the influence of temperature is included in the relative humidity effect, since relative humidity will change in response to temperature for a given vapour pressure (see Section 1.5.2).

The present analysis provides a flexible and relatively simple way of incorporating environmental effects directly into the description of stomatal conductance. However, it should be noted that this is an empirical approach and does account for the possible mechanisms that may be causing these responses. It must be emphasised that these responses relate to the physiological influence of the environment on stomatal aperture and not on the actual process of diffusion.

1.7 Final comments

The theory described in this Chapter covers the mathematical concepts of the background topics that are required for the theory of canopy photosynthesis and energy balance, including canopy transpiration and temperature, as described in the subsequent Chapters. Many of the topics presented in this Chapter are discussed in detail in Thornley and Johnson (2000) and Thornley and France (2007). These texts also cover a wide range of models and modelling approaches in plant and crop physiology, and agricultural simulation modelling in general.

1.8 References

Allen RG, Pereira LS, Raes D and Smith M (1998). FAO irrigation and drainage paper no. 56: crop evapotranspiration. www.kimberly.uidaho.edu/ref-et/fao56.pdf.

Ball JT, Woodrow IE & Berry JA (1987). A model predicting stomatal conductance and its contribution to the control of photosynthesis under different environmental conditions. In: *Progress in Photosynthesis Research*, vol IV, ed J Biggens. Martinus Nijhoff / American Society of Agronomy, Dordrecht, the Netherlands / Madison, WI, USA, 221-224.

Blonquist Jr JM, Norman JM & Bugbee B (2009). Automated measurement of canopy stomatal conductance based on infrared temperature. *Agricultural and Forest Meteorology,* **149,** 1931-1945.

Bunce JA (2000). Responses of stomatal conductance to light, humidity and temperature in winter wheat and barley grown at three concentrations of carbon dioxide in the field. *Global Change Biology,* **6,** 371-382.

Campbell GS and Norman JM (1998). *An Introduction to environmental biophysics*, second edition. Springer, New York, USA.

Gale, J (2004). Plants and altitude – revisited. *Annals of Botany*, **92(4)**, 199.

Johnson and Thornley (1985). Temperature dependence of plant and crop processes. *Annals of Botany,* **55,** 1-24.

Jones HG (1992). *Plants and microclimate*. Cambridge University Press, Cambridge, UK.

Mackowiak CL, Wheeler RM & Yorio NC (1992). Increased leaf stomatal conductance at very high carbon dioxide concentrations. *HortScience*, **27,** 683-684.

Monteith JL & Unsworth MH (2008). *Principles of environmental physic,* third edition. Elsevier, Oxford, UK.

Thornley JHM (1998). *Grassland dynamics: an ecosystem simulation model*. CAB International, Wallingford, UK.

Thornley JHM and France J (2007). *Mathematical models in agriculture*. CAB International, Wallingford, UK.

Thornley JHM & Johnson IR (2000). *Plant and crop modelling*. Blackburn Press, Caldwell, New Jersey, USA.

2 Radiation

2.1 Introduction

Radiation plays a crucial role in plant and crop physiological processes. The visible component of solar, or shortwave, radiation is the fundamental energy source for photosynthesis. The longwave radiation that is emitted by terrestrial bodies as well as the atmosphere, combined with solar radiation, is the key energy driver for the evaporation of water. A background to the basic principles relating to radiation components is now presented, but for a more complete discussion see, for example, Jones (1992), Campbell and Norman (1998), Monteith and Unsworth (2008).

In this Chapter, a background to the basic physics of radiation is presented, followed by the analysis that is required for canopy photosynthesis and energy balance, which includes the calculations of canopy transpiration and temperature in response to environmental conditions. Some of the symbols in the early sections are used with different definitions later for the canopy calculations. Symbols and their definitions are presented in Tables 2.1 and 2.2 at the end of the Chapter.

2.2 Black body radiation

The energy level distribution from a body is a function of its temperature, its wavelength and surface properties. If the surface properties are such that there is no reduction in energy emitted due to those surface properties, then that body is referred to as a *black body*. Planck's law, published in 1900, is derived from quantum mechanics, and states that

$$I(\lambda,T_K)=\frac{2hc^2}{\lambda^5}\left(\frac{1}{e^{hc/\lambda kT_K}-1}\right) \tag{2.1}$$

where $I(\lambda,T_K)$ is the *spectral emittance*, W m^{-2} (m wavelength)$^{-1}$ (sometimes written as W m^{-3}), which is the energy per unit surface area per unit wavelength of the emitting body as a function of its temperature T_K (K) (the subscript K is used to differentiate from °C), and wavelength λ (m) of the emitted radiation. $h=6.626\times10^{-34}$ J s is Planck's constant; $c=2.998\times10^{8}$ m s^{-1} is the speed of light; and $k=1.3807\times10^{-23}$ J K^{-1} is the Boltzmann constant. $I(\lambda,T)$ is illustrated in Fig. 2.1 for $T_K=6000$ K, which approximates to the external surface of the sun, and $T_K=300$ K (equivalent to 27°C) which is representative of temperatures on earth. The scales of these graphs are different since the energy emitted by the sun is much greater than that from the surface of the earth. The ultraviolet, photosynthetically active (see below) and infrared components of the solar radiation are also indicated. It can be seen that $I(\lambda,T_K)$ peaks at a shorter wavelength for the higher temperature, and Wein's law can be derived which states that the peak wavelength is

$$\lambda_m=\frac{2897}{T_K}\times10^{-6}\ \text{m} \tag{2.2}$$

so that $\lambda_m(T_K=6000)=0.480$ μm and $\lambda_m(T_K=300)=9.597$ μm, which means that the peak energy emitted by terrestrial bodies has a much longer wavelength than for the sun – hence the terms shortwave and longwave. The longwave radiation is sometimes referred to as terrestrial or far-infrared radiation.

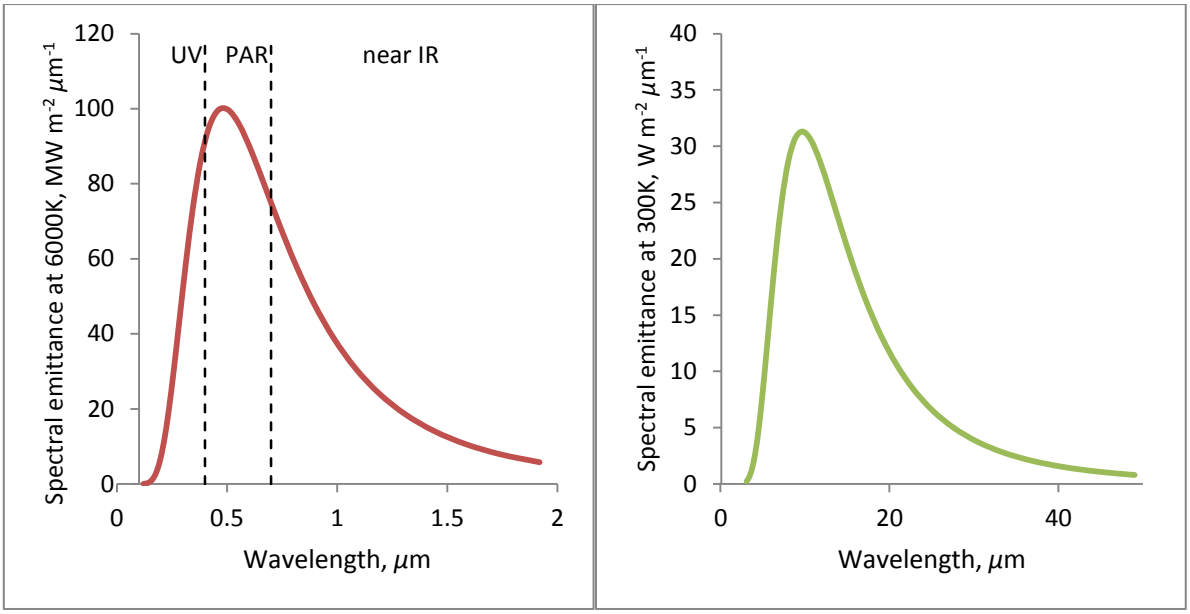

Figure 2.1: Spectral distribution of radiation emitted from black bodies for $T_K = 6000$ K (left) and $T_K = 300$ K (right), which correspond roughly to the surface of the sun and earth respectively, as a function of wavelength. The red line is shortwave, or solar, radiation, and the green line is longwave, or terrestrial, radiation. Also indicated for the shortwave radiation are the ultraviolet (UV), photosynthetically active radiation (PAR) and near-infrared (IR). The longwave radiation is also known as far-infrared. The components of radiation are discussed in the text. Note the scale for the shortwave radiation axis (left) is 10^6 times that on the right, which highlights the much greater energy emission by the sun.

The total energy emitted at a particular temperature is the integral of $I(\lambda, T_K)$ for all wavelengths, which is the area under the curve shown in Fig. 2.1. This can be derived from eqn (2.1) and is known as the Stefan-Boltzmann equation, which (for a black body) is

$$E = \sigma T_K^4 \tag{2.3}$$

with units W m^{-2}, where $\sigma = 5.670 \times 10^{-8}$ W m^{-2} K^{-4} is the Stefan-Boltzmann constant. Thus, $E(T_K = 6000) = 7.35 \times 10^7$ W m^{-2} $\equiv$ 73.5 MW m^{-2} and $E(T_K = 300) = 459$ W m^{-2}, demonstrating the greater energy emitted per unit area of the sun compared with the earth.

Of the radiation emitted by the sun about half of it is visible and this is the middle part of the frequency distribution, ranging from around 0.4 μm (blue light) to 0.7 μm (red light). Ultraviolet (UV) radiation is the component from below 0.4 μm, while the infrared (IR) component is the range 0.7 to 3 μm. These values, which are indicated in Fig. 2.1, are not exact since there is no sharp transition between the different components. The visible component of radiation is also known as *photosynthetically active radiation* (PAR) as this is the component of radiation that provides the energy for photosynthesis – this is discussed below. The wavelength of the radiation emitted by terrestrial bodies covers the range from about 3 to 100 μm, which is much greater than that for the sun, and hence is referred to as longwave, or far-IR, radiation.

2.3 Non-black body and gray body radiation

In practice, most terrestrial bodies do not behave like perfect black bodies and eqn (2.3) is modified to give

$$E = \varepsilon \sigma T_K^4 \tag{2.4}$$

where $\varepsilon, 0 < \varepsilon \leq 1$, (dimensionless) is the *emissivity*. Equation (2.4) applies to bodies where the emissivity is independent of wavelength. Black bodies therefore have an emissivity of 1 and bodies with $\varepsilon < 1$ are referred to as *gray bodies*. For most natural surfaces (including snow) ε lies between 0.95 and 1. Although it is reasonable to use the value 1, it is assumed that

$$\varepsilon = 0.97 \tag{2.5}$$

for calculation in PlantMod

2.4 Radiation energy for photosynthesis: PAR and PPF

As mentioned earlier, the visible component of the radiation emitted by the sun, which is in the range 0.4 to 0.7 μm (or 400 to 700 nm), provides the energy for photosynthesis. This is referred to as *photosynthetically active radiation*, or PAR, and is commonly assumed to be around half the total solar radiation. However, the precise fraction depends on climatic factors such as cloud cover and solar elevation. From the Clear Sky Calculator (www.clearskycalculator.com), it can be seen that a more accurate conversion is for PAR to be 45% of the total solar radiation. This fraction is not fixed, but increases when humidity increases and can reach close to 50%. The units for describing PAR are W $m^{-2} \equiv$ J m^{-2} s^{-1}.

For photosynthesis studies, the energy is generally expressed as the molar flux of photons between 0.4 to 0.7 μm, and is referred to as *photosynthetic photon flux*, or PPF. The term PPF will be used throughout PlantMod for the definition of the energy source for photosynthesis.

There is no precise conversion between PAR and PPF that can be applied for all atmospheric conditions since, as discussed above, the energy of the radiation depends on the wavelength and so depends on the spectral composition of the light. A reasonable value, using the Clear Sky Calculator and based on summer conditions at Logan, Ut, (Bruce Bugbee, *pers. comm.,* www.clearskycalculator.com) is

$$1\ \mu\text{mol photons PAR} \cong 0.218\ \text{J PAR}. \tag{2.6}$$

Finally, note that the term *photon flux density*, or PFD, is sometimes used, but this is now discouraged in the literature. I'm grateful to Professor Bruce Bugbee for clarifying these definitions.

2.5 Radiation units and terminology

In the theory presented above, both J m^{-2} s^{-1} (equivalent to W m^{-2}) and μmol photons m^{-2} s^{-1} have been used for radiation energy. In the physics literature, J m^{-2} s^{-1} (W m^{-2}) is almost universally used, while in photosynthesis studies the recent trend has been towards μmol photons m^{-2} s^{-1}. In PlantMod, both sets of units will be used, although this should not cause confusion. For discussions of photosynthesis, the convention for using μmol photons m^{-2} s^{-1} (PPF) is followed, but for energy dynamics and evaporation, J m^{-2} s^{-1} units are preferred, and this is referred to as irradiance which is the *total* solar radiation and not just the photosynthetically active component. The choice of J m^{-2} s^{-1} rather than W m^{-2}, which are equivalent, is because daily radiation values are also used which have units J m^{-2} d^{-1}.

2.6 Canopy light interception and attenuation

In order to model canopy photosynthesis in response to environmental factors, it is necessary to develop models of light interception and attenuation through the depth of the canopy. The canopy photosynthetic rate is then calculated in terms of the photosynthetic response to PPF of the leaves within the canopy and the variation of PPF through the depth of the canopy. The approach taken here is to look at the mean PPF through the canopy as well as the components of direct and diffuse sunlight. In doing so, the PPF components within the canopy and those that are actually incident on the leaf surfaces are considered. This component of the theory deals with the PPF with units μmol photons m^{-2}, where the area unit can refer either to ground or the leaf. The model for light interception and attenuation can be explored in PlantMod and so only a few illustrations are presented here.

2.6.1 Mean PPF

First consider the mean PPF within the canopy. In overcast conditions, there will be little variation in the PPF in the horizontal plane and so this approach is applicable without modification. However, for clear skies with strong sunflecks in the canopy, there will be considerable horizontal variation in the PPF. The following theory still applies to these situations but it has to be extended to identify the direct and diffuse components of PPF.

As light is intercepted and absorbed by leaves within the canopy, the PPF declines, as described by Beer's law:

$$I(\ell) = I_0 e^{-k\ell} \tag{2.7}$$

where I_0 is the PPF incident on the canopy and k is the canopy extinction coefficient. A derivation of this equation is given in Thornley and Johnson (2000, Chapter 8). Note that since ℓ has dimensions (m^2leaf) (m^{-2} ground) it follows that k has dimensions (m^2 ground) (m^{-2} leaf), and hence eqn (2.2) is dimensionally consistent. However, for most purposes it is sufficient to regard k as dimensionless. The PPF through the canopy as described by eqn (2.7) is illustrated in Fig. 2.2 for $k = 0.5$ which is typical of cereals and grasses, and $k = 0.8$ which is appropriate for canopies with more horizontally inclined leaves.

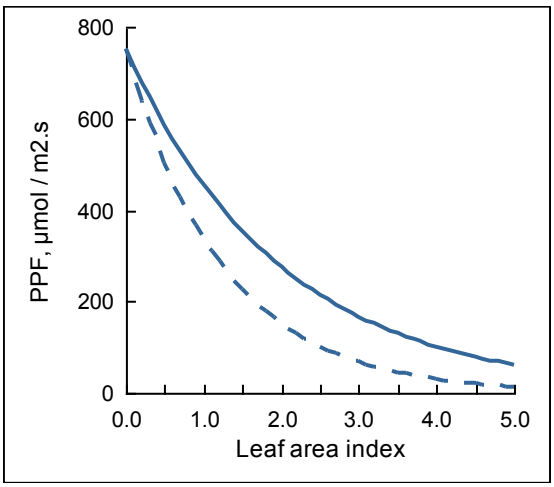

Figure 2.2: Mean PPF as a function of cumulative leaf area index through the canopy, as given by eqn (2.7) for $k = 0.5$ (solid) and $k = 0.8$ (dash), and with the PPF incident on the canopy given by $I_0 = 1000$ μmol m^{-2} s^{-1}. From PlantMod.

The default value

$$k = 0.5 \tag{2.8}$$

is used in PlantMod.

A simple interpretation of the extinction coefficient, k, is the cosine of the angle between the leaves and the horizontal plane. Thus, for perfectly horizontal leaves $k = \cos(0) = 1$.

Equation (2.7) defines the PPF per unit horizontal (or ground) area, but the PPF per unit leaf area is required in order to calculate the rate of photosynthesis of the leaves in the canopy. This is given by

$$I_\ell(\ell) = kI(\ell) \tag{2.9}$$

where the factor k projects the leaf area index onto the horizontal plane – for a derivation, see Thornley and Johnson (2000, p. 203)

2.6.2 Direct and diffuse PPF

The theory is now developed to identify the direct and diffuse components of PPF within the canopy. This approach is based on the early work of Norman (1980, 1982) as well as that by Campbell (1977) and Stockle and Campbell (1985). This treatment of direct and diffuse PPF is widely used and the analysis presented here closely follows Johnson *et al.* (1995) and has been applied, for example, by Thornley (2002).

Using subscripts s and d to denote the direct solar beam and diffuse PPF respectively, above the canopy, the PPF is

$$I_0 = I_{0,s} + I_{0,d} \tag{2.10}$$

Within the canopy at leaf area index ℓ it is

$$I = I_s + I_d \tag{2.11}$$

and the corresponding PPF incident on the leaf surfaces is

$$I_\ell = I_{\ell,s} + I_{\ell,d} \tag{2.12}$$

It is assumed that the direct and diffuse components of I_0 decline through the depth of the canopy according to eqn (2.7). Defining f_s as the fraction of total radiation that is direct, so that

$$I_{0,s} = f_s I_0 \tag{2.13}$$

it therefore follows that

$$I_s = f_s I_0 \mathrm{e}^{-k\ell} \tag{2.14}$$

and

$$I_d = (1 - f_s) I_0 \mathrm{e}^{-k\ell} \tag{2.15}$$

To calculate the incident PPF on the leaves, it is necessary to evaluate the components of leaf area index which are in direct sunlight and diffuse PPF, denoted by ℓ_s and ℓ_d respectively. ℓ_s is obtained by noting that the reduction in the direct beam is intercepted by ℓ_s , so that

$$k\ell_s I_{0,s} = I_{0,s}\left(1 - \mathrm{e}^{-k\ell}\right) \tag{2.16}$$

from which

$$\ell_s = \frac{1-\mathrm{e}^{-k\ell}}{k} \tag{2.17}$$

The factor k on the left hand side of eqn (2.16) is required as this projects the leaf area index, ℓ_s, onto the horizontal plane. The remainder of the leaves are in diffuse PPF and have leaf area index

$$\ell_d = \ell - \ell_s \tag{2.18}$$

The incident PPF on ℓ_d is, applying eqns (2.9) and (2.15)

$$\begin{aligned} I_{\ell,d} &= kI_d \\ &= kI_0\left(1-f_s\right)\mathrm{e}^{-k\ell} \end{aligned} \tag{2.19}$$

The PPF incident on ℓ_s is the combination of the diffuse component and the direct solar beam, as given by

$$\begin{aligned} I_{\ell,s} &= kI_{0,s} + I_{\ell,d} \\ &= kI_0\left[f_s + \left(1-f_s\right)\mathrm{e}^{-k\ell}\right] \end{aligned} \tag{2.20}$$

Note that Norman (1982) relates the extinction coefficient, k to solar elevation. While this is a good objective for detailed study of light interception in canopies, difficulties arise when looking at mean values over the day (for further discussion, see Johnson *et al.*, 1995). In PlantMod, one value for the extinction coefficient for both direct and diffuse PPF is used and it is assumed to be constant.

The mean PPF, I, direct and diffuse components, I_s, I_d, and PPF incident on leaves in direct and diffuse light, $I_{l,s}$, $I_{l,d}$, are shown in Fig. 2.3.

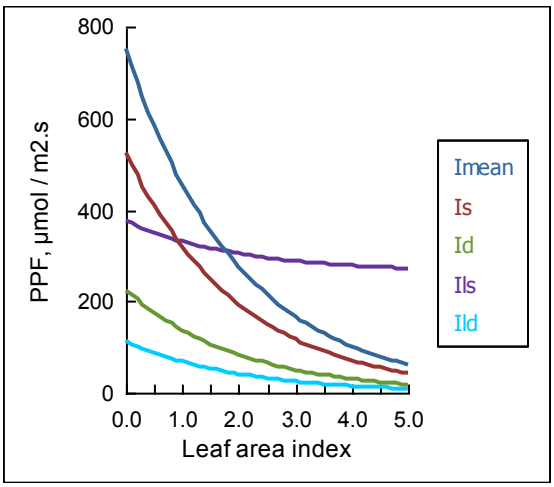

Figure 2.3: The mean PPF, I, direct and diffuse components, I_s, I_d, and PPF incident on leaves in direct and diffuse light, $I_{l,s}$, $I_{l,d}$, with $k = 0.5$. From PlantMod.

The theory presented here provides a complete description of the attenuation and interception of the direct and diffuse PPF components through the canopy. It is necessary to define the canopy light extinction coefficient, k, the PPF on the canopy, I_0, and the fraction of I_0 that is from the direct solar beam, f_s. In practice, the extinction coefficient may vary from around 0.5 for cereals and grasses to 0.8 for species with more horizontally inclined leaves such as clover. For skies where the sun is not obscured by cloud, f_s may be typically around 0.7, although this can depend on atmospheric composition.

There are some simplifying assumptions in this approach, as discussed by Thornley and France (2007). The main simplifications are that the leaves are assumed to be randomly distributed (see Thornley and Johnson, 2000, for a discussion on leaf distribution), and variation in the direction of the direct solar beam throughout the day is not included. Also, light reflection and transmission through the leaves has not been incorporated directly, although in photosynthesis studies, the rate of leaf photosynthesis is generally calculated in terms of incident light and not absorbed light. By working with eqn (2.7) directly (Beer's law), it is reasonable to assume that the reflected and transmitted components are incorporated implicitly. While the analysis is relatively simple, this level of complexity is widely used in crop and pasture studies for the calculation of canopy photosynthesis, which is considered in Chapter 4.

2.6.3 Ground cover

In the analysis for the canopy energy balance the fractional ground cover is required. According to eqn (2.7), the solar radiation that is transmitted through the canopy is

$$I_t = I_0 e^{-kL} \tag{2.21}$$

Defining the fractional ground cover, f_g, as the proportion of solar radiation that is not transmitted, it follows that

$$f_g = 1 - e^{-kL} \tag{2.22}$$

This simple expression will be used in the analysis for the canopy radiation balance.

2.7 Clear-sky solar radiation and daylength

In the treatment of canopy transpiration, temperature and energy balance, it is necessary to estimate the clear-sky daily solar radiation, $R_{S,0}$, MJ m^{-2} day. The theory presented here follows Campbell (1977) and Thornley and France (2007).

Three standard equations relating to the geometry of the earth's rotation and its orbit around the sun are first presented without derivation. These are the solar declination angle, δ (rad), which is the angle between the earth's equatorial plane and the line from the earth to the sun, and accounts for the tilt of the earth's axis relative to the sun; the solar elevation angle at local noon, ϕ (rad); and the daylength, f_d, as a fraction of the 24 hour period. If t is the day of year from 1 January, λ (rad) the latitude, then

$$\delta = \frac{\pi}{180} 23.45 \sin\left(2\pi \frac{t-81}{365}\right) \tag{2.23}$$

$$\phi = \sin^{-1}\left(\sin\lambda \sin\delta + \cos\lambda \cos\delta\right) \tag{2.24}$$

$$f_{day} = \frac{1}{\pi} \cos^{-1}\left(-\tan\lambda \tan\delta\right) \tag{2.25}$$

and the number of daylight hours per day is

$$h_{day} = 24 \times f_{day} \tag{2.26}$$

If λ is prescribed in degrees then, using obvious notation,

$$\lambda = \frac{\pi}{180} \lambda_{deg} \tag{2.27}$$

To convert δ and ϕ to degrees, multiply by $180/\pi$. Also note that latitudes in the northern hemisphere are positive while they are negative in the southern hemisphere.

δ, ϕ and h_{day} are illustrated in Fig. 2.4 for elevations of 0 (the equator), 20, 40, 60°. It can be seen that the solar declination is positive in summer, negative in winter and zero at the spring and autumn equinoxes (which are around 21 March and 22 Sept). For latitudes outside locations between the tropic of Cancer and Capricorn, which are $\pm$ 23.4° respectively, the solar elevation angle at local noon, ϕ, is maximum in the middle of summer. However, at the equator, ϕ is maximum at the spring and autumn equinoxes and, moving towards the tropics, the two maxima converge. Finally, the daylength follows a familiar pattern and is seen to be fixed at 12 hours for the equator while, for other locations it is, of course, greater in summer, with longer days and shorter nights as the latitude increases.

Turning to irradiance, three sets of variables are used with appropriate subscripts (R_S has already been defined above). These are:

J, instantaneous irradiance outside the earth's atmosphere: W m^{-2} or J m^{-2} s^{-1};

I, instantaneous irradiance at the earth's surface: W m^{-2} or J m^{-2} s^{-1};

In all cases, irradiance is measured parallel to the horizontal plane at the surface of the earth.

The irradiance outside the earth's surface at solar noon, J_{noon}, is

$$J_{noon} = \gamma \sin\phi \tag{2.28}$$

where

$$\gamma = 1367 \text{ J m}^{-2} \text{ s}^{-1} \tag{2.29}$$

is the solar constant, and is the irradiance perpendicular to the sun at the edge of the earth's atmosphere. It is now assumed that the potential, or clear-sky, irradiance at the earth's surface, $I_{p,noon}$, is given by

$$I_{p,noon} = \tau J_{noon} \tag{2.30}$$

where τ is an atmospheric diffusivity coefficient. While more complex equations have been used this approach works well for a range of locations in Australia, as will be seen shortly, and there is no obvious reason to suggest other locations will behave much differently. Comparisons with experimental data suggest

$$\tau = 0.73 \tag{2.31}$$

is a good default value, although it may be necessary to adjust this parameter for different sites. However, this is relatively easy to estimate, as discussed below. It should be noted that a slightly different approach than a fixed constant in eqn (2.30) is used by Allen *et al*, (1998) although, as will be seen below, the present approach works well. $I_{p,noon}$ is illustrated in Fig. 2.5 for the latitudes used in Fig. 2.4. It can be seen that the variation in $I_{p,noon}$ is most apparent as the latitude moves further from the equator. It peaks at the equinoxes at the equator and, outside the tropics, it peaks in mid-summer, with the range between summer and winter increasing as the distance from the equator increases.

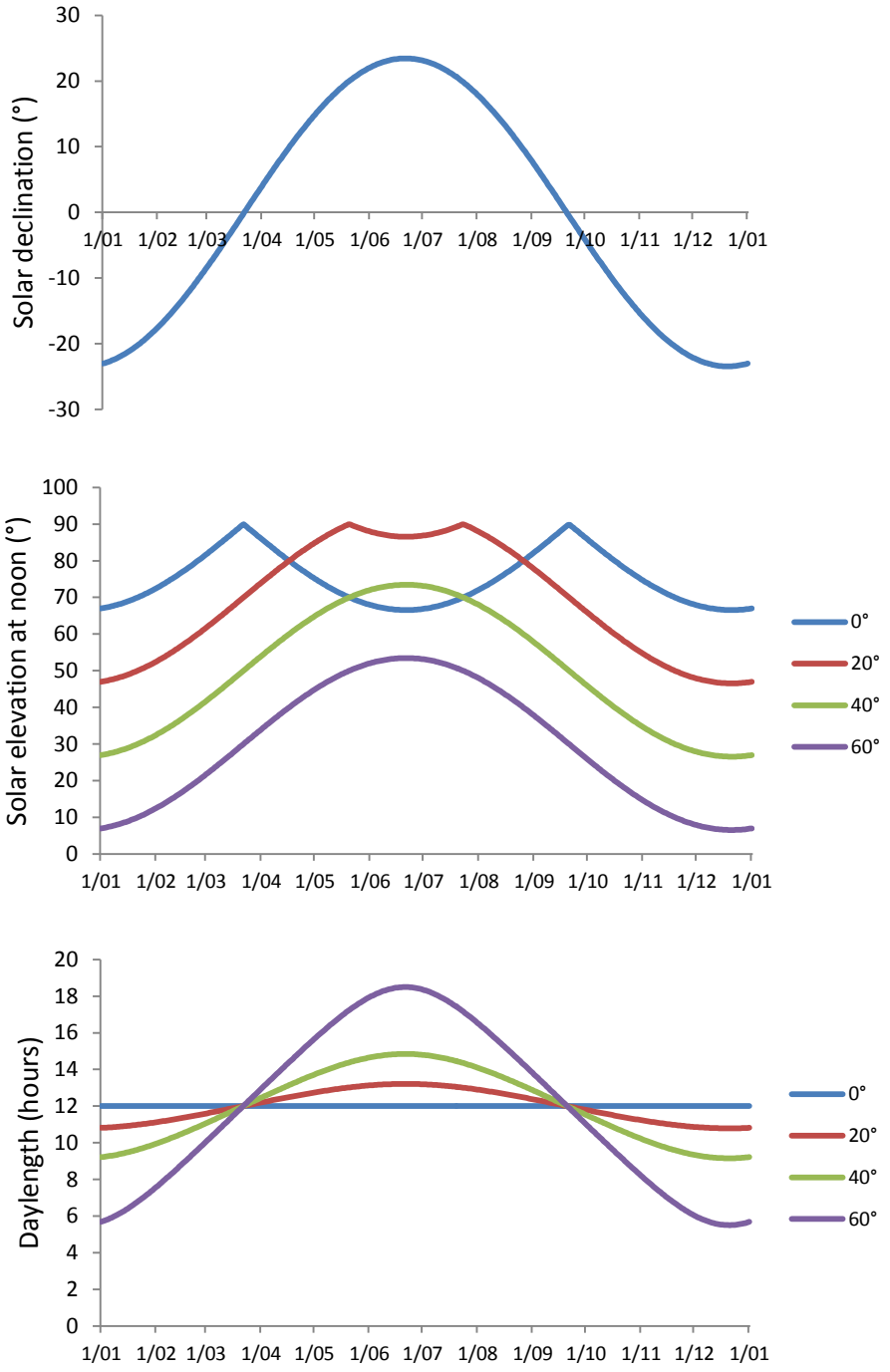

Figure 2.4: Solar declination angle, δ (°), solar elevation angle at local noon, ϕ (°), and the daylength, h_{day} (hours), as given by eqns (2.23) to (2.26). The latitude is as indicated (δ is independent of latitude). Note that in the theory δ and ϕ are prescribed in radians.

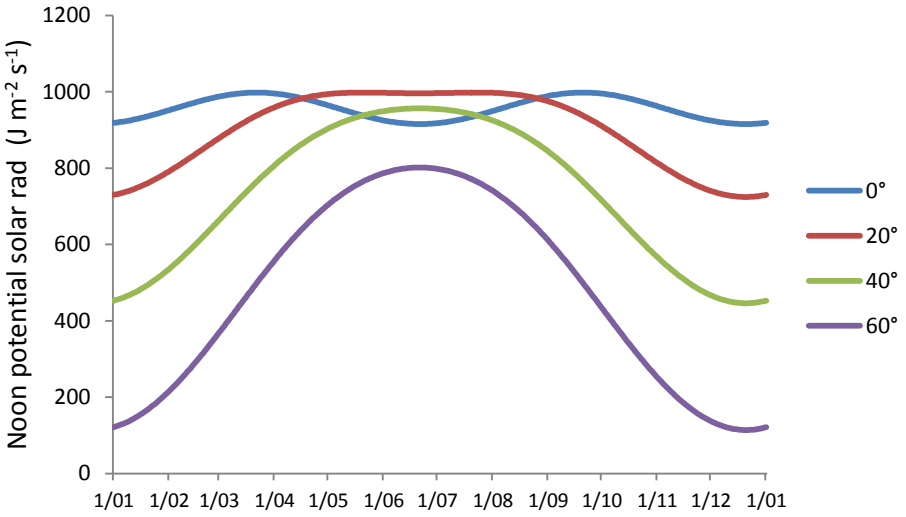

Figure 2.5: Noon potential solar radiation, $I_{p,noon}$, as given by eqn (2.30).

To calculate the potential daily solar radiation, it is assumed that the potential solar radiation throughout the day, I_p, varies sinusoidally, and can be written

$$I_p = I_{p,noon} \sin(\pi d),\ d = 0\text{–}1 \text{ over the daylight period} \tag{2.32}$$

so that the mean daily potential, or daily clear-sky, irradiance is

$$R_{S,p} = 86{,}400\, f_{day} \frac{2}{\pi} I_{p,noon} \tag{2.33}$$

where 86,400 is the number of seconds in a day. Thus,

$$R_{S,p} = 86{,}400\, f_{day} \frac{2}{\pi} \tau\gamma \sin\phi \tag{2.34}$$

This is a simple equation for the clear-sky irradiance in terms of latitude and day of year, and is illustrated in Fig. 2.6 for the latitudes used in Figs 2.4 and 2.5. The general trend for $R_{S,p}$ is similar to that for $I_{p,noon}$, although the maximum value for $R_{S,p}$ is greater as latitudes increase, whereas this is not the case for $I_{p,noon}$. This difference is due to the fact that the maximum daylength increases at higher latitudes and the total potential daily solar radiation ($R_{S,p}$) is the combination of the potential instantaneous solar radiation (I_p) and daylength.

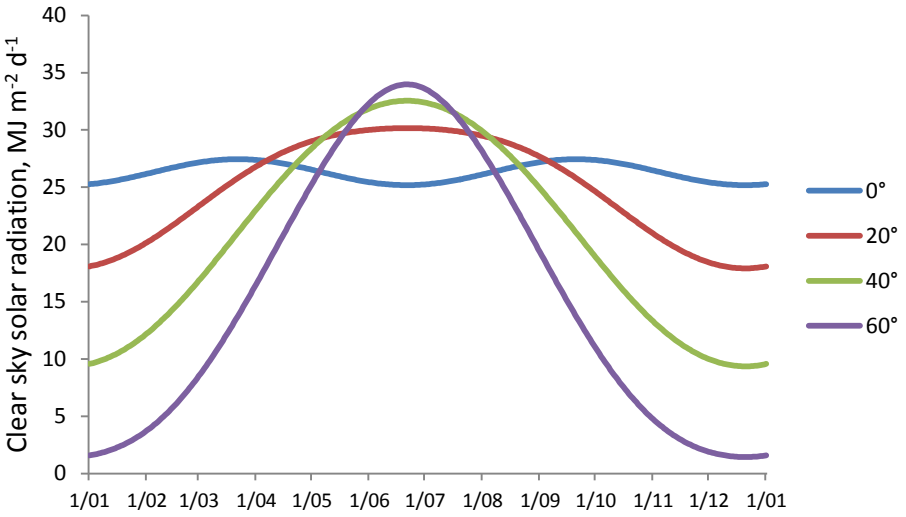

Figure 2.5: Clear-sky potential solar radiation, $R_{S,p}$ (MJ m^{-2} d^{-1}), as given by eqn (2.34) for the latitudes as indicated.

In order to test the approach, data from two sites in Australia from 1901 to 2008 are used from the SILO data set (Jeffrey, 2001). These sites are Barraba, NSW, at latitude -30.5°, and Albany, WA, at latitude -35°. Potential irradiance for each day of the year is estimated as the maximum observed for each day in the climate file. This assumes, therefore, that for each day of the year there was at least one occasion in the 108 years where the sky was clear. Figure 2.6 shows the observed and predicted clear-sky irradiance. Also shown are the mean and minimum irradiance, to illustrate the range of values that occur. There are occasional 'blips' in the data for maximum and minimum irradiance, but these may well be due to fluctuations in the accuracy of the measurement equipment. The data and model for clear-sky irradiance are virtually identical which gives confidence in the theoretical approach.

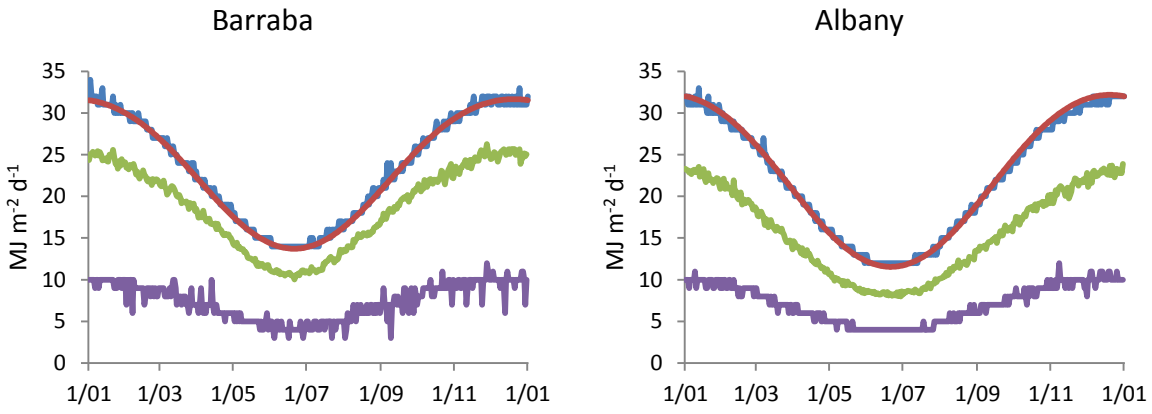

Figure 2.6: Observed maximum daily irradiance (blue) and predicted values (red) using eqn (2.34). Note that the blue lines are obscured for much of the data due to the close similarity of the values. Also shown are the mean (green) and minimum (purple) daily irradiance values.

Equation (2.34) has been tested for several other sites around Australia with similar close agreement with the data. The key parameter defining potential solar radiation is the atmospheric diffusivity, τ, which may vary for different locations, although the value 0.73 has been found to be appropriate in

many cases. This equation will be used in Chapter 5 which considers canopy transpiration, temperature and energy budget.

2.8 Net radiation

The net radiation balance, which accounts for both shortwave and longwave radiation components, is central to the treatment of canopy transpiration, temperature and energy budget. The discussions here relating to the net radiation balance at the canopy can be defined either for instantaneous (s) or daily (d) time scales. The notation uses J (W m^{-2} ≡ J m^{-2} s^{-1}) for instantaneous radiation components and R (J m^{-2} d^{-1}, although it is often expressed as MJ m^{-2} d^{-1}) for daily radiation.

The radiation balance of the canopy is shown in Fig. 2.7. Solar radiation is incident on the canopy, which is either reflected and absorbed by the canopy or transmitted through the canopy. Longwave radiation transmitted from the atmosphere is intercepted and absorbed by the canopy with a small component that is reflected (and often ignored). Longwave radiation is also emitted by the canopy as a function of its temperature. Both shortwave and longwave radiation components that are not intercepted by the canopy will be transmitted through the canopy.

The theory for the radiation balance of canopies is often presented with the assumption of full ground cover. In the present analysis, partial ground cover is considered by using eqn (2.22) for the fractional ground cover, f_g, as a function of canopy leaf area index, L.

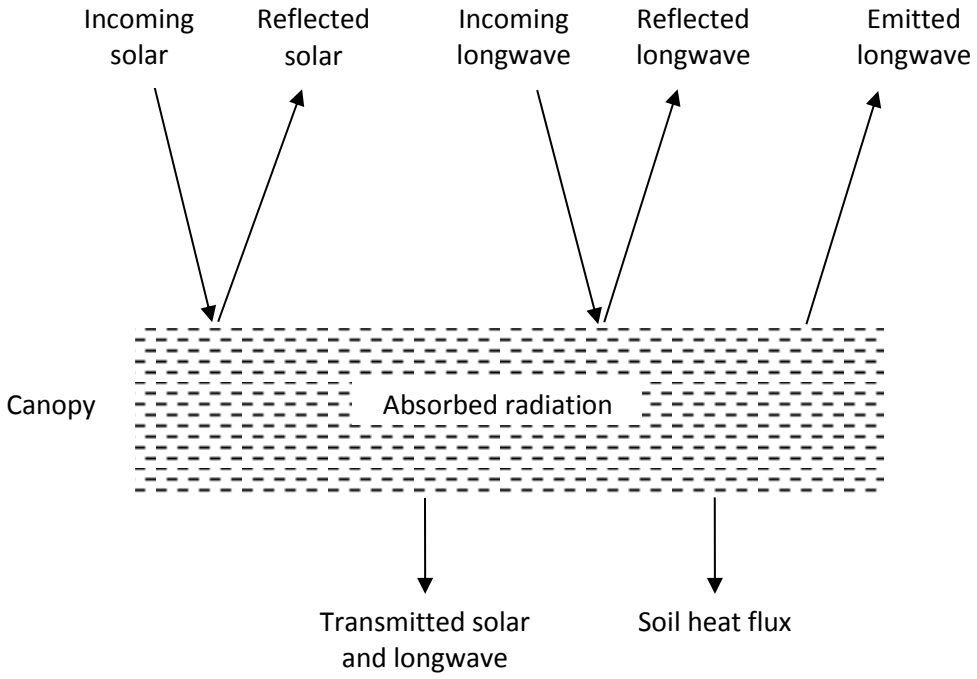

Figure 2.7: Schematic representation of the radiation balance of the canopy.

Denoting the incoming shortwave radiation component by J_S, and the absorbed, transmitted and reflected components by $J_{S,a}, J_{S,t}, J_{S,r}$ respectively, the solar radiation balance is

$$J_{S,a} = J_S - J_{S,t} - J_{S,r} \tag{2.35}$$

Longwave radiation is generally not absorbed, but emitted by the canopy. Let the incoming, reflected and transmitted components of longwave radiation be $J_{L,i}$, $J_{L,r}$, $J_{L,t}$ respectively, and

denoting the longwave component that is emitted as a function of temperature by $J_{L,e}$, the net *outgoing* longwave radiation, $J_{L,n}$, is

$$J_{L,n} = J_{L,e} - \left(J_{L,i} - J_{L,r} - J_{L,t}\right) \tag{2.36}$$

In addition to these terms for the shortwave and longwave components between the canopy and the atmosphere, there can also be a heat flux between the canopy and the soil. However, this is generally small and can be ignored. Note that although the heat flux between the canopy and soil is ignored, the radiation input to the soil from shortwave and longwave radiation that is transmitted through the canopy is included in the analysis.

The net radiation balance for the canopy is now

$$J_n = J_{S,a} - J_{L,n} \tag{2.37}$$

These components will be considered in turn.

2.8.1 Incoming shortwave radiation

In order to calculate the absorbed solar radiation, $J_{S,a}$, the transmitted and reflected components in eqn (2.35) must be derived. Applying eqns (2.21) and (2.22),

$$\begin{aligned} J_{S,t} &= J_S e^{-kL} \\ &= \left(1 - f_g\right) J_S \end{aligned} \tag{2.38}$$

Defining the reflection coefficient, or albedo, as α, the absorbed and reflected components of solar radiation are simply

$$J_{S,a} = f_g \left(1 - \alpha\right) J_S \tag{2.39}$$

$$J_{S,r} = f_g \alpha J_S \tag{2.40}$$

Note that eqns (2.38), (2.39), (2.40) sum to the total incoming solar radiation, J_S, as required. The expression for $J_{S,a}$ in eqn (2.39) will be used in the analysis for the net radiation balance for the canopy.

For daily values, the radiation components use the symbol R with the same subscripts as above and units J m^{-2} d^{-1}, or MJ m^{-2} d^{-1}. Thus, the daily absorbed solar radiation is

$$R_{S,a} = f_g \left(1 - \alpha\right) R_S \tag{2.41}$$

2.8.2 Outgoing longwave radiation

Longwave, or terrestrial radiation is the radiation emitted by a body as a function of its temperature. Incoming longwave radiation from the atmosphere depends primarily on atmospheric properties and temperature, generally increasing in response to vapour density and cloud cover. Note that in the analysis presented here, the net longwave radiation term is defined as outgoing rather than incoming. In some texts, it is defined as incoming to be consistent with incoming solar radiation. The choice to use outgoing here is because this term is generally positive.

Instantaneous longwave radiation

First consider the emitted longwave radiation which, according to the Stefan-Boltzmann equation (see section 2.3 above) is given by

$$J_{L,e} = f_g \varepsilon \sigma T_{K,c}^4 \tag{2.42}$$

where $\sigma = 5.670 \times 10^{-8}$ W m^{-2} K^{-4} is the Stefan-Boltzmann constant, $T_{K,c}$ (K) is the canopy temperature in absolute degrees, and ε is the canopy emissivity. For leaves, ε is generally in the range 0.95 to 0.99, and is taken to be 0.97 here. The factor f_g is used to account for the ground cover so that it is assumed that the longwave radiation emitted by the canopy is proportional to the canopy ground cover.

According to Kirchoff's law, the *absorptivity* coefficient for longwave radiation is equal to the emissivity, and hence the absorbed longwave radiation is

$$J_{L,a} = \varepsilon f_g J_{L,i} \tag{2.43}$$

where, again, the fractional ground cover accounts for the component of incoming longwave radiation that is actually intercepted by the canopy. Thus, the reflected longwave radiation, $J_{L,r}$, is

$$\begin{aligned} J_{L,r} &= f_g J_{L,i} - J_{L,a} \\ &= f_g \left(1-\varepsilon\right) J_{L,i} \end{aligned} \tag{2.44}$$

The transmitted longwave radiation is given by, analogous to eqn (2.38),

$$J_{L,t} = \left(1-f_g\right) J_{L,i} \tag{2.45}$$

Substituting in eqn (2.36) for the overall longwave radiation balance becomes

$$J_{L,n} = f_g \varepsilon \left(\sigma T_{K,c}^4 - J_{L,i}\right) \tag{2.46}$$

Now, in the following analysis to look at the canopy energy balance, the aim is to be able to eliminate, or calculate directly, the canopy temperature $T_{K,c}$. As will be seen, this requires eqn (2.46) to be written in terms of the air temperature and the temperature difference between the canopy and air. To do so, write

$$T_{K,c} = T_{K,a} + \Delta T \tag{2.47}$$

where $T_{K,a}$ (K) is the air temperature and

$$\begin{aligned} \Delta T &= T_{K,c} - T_{K,a} \\ &= T_c - T_a \end{aligned} \tag{2.48}$$

which can use temperatures in either K or °C. It follows that

$$T_{K,c}^4 = T_{K,a}^4 + 4T_{K,a}^3 \Delta T + 6T_{K,a}^2 \Delta T^2 + 4T_{K,a}^2 \Delta T^3 + \Delta T^4 \tag{2.49}$$

It is readily confirmed that terms of order ΔT^2 and higher are negligible, so that a good approximation is

$$\begin{aligned} T_{K,c}^4 &= T_{K,a}^4 + 4T_{K,a}^3 \Delta T \\ &= T_{K,a}^4 + 4T_{K,a}^3 \left(T_{K,c} - T_{K,a}\right) \end{aligned} \tag{2.50}$$

Equation (2.46) can now be written

$$J_{L,n} = \varepsilon f_g \left[\sigma T_{K,a}^4 - J_{L,i} + f_g c_p g_r \left(T_c - T_a\right)\right] \tag{2.51}$$

which uses the *radiative conductance*, g_r (mol m^{-2} s^{-1}), given by

$$g_r = \frac{4\varepsilon\sigma T_{K,a}^3}{c_p} \tag{2.52}$$

where $c_p = 29.3$ J mol^{-1} K^{-1} is the specific heat capacity of air, so that g_r is a function of air temperature only. The advantage of introducing the radiative conductance is that it defines longwave radiative heat loss in a way that is analogous to the sensible heat loss which will be considered in the net radiation balance for the canopy. Although this equation has temperature raised to the third power, the response is virtually linear for practical temperature conditions since this is absolute temperature, with g_r ranging from 4.6 J mol^{-1} K^{-1} at 0°C to 7.0 J mol^{-1} K^{-1} at 40°C, where $\varepsilon = 0.97$, eqn (2.5), is used.

If the incoming longwave radiation, $J_{L,i}$, is known, then eqn (2.51) can be used directly. However, in many situations it is only the incoming solar radiation that is known and so an estimation of $J_{L,i}$ is required. For full canopy ground cover and isothermal conditions, when the air and canopy are at the same temperature, which is most likely to occur (at least approximately) to systems that are freely transpiring, the net longwave radiation is termed the *isothermal net outgoing longwave radiation*, which is denoted by $J'_{L,n}$, and setting $T_{K,c} = T_{K,a}$ and $f_g = 1$ in eqn (2.51), is given by

$$J'_{L,n} = \varepsilon\left(\sigma T_{K,a}^4 - J_{L,i}\right) \tag{2.53}$$

This can be used in eqn (2.51) to eliminate $J_{L,i}$ to give

$$J_{L,n} = f_g\left[J'_{L,n} + c_p g_r\left(T_c - T_a\right)\right] \tag{2.54}$$

which defines the net outgoing longwave radiation in terms of the corresponding value for isothermal full ground cover systems, the temperature difference between the canopy and air, and the fractional ground cover.

The use of the isothermal net radiation in the study of the energy balance of the canopy, rather than assuming a fixed longwave radiation component, improves the accuracy of the analysis considerably (Thornley and France, 2007).

Daily longwave radiation

The above equations for instantaneous longwave radiation can be applied directly to daily values, so that the equations corresponding to (2.53) and (2.54) are

$$R'_{L,n} = \varepsilon\left(86{,}400\sigma T_{K,a}^4 - R_{L,i}\right) \tag{2.55}$$

and

$$R_{L,n} = f_g\left[R'_{L,n} + 86{,}400 c_p g_r\left(T_c - T_a\right)\right] \tag{2.56}$$

where the daily radiation values have units J m^{-2} d^{-1}.

2.8.3 Isothermal net radiation

An acceptable expression for the *daily* isothermal net outgoing longwave radiation, $R'_{L,n}$, is the approach used by Allen *et al.* (1998, eqn (39)), which is

$$R'_{L,n} = 86,400\sigma T_{K,a}^4 \left(0.34 - 0.14\sqrt{e_{v,a}}\right)\left(1.35\frac{R_S}{R_{S,p}} - 0.35\right) \quad (2.57)$$

T_K (K) now represents the mean daily temperature, σ is the Stefan-Boltzmann constant, where $\sigma = 5.6704 \times 10^{-8}$ J m^{-2} s^{-1}K^{-4}, $e_{v,a}$ (kPa) is vapour pressure, R_S (J m^2 d^{-1}) as defined above is daily solar radiation, and $R_{S,p}$ (J m^2 d^{-1}) is the potential, or clear-sky, solar radiation with $R_S \leq R_{S,p}$. Clear-sky solar radiation was derived in terms of the latitude and day of year in section 2.6 above. The factor 86,400 is the number of seconds per day and converts the radiation components in the Stefan-Boltzmann equation to daily values. According to Allen *et al.* (1998), the $\left(0.34 - 0.14\sqrt{e_{v,a}}\right)$ term corrects for air humidity and declines as humidity increases. The $\left(1.35\, R_S/R_{S,p} - 0.35\right)$ term incorporates the influence of cloud cover and decreases as cloud cover increases, since this will result in a reduction in R_S. The approach of eqn (2.57) is widely used – for example the SILO dataset (Jeffrey, 2001) available in Australia, which gives access to daily climate data from the late 1800s to the present day for any location in Australia, uses this approach for the calculation of the net radiation balance. Note that Allen *et al.* (1998) incorporated the daily maximum and minimum temperatures, although using a single mean daily temperature gives very similar results. Equation (2.57) can be used in eqn (2.56) to give the canopy daily net radiation balance in terms of readily measured quantities.

$R'_{L,n}$ is illustrated in Fig. 2.8 for the same two sites in Australia that were used to illustrate clear-sky solar radiation in Fig. 2.6 above. It can be seen that the minimum, mean and maximum values for $R'_{L,n}$ are relatively constant throughout the year at both these sites. Furthermore, comparing Figs 2.6 and 2.8 it is apparent that $R'_{L,n}$ is generally considerably smaller than the solar radiation component, although it is certainly not negligible. Note also that the minimum values are occasionally negative, although the values are small, which is likely to occur for cloudy conditions and means there is a net inward flux of longwave radiation. The range of values shown in Fig. 2.8 for the daily net outgoing longwave radiation is typical of most locations around the world.

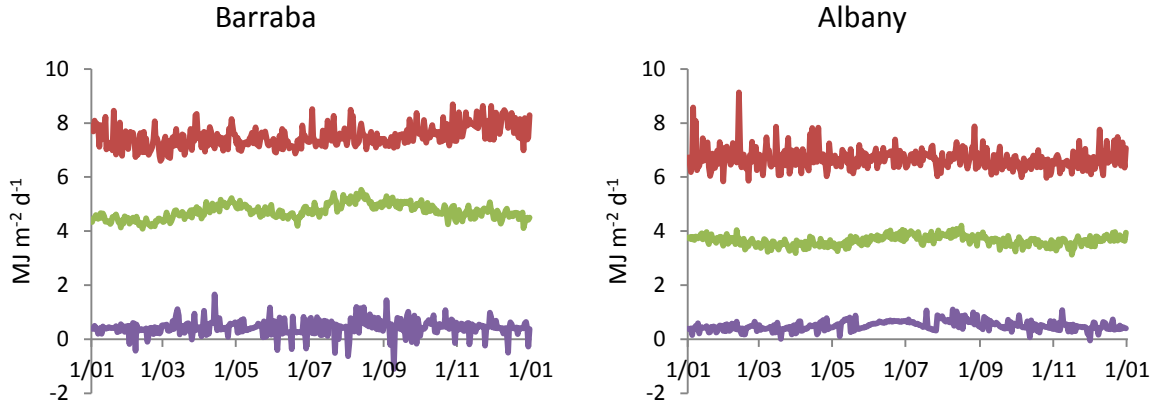

Figure 2.8: Minimum (purple), mean (green) and maximum (red) isothermal net outgoing longwave radiation as given by eqn (2.57) for Barraba (latitude -30.5°) and Albany (latitude -35°). Note that the minimum values are occasionally negative.

In the analysis for canopy transpiration, temperature and energy balance, Chapter 5, separate day and night conditions are considered. Thus, if T_{day} and T_{night} are the mean day and night temperatures, then the mean day and night isothermal net outgoing longwave radiation are given by

$$J'_{L,n,day} = \sigma T_{K,a,day}^4 \left(0.34 - 0.14\sqrt{e_{v,a}}\right)\left(1.35\frac{R_S}{R_{S,p}} - 0.35\right) \tag{2.58}$$

and

$$J'_{L,n,night} = \sigma T_{K,a,night}^4 \left(0.34 - 0.14\sqrt{e_{v,a}}\right)\left(1.35\frac{R_S}{R_{S,p}} - 0.35\right) \tag{2.59}$$

so that the total daily values are

$$R'_{L,n,day} = 86,400 f_{day} J'_{L,n,day} \tag{2.60}$$

and

$$R'_{L,n,night} = 86,400\left(1 - f_{day}\right) J'_{L,n,night} \tag{2.61}$$

with the total given by

$$R'_{L,n} = 86,400\left[f_{day} J'_{L,n,day} + \left(1 - f_{day}\right) J'_{L,n,night} \right] \tag{2.62}$$

where f_{day} is the daytime fraction as given by eqn (2.25). In practice, since T_K is almost linear over realistic temperature ranges, separating out day and night components, eqn (2.62), is virtually identical to using a single daily temperature value, eqn (2.57). However, since the analysis does use day and night temperature it is simple to apply eqn (2.62) with (2.58) and (2.59)

For studies where the instantaneous solar radiation, J_S, is used rather than the daily value, R_S, eqns (2.58) and (2.59) are not used. In this case, eqn (2.57) can be adapted for the instantaneous isothermal net outgoing longwave radiation, $J'_{L,n}$, as

$$J'_{L,n} = \sigma T_{K,a}^4 \left(0.34 - 0.14\sqrt{e_{v,a}}\right)\left[1.35 f_c\left(c\right) - 0.35\right] \tag{2.63}$$

where f_c is a function of cloud cover, c, with $c = 0, 1$ being no cloud cover and full cover respectively. It is assumed that

$$f_c\left(c\right) = 1 - 0.7c \tag{2.64}$$

According to this definition, no cloud cover, where $c = 0$, corresponds to the actual daily solar radiation being equal to the potential value, and for full cloud cover, which is $c = 1$, the actual daily value is 30% of potential. Equation (2.63) with (2.64) is used in PlantMod. From the daily values, $R'_{L,n}$, shown in Fig. 2.8, it follows that $J'_{L,n}$ will generally be lower than 100 J m^{-2} s^{-1}.

2.8.4 Net radiation balance

Using eqn (2.54) for $J_{L,n}$, the instantaneous net radiation balance for the canopy, eqn (2.37), is now

$$J_n = f_g J_{S,a} - f_g\left[J'_{L,n} + c_p g_r \left(T_c - T_a\right)\right] \tag{2.65}$$

where $J_{S,a}$ is given by eqn (2.39).

It is convenient to define the *canopy isothermal net radiation*, analogous to the canopy isothermal net outgoing *longwave* radiation, eqn (2.53), as the net incoming radiation balance for a canopy with full ground cover and with no temperature difference between the canopy and air. Using eqn (2.39) with $f_g = 1$ and setting $T_c = T_a$ in (2.65) and $f_g = 1$, this is given by

$$J'_n = (1-\alpha) J_S - J'_{L,n} \tag{2.66}$$

and hence eqn (2.65) may be written

$$J_n = f_g \left[J'_n - c_p g_r (T_c - T_a) \right] \tag{2.67}$$

where J'_n is evaluated during the daytime or nighttime from eqns (2.58) or (2.59) as appropriate. Equation (2.67) is the expression for the net radiation balance that will be used in the energy balance calculations in Chapter 5.

The corresponding total daily net radiation balance is

$$R_n = f_g \left[R'_n - c_p g_r (T_c - T_a) \right] \tag{2.68}$$

where the daily isothermal net radiation balance is

$$R'_n = (1-\alpha) R_S - R'_{L,n} \tag{2.69}$$

where $R'_{L,n}$ is evaluated from eqn (2.60), (2.61) or (2.62) as appropriate for daytime, nighttime or total daily net radiation calculations.

2.9 Final comments

This Chapter starts with the basic physics of radiation and then deals with the theory of radiation as it is required to model canopy photosynthesis and energy balance, including canopy transpiration and temperature, which are considered in the following Chapters and are the main focus of PlantMod. The distinction between shortwave and longwave radiation is crucial in the study of photosynthesis and energy dynamics. The visible component of shortwave radiation is the source of energy for photosynthesis, and is known as photosynthetic photon flux (PPF). The direct and diffuse components of PPF have been considered, and are used in the description of canopy photosynthesis. The overall canopy energy balance includes both shortwave and longwave radiation, and care must be taken to ensure that these components are described appropriately. Direct measurements of longwave radiation are often not available and methods have been discussed in this Chapter for estimating longwave radiation, and the overall canopy energy balance, in relation to incoming shortwave radiation, air temperature and relative humidity.

2.10 Variables and parameters

Table 2.1: Model variables, definitions and units. Model parameters are defined in Table 2.2. Unless stated otherwise, areas refer to ground area. Note that J (m^{-2} ground) s^{-1} ≡ W (m^{-2} ground).

Variable	Definition	Units
	Sections 2.2, 2.3: Physics of radiation	
E	Energy emitted by a body	W m^{-2}
I	Spectral emittance	W m^{-2} (m^{-1} wavelength)
T_K	Temperature	K
λ	Wavelength	m
λ_m	Peak wavelength as a function of temperature	m

Section 2.6: Canopy light interception and attenuation
s – direct solar; d – diffuse solar.

f_g	Fractional ground cover	dimensionless
$I_0, I_{0,s}, I_{0,d}$	Solar radiation incident on the canopy	J m^{-2} s^{-1}
I, I_s, I_d	Solar radiation at LAI ℓ in canopy.	J m^{-2} s^{-1}
$I_\ell, I_{\ell,s}, I_{\ell,d}$	Solar radiation incident on leaves at LAI ℓ in canopy	J (m^{-2} leaf) s^{-1}

Section 2.7: Clear-sky solar radiation and daylength

h_{day}	Daylight hours	hours
f_{day}	Daylength as a fraction of 24 hours	dimensionless
I_p	Potential clear-sky solar radiation during the day	J m^{-2} s^{-1}
$I_{p,noon}$	Potential clear-sky solar radiation at solar noon	J m^{-2} s^{-1}
J	Instantaneous Irradiance outside the earth's atmosphere parallel to the horizontal plane	J m^{-2} s^{-1}
J_{noon}	J evaluated at solar noon	J m^{-2} s^{-1}
ℓ, ℓ_s, ℓ_d	Leaf area index in canopy	m^2 leaf (m^{-2} ground)
$R_{S,p}$	Potential clear-sky daily solar radiation	J m^{-2} d^{-1}
δ	Solar declination angle	Rad
ϕ	Solar elevation angle at solar noon	rad

Section 2.8: Net radiation
e – emitted; i – incoming; r – reflected; t – transmitted; a – absorbed

f_g	Fractional ground cover	dimensionless
g_r	Radiative conductance	mol m^{-2} s^{-1}
$J_{L,e}, J_{L,i}, J_{L,r}, J_{L,t}, J_{L,a}$	Longwave radiation components for the canopy	J m^{-2} s^{-1}
$J_{L,n}$	Net outgoing longwave canopy radiation balance	J m^{-2} s^{-1}
$J'_{L,n}$	Isothermal net outgoing longwave radiation for the canopy	J m^{-2} s^{-1}
$J'_{L,n,day}, J'_{L,n,night}$	Day and night values for $J'_{L,n}$	J m^{-2} s^{-1}
J_n	Canopy net radiation balance (shortwave and longwave)	J m^{-2} s^{-1}
J'_n	Canopy isothermal net radiation balance (shortwave and longwave)	J m^{-2} s^{-1}
J_S	Incoming solar radiation	J m^{-2} s^{-1}
$J_{S,a}, J_{S,t}, J_{S,r}$	Solar radiation components for the canopy	J m^{-2} s^{-1}
L	Canopy leaf area index	m^2 leaf (m^{-2} ground)
$R_{L,n}$	Daily net outgoing longwave radiation	J m^{-2} d^{-1}
$R'_{L,n}$	Daily isothermal net outgoing longwave radiation	J m^{-2} d^{-1}
$R'_{L,n,day}, R'_{L,n,night}$	Day and night values for $R'_{L,n}$	J m^{-2} d^{-1}
R_S	Incoming daily solar radiation	J m^{-2} d^{-1}
$R_{S,a}$	Daily solar radiation absorbed by the canopy	J m^{-2} d^{-1}
T_c	Canopy temperature	°C
$T_{K,c}$	Canopy temperature	K

Table 2.2: Model parameters, definitions, units, and default values. Model variables are defined in Table 2.2. Unless stated otherwise, areas refer to ground area. Note that J (m^{-2} ground) $s^{-1} \equiv$ W (m^{-2} ground).

Parameter	Definition	Default value
	Sections 2.2, 2.3: Physics of radiation	
c	Speed of light	2.998×10^{8} m s^{-1}
h	Planck's constant	6.626×10^{-34} J s
k	Boltzmann constant	1.3807×10^{-23} J K^{-1}
ε	Emissivity	0.97 (dimensionless)
σ	Stefan-Boltzmann constant	5.670×10^{-8} J m^{-2} s^{-1} K^{-4}
	Section 2.6: Canopy light interception and attenuation	
f_s	Direct solar fraction of solar radiation incident on the canopy	0.7 (dimensionless)
k	Canopy extinction coefficient	0.5 m^2 ground (m^{-2} leaf)
	Section 2.7: Clear-sky solar radiation and daylength	
γ	Solar constant	1367 J m^{-2} s^{-1}
λ	Latitude	rad
λ_{deg}	Latitude	°
τ	Atmospheric diffusivity coefficient	0.73 (dimensionless)
	Section 2.8: Net radiation	
c	Fractional cloud cover (0-1)	Dimensionless
c_p	Specific heat capacity of air	29.3 J mol^{-1} K^{-1}
$e_{v,a}$	Atmospheric vapour pressure	1.4 kPa (60% relative humidity at 20°C)
T_a	Air temperature	20°C
$T_{K,a}$	Air temperature	293 K
α	Canopy reflection coefficient, or albedo	0.23 (dimensionless)

2.11 References

Allen RG, Pereira LS, Raes D and Smith M (1998). FAO irrigation and drainage paper no. 56: crop evapotranspiration. www.kimberly.uidaho.edu/ref-et/fao56.pdf.

Campbell GS (1977). *An introduction to environmental biophysics*. Springer-Verlag, New York, USA.

Campbell GS and Norman JM (1998). *An Introduction to environmental biophysics*, second edition. Springer, New York, USA.

Jeffrey SG, Carter JO, Moodie KB and Beswick AR (2001) Using spatial interpolation to construct a comprehensive archive of Australian climate data. *Environmental Modelling & Software* **16,** 309–330.

Johnson IR, Riha SG and Wilks DS (1995). Modelling daily net canopy photosynthesis and its adaptation to irradiance and atmospheric CO_2 concentration. *Agricultural Systems* **50,** 1-35.

Jones HG (1992). *Plants and microclimate*. Cambridge University Press, Cambridge, UK.

Monteith JL & Unsworth MH (2008). *Principles of environmental physic,* third edition. Elsevier, Oxford, UK.

Norman JM (1980). Interfacing leaf and canopy light interception models. In: *Predicting photosynthesis for ecosystem models,* (Eds JD Hesketh and JW Jones), CRC Press, Boca Raton, Fl, USA.

Norman JM (1982). Simulation of microclimates. In *Biometeorology in integrated pest management.* Academic Press, New York, USA.

Stockle CO & Campbell GS (1985). A simulation model for predicting effect of water stress on yield: an example using corn. *Advances in Irrigation,* **3,** 283-323.

Thornley JHM (2002). Instantaneous canopy photosynthesis: analytical expressions for sun and shade leaves based on exponential light decay down the canopy and an acclimatized non-rectangular hyperbola for leaf photosynthesis. *Annals of Botany,* **89,** 451-458.

Thornley JHM and France J (2007). *Mathematical models in agriculture*. CAB International, Wallingford, UK.

Thornley JHM & Johnson IR (2000). *Plant and crop modelling*. Blackburn Press, Caldwell, New Jersey, USA.

3 Leaf photosynthesis and respiration

3.1 Introduction

Photosynthesis refers to the fixation of CO_2 by plants in response to environmental conditions, particularly solar radiation, temperature and atmospheric CO_2 concentration. The aim in this component of PlantMod is to explore the response of leaf photosynthesis to environmental factors. As discussed in Chapter 2, the source of energy for photosynthesis is the photosynthetically active component of solar radiation, referred to as irradiance (PAR), or photosynthetic photon flux (PPF), which is the term used throughout PlantMod. Other environmental factors included are temperature and atmospheric CO_2 concentration. For general reviews of aspects of the effects of changes in atmospheric CO_2 on plant and crop growth, see, for example, Allen (1989) and Gifford (1992), Ziska and Bunce (2007).

When studying the carbon assimilation in plants, both gross photosynthesis and respiratory losses must be considered. Gross photosynthesis is the synthesis of carbon via the Calvin cycle, which can be summarized by the reaction:

$$6CO_2 + 6H_2O \xrightarrow{\text{light}} C_6H_{12}O_6 + 6O_2 \tag{3.1}$$

This reaction is catalysed by the enzyme ribulose bisphosphate carboxylase (RuBP carboxylase), and is referred to as the photosynthetic carbon reduction (PCR) cycle which is illustrated schematically in Fig. 3.1.

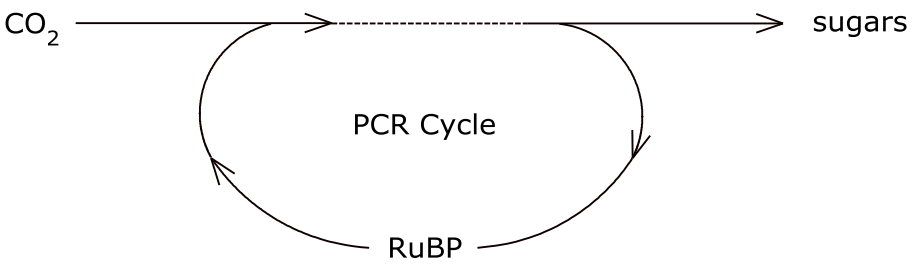

Figure 3.1. Schematic representation of the photosynthetic carbon reduction cycle.

Respiration is associated with the production of energy (ATP: adenosine triphosphate) for plant metabolic processes, and is summarized by the reaction:

$$C_6H_{12}O_6 + 6O_2 \longrightarrow 6H_2O + 6CO_2 + 36\text{ATP} \tag{3.2}$$

This is the process whereby the plant can utilize sugars to release energy in the form of ATP for plant metabolic processes, during which CO_2 is produced – hence the term 'respiration'.

The other form of respiration is photorespiration, which differs from the respiration defined by eqn (3.2), in that there is no production of energy in the form of ATP and it also requires light energy. Photorespiration is the reverse of the carbon assimilation reaction, eqn (3.1), so that RuBP oxygenation rather than carboxylation occurs.

The following definitions are widely used and can be applied to the leaf, plant or canopy:

- *net photosynthesis* is the net CO_2 exchange, taking into account CO_2 fixation and respiratory losses;
- *gross photosynthesis* is the sum of net photosynthesis and respiration, and so is the total CO_2 fixed after accounting for photorespiration losses.

Denoting gross photosynthesis, net photosynthesis, and respiration rates, by P_g, P_n, R respectively, with units μmol CO_2 m^{-2} s^{-1},

$$P_g = P_n + R \tag{3.3}$$

In practice, P_n is measured in the light, R in the dark and P_g is then estimated from those measurements. These definitions do raise the question as to whether respiration proceeds at the same rate in the light and dark, although it is almost universally assumed that they do.

Note that the term 'dark' respiration is sometimes used since the reaction in eqn (3.2) does not need light energy, although this reaction can occur in both light and dark periods. However, this can be misleading as it may be interpreted as saying this form of respiration *only* occurs during the dark which is not correct. The term 'respiration' will be used here to describe the respiration associated with the production of ATP in eqn (3.2), as distinct from photorespiration.

Before looking at the model for leaf photosynthesis, a brief background to C_3 and C_4 photosynthesis is presented.

3.1.1 C_3 and C_4 photosynthesis

The two main forms of photosynthesis are known as C_3 and C_4 because the initial products in the reactions are 3- and 4-carbon molecules respectively. In practice, the principal difference is that C_4 plants are able to suppress photorespiration and, since in C_3 plants there tends to be a shift towards photorespiration at the expense of photosynthesis at higher temperatures, C_4 plants are therefore generally able to continue to photosynthesise at higher temperatures, whereas this is not normally the case for C_3 plants. Some caution must be applied when generalizing about C_3 and C_4 plants since there are C_4 species that grow well in fairly cool conditions, such as kikuyu, and some C_4 species, such as cotton, that grow well in hot conditions.

The C_3 photosynthetic process involves the conversion of atmospheric carbon dioxide to organic carbon (sugars), as summarized in eqn (3.1) and illustrated in Fig. 3.1. The chloroplasts in the mesophyll cells capture light energy to produce ATP which is the light reaction of photosynthesis: this ATP supplies the energy for the dark reactions. Using this ATP, CO_2 is converted to sugars (dark reactions) via the photosynthetic carbon reduction cycle (PCR) or Calvin cycle, which involves the carboxylation of ribulose bisphosphate (RuBP). The first product in this process is the 3-carbon compound 3-phosphoglyceric acid (PGA): hence the term C_3. PGA is then used to produce sugars and regenerate RuBP.

The scheme for C_4 plants is illustrated in Fig. 3.2. In this case, the light reactions produce ATP as for C_3 plants. However, the initial CO_2 fixation is catalyzed by the enzyme phosphoenolpyruvate carboxylase (PEP carboxylase) to produce oxaloacetate (OAA), which is a 4-carbon molecule – hence the term C_4. Other 4-carbon molecules are rapidly produced, mainly malate and aspartate. Malate and aspartate are then transported into the chlorophyll rich bundle sheath cells. Here, decarboxylation of the C_4 acids occurs to produce C_3 compounds and CO_2, so that effectively CO_2 is being pumped into the bundle sheath cells. The C_3 compounds are transported back to the

mesophyll cells where PEP carboxylase is regenerated. The RuBP carboxylase enzyme is located in the bundle sheath cells and the normal PCR cycle (C_3 photosynthesis) takes place.

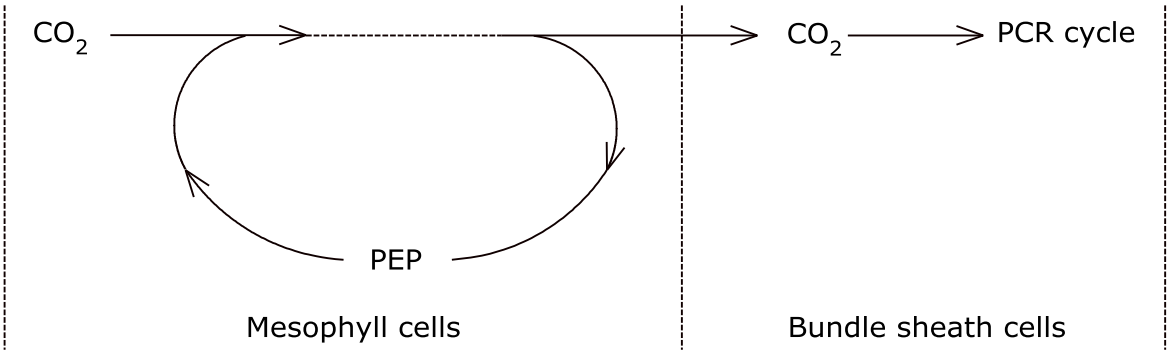

Figure 3.2. Schematic representation of the C_4 photosynthetic pathway.

Since PEP carboxylase has a higher affinity for CO_2 than RuBP carboxylase, C_4 plants have a lower substomatal CO_2 concentration than do C_3 plants (approximately 40% and 70% of the atmospheric CO_2 concentration respectively). Consequently, C_4 plants can maintain the flux of CO_2 across the stomata while the stomata are partially closed, which helps reduce water loss. Thus, water use efficiency values (kg dry matter produced per kg water used) for C_4 plants are usually lower than for C_3. Secondly, because of this high affinity for CO_2 of PEP carboxylase, the CO_2 concentration in the vicinity of RuBP carboxylase is higher in C_4 leaves (bundle sheath cells) than in C_3 leaves (mesophyll cells). This increases the activity of the RuBP carboxylase and also effectively causes the carboxylation of RuBP to out-compete oxygenation, so that photorespiration is inhibited. Furthermore, if any photorespiration does occur, the emitted CO_2 may be re-fixed as it passes the mesophyll cells, owing to the high affinity of PEP carboxylase for CO_2.

While it is common to refer to C_4 species as tropical species and C_3 as temperate species, the distinction is not always that clear. For example, the genus *Panicum* contains both C_3 and C_4 species. There are also plant species that appear to have both C_3 and C_4 characteristics.

In spite of the fact that C_4 plants have a higher water use efficiency than C_3 plants, the distribution of C_3 and C_4 species is more closely related to temperature than available water. C_4 plants are generally able to withstand higher temperatures than C_3 plants, and this seems to be the more important attribute in terms of geographical distribution.

Many pastures contain both C_3 and C_4 species, with each growing when conditions are suitable. For example, in Australian native pastures, it is common for the pasture to comprise *Danthonia* (C_3) and *Themeda* (C_4) species. Another example is in managed dairy pastures in sub-tropical regions where C_4 species such as Rhodes grass or kikuyu are grown in the summer and ryegrass, which is a C_3 species, in winter.

There is a third photosynthetic system, known as CAM plants (crassulacean acid metabolism). This system is similar to C_4 in that it utilizes PEP carboxylase. However, the PEP carboxylase is active at night and then supplies CO_2 for the carboxylation of RuBP during the day. By this means, the stomata are only open at night, which reduces water loss. During the day, the stomata close and the supply of CO_2 for the carboxylation of the RuBP comes from the C_4 acids. The CAM pathway is mainly found in succulents, and one of the few economically important CAM plants is pineapple.

Further discussions of C_3 and C_4 photosynthesis can be found in most standard plant physiology texts, and detailed mathematical discussions can be found in Thornley and Johnson (2000), von Caemmerer (2000), Thornley and France (2007).

3.2 Leaf photosynthesis

Leaf gross photosynthesis is affected primarily by light energy, temperature, atmospheric CO_2 concentration, and photosynthetic enzyme concentration, while respiration responds to temperature and enzyme concentration. The gross photosynthetic response is considered first and then respiration is addressed. At the leaf level, the treatment of respiration is quite simple, whereas the concepts of growth and maintenance respiration are incorporated at the canopy level when canopy photosynthesis is considered in the next Chapter. Applying eqn (3.3) to the leaf, the rates of leaf gross photosynthesis, net photosynthesis and respiration are related by

$$P_{g,\ell} = P_{n,\ell} + R_\ell \tag{3.4}$$

This equation is applied by describing $P_{g,\ell}$ and R_ℓ in relation to environmental conditions and then evaluating $P_{n,\ell}$.

Biochemical models of leaf photosynthesis of varying levels of complexity, such as Thornley (1976), Farquhar *et al.* (1980), Collatz *et al.* (1991), Thornley and Johnson (2000), von Caemmerer (2000) have been presented in the literature, with the model of Farquhar *et al.* (1980) being widely used. The main value of these models is in the study of the underlying biochemistry of leaf photosynthesis but, due to their complexity they are generally less suited to the study of canopy photosynthesis than simpler empirical, or semi-empirical models. As discussed in Section 1.2, the hierarchical structure of the processes in plant biology, means that the more organizational levels that are incorporated in a model, the greater the model complexity. As complexity increases, models become more challenging to parameterize, and more difficult to interpret. The model of Farquhar *et al.* (1981) is widely used in leaf photosynthesis studies, but models of crop and pasture systems generally use simpler approaches that are more readily adapted to individual species: examples are Reyenga *et al*. (1999), for crop modelling; Thornley (1998) and Johnson *et al.* (2008), for pasture models. Furthermore, in spite of their complexity, biochemical models may have limitations that need to be addressed (eg Ethier and Livingston, 2000). A final, practical limitation to using complex biochemical models of photosynthesis in the study of canopy photosynthesis is that it is difficult to define parameter sets routinely for different plant species for use in crop, pasture and ecosystem models (eg Grace and Zhang, 2006). Biochemical models of leaf photosynthesis are therefore not used in PlantMod, although discussion can be found in Thornley and Johnson (2000) and von Caemmerer (2000).

The approach adopted here is to define the underlying photosynthetic response to PPF and then to use empirical equations to define the responses of the parameters in this response curve to temperature CO_2 and leaf enzyme concentration, for both C_3 and C_4 plants. The objective is to provide robust and realistic descriptions of leaf photosynthesis that can be used to calculate canopy photosynthesis and that can easily be related to the varying photosynthetic responses of different plant species with readily interpreted parameters – for example, the light saturated rate of leaf photosynthesis will be defined with a minimum, optimum and maximum temperature.

Before proceeding, recall that the energy source for photosynthesis is the photosynthetic photon flux (PPF) with units μmol photons m^{-2} s^{-1}, which was defined in Section 2.4 in Chapter 2, while atmospheric CO_2 concentration was considered in Chapter 1. For CO_2, the true concentration has

units mol CO_2 m^{-3} while the more commonly used fractional concentration is expressed as μmol CO_2 (mol air)$^{-1}$ or parts per million (ppm). Following convention, the fractional concentration will be used here and referred to simply as *concentration*. However, it should be noted that true concentration may be more appropriate for detailed biochemical analysis, since this is the absolute amount of CO_2 per unit volume of air. Symbols and their definitions are presented in Tables 3.1, 3.2, 3.3 at the end of the Chapter.

Some model illustrations are presented, but you are encouraged to explore the behaviour of the model in the PlantMod program.

3.2.1 Light response

The rate of single leaf gross photosynthesis, $P_{\ell,g}$ μmol CO_2 (m^{-2} leaf) s^{-1}, is described as a function of PPF, I_ℓ μmol PAR (m^{-2} leaf) s^{-1}, by the widely used non-rectangular hyperbola, which can be written as

$$\theta P_{\ell,g}^2 - (\alpha I_\ell + P_m) P_{\ell,g} + \alpha I_\ell P_m = 0 \tag{3.5}$$

where the parameters are:

P_m	rate of single leaf gross photosynthesis at saturating irradiance	μmol CO_2 (m^{-2} leaf) s^{-1}
α	leaf photosynthetic efficiency	μmol CO_2 (μmol photons)$^{-1}$
θ $(0 \le \theta \le 1)$	curvature parameter	dimensionless

The non-rectangular hyperbola was discussed in detail in Chapter 1. Note that all model variables are listed in Table 3.2 and model parameters, with default values, in Table 3.3 at the end of this Chapter.

Equation (3.5) is the fundamental equation upon which the treatment of photosynthesis is built in this modelling approach. This equation is almost universally used for the leaf photosynthetic response to PPF – see for example Sands (1995), Anten *et al.* (1995), Anten (1997), Thornley and Johnson (2000), Thornley and France (2007), where numerous references can be found. It can be derived from a range of simplified biochemical schemes, including Thornley (1976), Collatz *et al.* (1991). It is also used by several authors in Boote and Loomis (1991), including Evans and Farquhar (1991), Norman and Arkebaur (1991), Gutschick (1991). One point to note is that the light-saturated rate of photosynthesis, P_m, can be reached either when photosynthesis is RuBP limited or when the rate of RuBP regeneration is limited which is due to the maximum rate of electron transport.

$P_{\ell,g}$ is given by the lower root of eqn (3.5), which is

$$P_{\ell,g} = \frac{1}{2\theta}\left[\alpha I_\ell + P_m - \left\{(\alpha I_\ell + P_m)^2 - 4\theta\alpha I_\ell P_m\right\}^{1/2}\right] \tag{3.6}$$

When $\theta = 0$ it reduces to the simpler rectangular hyperbola

$$P_{\ell,g} = \frac{\alpha I_\ell}{\alpha I_\ell + P_m} \tag{3.7}$$

and with $\theta = 1$ it becomes the Blackman limiting response given by

$$P_{\ell,g} = \begin{cases} \alpha I_\ell, & I_\ell \le P_m/\alpha; \\ P_m, & I_\ell > P_m/\alpha. \end{cases} \tag{3.8}$$

The influence of the parameters α, θ, P_m on the $P_{\ell,g}(I_\ell)$ is:

α: initial slope;

P_m: asymptote as the curve approaches saturating irradiance;

θ: curvature of the curve.

In practice, the parameters α and θ vary little and, within their physiological range, typical variation is likely to have a relatively small influence in the leaf photosynthetic response. On the other hand, P_m is much more variable and responds quite markedly to temperature, CO_2 concentration, and photosynthetic enzyme status, as well as other factors such as plant morphology. Further discussion of the parameters can be found in Cannell and Thornley (1998, Appendix), where they emphasize the fact that variation in leaf photosynthetic rates is dominated by the large variation that is observed in the light-saturated leaf photosynthetic rate, P_m. Typical values for α and θ are

α = 0.08 mol CO_2 (mol photons)$^{-1}$ and θ = 0.8. (3.9)

While P_m can vary considerably, representative values are

C_3: P_m= 20; C_4: P_m = 30 μmol CO_2 (m^{-2} leaf) s^{-1} (3.10)

Equation (3.6) is shown in Fig. 3.3 for a range of θ values as indicated.

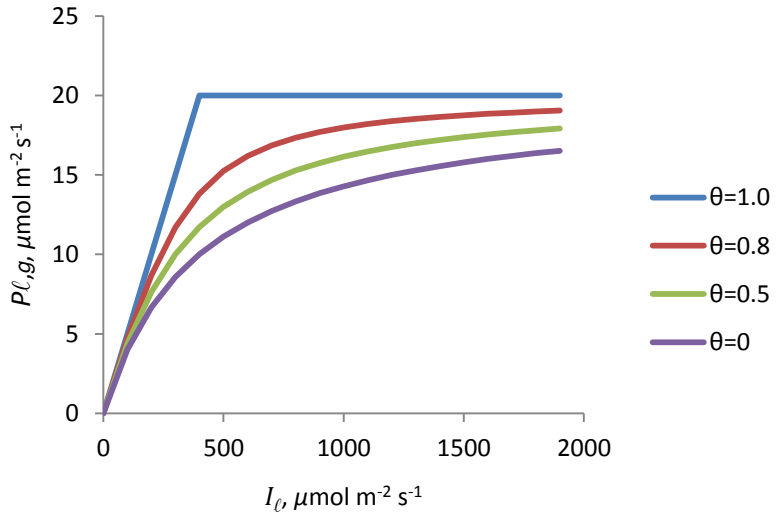

Figure 3.3: Leaf gross photosynthesis in response to PPF, eqn (3.6) for α = 0.08 mol CO_2 (mol photons)$^{-1}$, P_m = 20 μmol CO_2 (m^{-2} leaf) s^{-1}, and θ as indicated.

The non-rectangular hyperbola, eqn (3.6), is the key equation used in this analysis for the description of leaf gross photosynthesis in response to environmental factors. The equation has the direct effect of PPF – the effects of temperature, CO_2 and photosynthetic enzyme content are described through their influence on the model parameters.

3.2.2 Leaf photosynthetic response to temperature, CO_2 and enzyme concentration

The influence of temperature, CO_2 and nitrogen concentration on leaf gross photosynthesis is dominated by the effect on the parameter P_m in eqn (3.6). The leaf photosynthetic efficiency α also depends on temperature and CO_2, although to a lesser extent than P_m. There is less evidence that the curvature parameter θ responds to these factors (Sands, 1995; Cannel and Thornley 1998) and so this parameter is treated as constant. The methods used here follow, or are adapted from,

Cannel and Thornley (1998), Thornley (1998), and Thornley and France (2007). Before looking at the parameters P_m and α, the generic CO_2 function that was presented in Section 1.3.4 in Chapter 1 is discussed.

CO_2 response function, f_C

To recap the discussion in Chapter 1, the generic CO_2 response function, $f_C(C)$, is given by the non-rectangular hyperbola

$$f_C(C)=\frac{1}{2\phi}\left[\beta C+f_{C,m}-\left\{\left(\beta C+f_{C,m}\right)^2-4\phi\beta f_{C,m}C\right\}^{1/2}\right] \tag{3.11}$$

where C is atmospheric CO_2 concentration, β is the initial slope, ϕ $(0 \le \phi \le 1)$ the curvature, and $f_{C,m}$ the asymptote. Rather than prescribe β and ϕ, the function is defined to take the value unity at ambient CO_2 and λ at double ambient, so that

$$\left.\begin{aligned} f_C\left(C=C_{amb}\right)&=1\\ f_C\left(C=2C_{amb}\right)&=\lambda\end{aligned}\right\} \tag{3.12}$$

where C_{amb} is the ambient atmospheric CO_2 concentration, taken to be $C_{amb}=380\ \mu\text{mol mol}^{-1}$ (eqn 1.70). Thus, $f_C(C)$ is defined in terms of the parameters λ and $f_{C,m}$. The default values for $(\lambda, f_{C,m})$ are (1.5, 2) for C_3 and (1.1, 1.15) for C_4 so that, for C_3 plants, P_m increases by 50% at double ambient CO_2 concentration and doubles at saturating CO_2, while for C_4 plants the response is more moderated with a 10% increase at double ambient CO_2 and 15% increase at saturation. This difference in parameters for C_3 and C_4 species is due to the relatively small influence of CO_2 on C_4 plants as discussed later. The analysis for deriving β and ϕ in eqn (3.11) subject to (3.12) is discussed in Section 1.3.4 in Chapter 1.

Equation (3.11) is illustrated in Fig. 3.4 with the default parameter values for C_3 and C_4 plants. It can be seen that, with these parameter values, the variation in the CO_2 response is much lower for C_4 than for C_3.

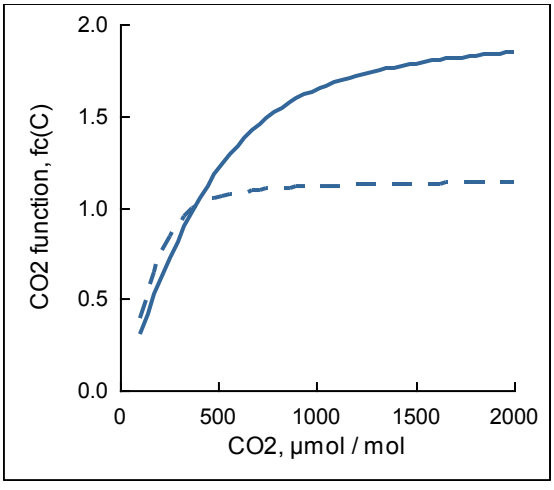

Figure 3.4: CO_2 response function, eqn (3.11), with $(\lambda, f_{C,m})$ = (1.5, 2) for C_3 plants (solid line) and (1.1, 1.15) for C_4 plants (broken line). From PlantMod.

Light saturated photosynthesis, P_m

The general characteristics of the response of P_m to temperature, CO_2, and enzyme concentration are:

- P_m increases from zero as temperature increases from some low value.
- There is an optimum temperature above which there is no further increase in P_m.
- The temperature optimum increases in response to atmospheric CO_2 concentration, C, which is due to the fall in photorespiration.
- As temperature continues to rise there is a decline in P_m for C_3 species, also due to the increase in photorespiration.
- For C_4 species, P_m may remain stable or may decline slightly as temperature increases past the optimum.
- P_m increases in response to increasing C in an asymptotic manner, approaching a maximum value at saturating C.
- P_m increases as the photosynthetic enzyme concentration increases, and it is assumed that this enzyme concentration is proportional to the nitrogen content.

In addition, enzymes can be damaged at low or high temperature extremes. At low temperatures, chilling stress can cause a phase change in the cell membranes from a liquid to solid gel, although this does not generally affect temperate species. Freezing stress can result in severe cell wall damage, although some cold-tolerant plants have a variety of mechanisms to help tolerate freezing conditions. At high temperatures, heat injury can lead to leaking cell membranes as the viscosity of the membrane lipids falls. Enzyme inactivation can also result from the denaturing of protein molecules. The effects of extreme temperature stress are not considered in PlantMod.

To incorporate the factors listed above, the light saturated leaf photosynthetic rate, P_m, is defined by

$$P_m = P_{m,ref} f_C(C) f_{Pm,TC}(T,C) f_{Pm,fp}(f_p) \tag{3.13}$$

where $f_C(C)$ is the CO_2 response function discussed in the previous section, $f_{Pm,TC}(T,C)$ is a combined response to temperature and CO_2, $f_{Pm,fp}$ is the response to plant enzyme, or protein, concentration f_p mol protein C (mol leaf C)$^{-1}$, and $P_{m,ref}$ is a reference value for P_m, and is the value of P_m at a reference temperature, ambient CO_2 concentration, C_{amb}, and reference enzyme concentration, as discussed below.

The function $f_{Pm,TC}(T,C)$ is constrained by

$$f_{Pm,TC}(T = T_{ref}, C = C_{amb}) = 1 \tag{3.14}$$

$$f_{Pm,fp}(f_p = f_{p,ref}) = 1 \tag{3.15}$$

The default values for $P_{m,ref}$ are

C_3: $P_{m,ref}$ = 20; C_4: $P_{m,ref}$ = 30 μmol CO_2 (m^{-2} leaf) s^{-1} (3.16)

The enzyme response function is the same for both C_3 and C_4 species and is defined simply as a ramp function, so that

$$f_{Pm,fp}\left(f_p\right)=\begin{cases} f_p/f_{p,ref}, & f_p \le f_{p,ref} \\ f_{p,mx}/f_{p,ref}, & f_p > f_{p,mx} \end{cases} \tag{3.17}$$

According to this function, $f_{Pm,fp}$ increases linearly as the enzyme concentration increases to the maximum value, above which there is no further increase in the rate of photosynthesis in response to the enzyme concentration. The default parameter values are

$$\begin{aligned} &C_3: \quad f_{p,ref}=0.25; \quad f_{p,mx}=0.3; \\ &C_4: \quad f_{p,ref}=0.2 \qquad f_{p,mx}=0.25; \end{aligned} \tag{3.18}$$

with units mol protein C (mol leaf C)$^{-1}$. The lower value for C_4 plants reflects the fact that these species generally have lower nitrogen contents – this will be explored theoretically later. This simple function is illustrated in Fig. 3.5.

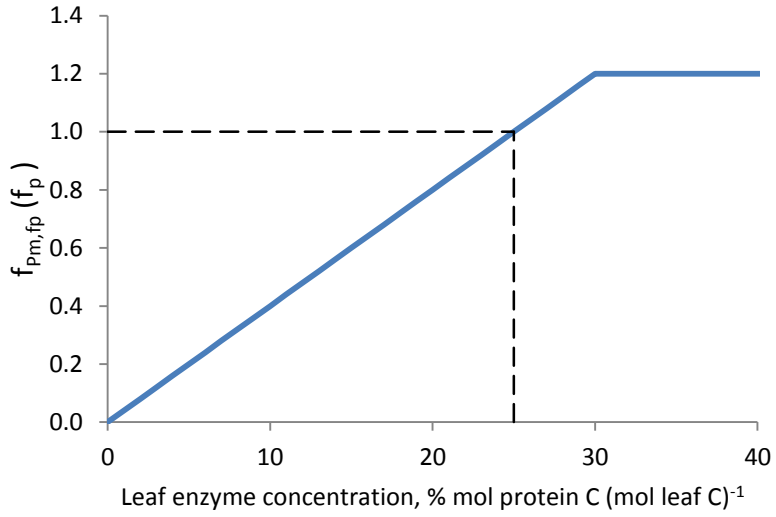

Figure 3.5: Enzyme function, $f_{Pm,fp}\left(f_p\right)$, eqn (3.17), with the default parameter values for C_3 plants as given by eqn (3.18). The function takes the value unity at $f_{p,ref}$.

Various options are available for describing the temperature response, and this was discussed in some detail in Section 1.3.5 in Chapter 1. The approach used here, following Cannel and Thornley (1998) is to define the combined temperature and CO_2 response as

$$f_{Pm,TC}\left(T,C\right)=\left(\frac{T-T_{mn}}{T_{ref}-T_{mn}}\right)^q\left(\frac{(1+q)T_{opt}-T_{mn}-qT}{(1+q)T_{opt}-T_{mn}-qT_{ref}}\right) \tag{3.19}$$

where T_{mn} is the minimum temperature, with

$$f_{Pm,TC}\left(T_{mn}\right)=0 \tag{3.20}$$

$q \ge 1$ is a curvature parameter, and T_{ref} is a reference temperature where

$$f_{Pm,TC}\left(T_{ref}\right)=1 \tag{3.21}$$

T_{opt} is the optimum temperature and is related to C according to

$$T_{opt,Pm}=T_{opt,Pm,amb}+\gamma_{Pm}\left[f_C\left(C\right)-1\right] \tag{3.22}$$

where $f_C(C)$ is once again defined by the CO_2 function, eqns (3.11), (3.12). The default value

$$\gamma_{Pm} = 10\,^{\circ}\mathrm{C} \tag{3.23}$$

is used. Note that there is a maximum temperature at

$$T_{mx} = \frac{(1+q)T_{opt} - T_{mn}}{q} \tag{3.24}$$

The constraint

$$f_{PmTC}(T,C) = 0\text{, if } T < T_{mn} \text{ or } T > T_{mx} \tag{3.25}$$

is applied to ensure the function is never negative. The default parameter values are listed in Table 3.3. Also, the optimum temperature is constrained not to fall below the reference temperature, so that

$$T_{opt} \geq T_{ref} \tag{3.26}$$

This constraint is required to ensure sensible behaviour of the temperature functions.

Equation (3.19), is illustrated in Fig. 3.6 at ambient CO_2 for a range of q values, and it can be seen that it is a versatile, flexible function for describing the temperature response.

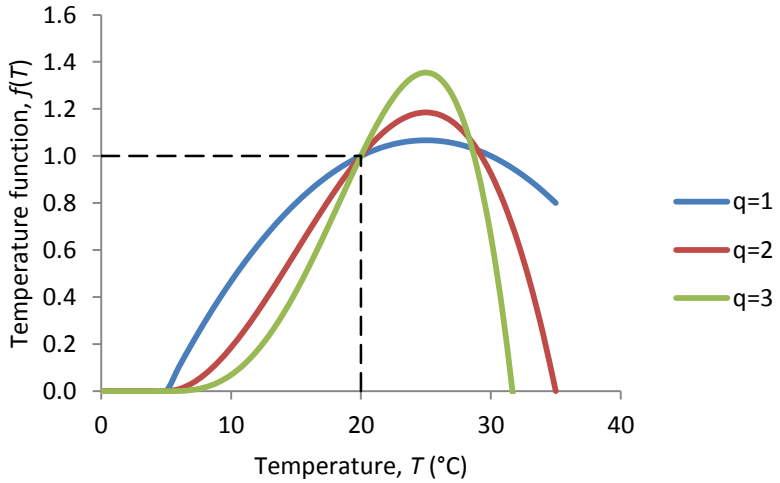

Figure 3.6. Temperature function, $f_{Pm,TC}(T)$ eqn (3.19), at ambient CO_2. Parameters are: $T_{ref} = 20$°C, $T_{mn} = 5$°C, $T_{opt} = 25$°C, q as indicated.
Note that $f_{Pm,TC}(T = T_{ref}) = 1$.

C_3 and C_4 species are treated in the same way, with the exception that for C_4 species the constraint

$$C_4\text{: } f_{Pm,TC}(C,T) = f_{Pm,TC}(C,T_{opt,Pm}), \quad \text{for } T > T_{opt,Pm} \tag{3.27}$$

applies, so that the temperature response does not fall when temperatures exceed the optimum. In practice, photosynthesis may decline at high temperatures due either to water stress or enzyme damage. However, the analysis here aims to capture only the decline due to a shift towards photorespiration and, since this is assumed to be eliminated in C_4 plants, the constraint in eqn (3.27) is reasonable. Note that although P_m may not decline at high temperatures, there can be a fall in net photosynthesis due to increases in respiration rate.

Equations (3.19)-(3.27) completely define the function $f_{Pm,TC}$ for C_3 and C_4 species. The default parameter values are given in Table 3.3. P_m is illustrated in Fig. 3.7 for both C_3 and C_4 species with the parameter values from Table 3.3.

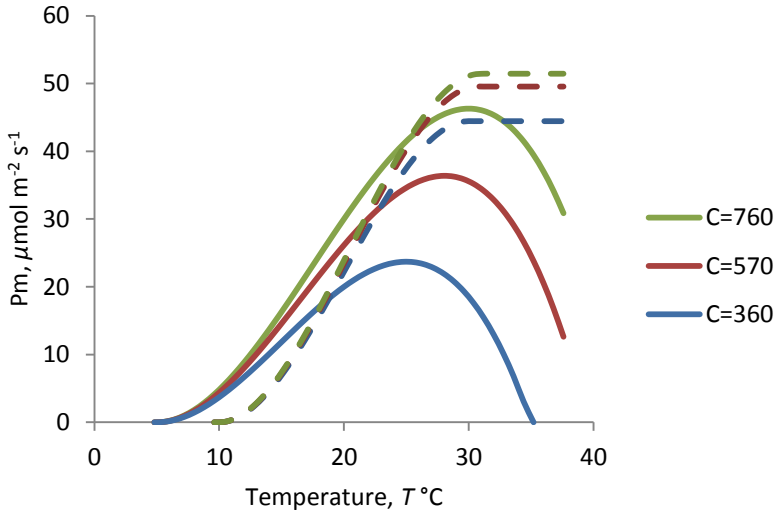

Figure 3.7. Light saturated leaf gross photosynthetic rate, P_m eqn (3.13), in response to temperature for CO_2 concentrations of 380 (current ambient), 570 (50% increase) and 760 (doubling) μmol mol^{-1} as indicated, with the parameters in Table 3.3. The solid lines are for C_3 plants and the broken lines for C_4 plants.

Leaf photosynthetic efficiency, α

The general characteristics of the photosynthetic efficiency, α, to temperature and CO_2 are:

- α increases with atmospheric CO_2 concentration, C, although this is relatively modest for C_4 plants.
- In C_3 plants, at ambient CO_2 concentration α declines as temperature increases above 15°C due to a shift from carboxylation (carbon fixation) to oxygenation (photorespiration) in the photosynthesis reactions. The critical temperature above which α starts to decline increases as the CO_2 concentration rises.
- The impact of increasing temperature on α is reduced as CO_2 concentration increases.
- a increases in response to protein concentration.

In order to capture these responses, the photosynthetic efficiency α is given by

$$\begin{aligned} &C_3: \quad \alpha = \alpha_{amb,15} f_C(C) f_{\alpha,fp}(f_p) f_{\alpha,T}(T) \\ &C_4: \quad \alpha = \alpha_{amb,15} f_C(C) f_{\alpha,fp}(f_p) \end{aligned} \tag{3.28}$$

where $\alpha_{amb,15}$, mol CO_2 (mol photons)$^{-1}$, is the value of α at the ambient CO_2 concentration C_{amb}, 15°C, and reference protein concentration, with default value

$$\alpha_{amb,15} = 80 \text{ mmol } CO_2 \ (\text{mol photons})^{-1} \tag{3.29}$$

The function $f_C(C)$ captures the direct influence of C on α, and is given by the CO_2 function that was discussed in Chapter 1, Section 1.3.5 and used above, eqns (3.11) and (3.12).

The function $f_{\alpha,T}(T)$ in eqn (3.28) defines the temperature response on α, as given by

$$f_{\alpha,TC}(T,C)=\begin{cases}\left\{1-\dfrac{\sigma_\alpha}{f_C(C)}\left(T-T_{opt,\alpha}\right)\right\}, & T\geq T_{opt,\alpha}\\ 1, & T<T_{opt,\alpha}\end{cases} \tag{3.30}$$

where σ_α is a constant and

$$T_{opt,\alpha}=15+6\left[f_C(C)-1\right] \tag{3.31}$$

where again the CO_2 response function, eqns (3.11) and (3.12) is used. As a precaution, the constraint

$$f_{\alpha,T}(T)\geq 0, \quad \text{for all } T \tag{3.32}$$

is imposed, although it would require fairly unrealistic parameter values to cause $f_{\alpha,T}(T)$ to have negative values.

Default parameter value in eqn (3.30) is

$$\sigma_\alpha=0.02\,^\circ\text{C}^{-1} \tag{3.33}$$

In PlantMod, σ_α is restricted to

$$\sigma_\alpha\leq 0.03^\circ\text{C}^{-1} \tag{3.34}$$

to ensure realistic values for α.

The coefficients in eqn (3.31) are fixed since the value 15 is widely used and the value 6 is unlikely to vary significantly and the model is relatively insensitive to changes in this value. According to eqn (3.31) $T_{opt,\alpha}$ increases from its ambient value of 15°C by 3°C for a doubling of CO_2 from ambient.

The protein response function is defined as a simple ramp function (Peri *et al.*, 2005), taken to be

$$f_{\alpha,fp}(f_p)=\begin{cases}0.5+0.5\,f_p/f_{p,ref}, & f_p\leq f_{p,ref}\\ 1, & f_p>f_{p,ref}\end{cases} \tag{3.35}$$

This equation will not be valid for very low f_p, but, for that situation, photosynthesis will be primarily restricted by the influence on P_m

With these equations, the photosynthetic efficiency α increases with increasing C for both C_3 and C_4 species, but for C_3 plants there is also a decline for temperatures above 15 °C. The increase in α in response to C reflects the greater availability of CO_2, while the decline in response to temperature for C_3 species indicates a shift towards photorespiration as temperature increases, while this shift is reduced at increasing C. The lack of temperature response for C_4 species is due to the lack of photorespiration in those plants. Furthermore, the CO_2 response for C_4 plants is small, again due to the lack of photorespiration, as reflected by the parameters in $f_C(C)$, eqns (3.11) and (3.12). The default parameter values are summarised in Table 3.3, and the response of α to temperature at three CO_2 concentrations is illustrated in Fig. 3.8 for both C_3 and C_4 species.

The increase in α in response to C and the decline as T increases for C_3 plants is consistent with observations (eg Long and Drake, 1991), and the modest response of C_4 plants is due to their lack of photorespiration (eg Ehleringer and Björkman, 1977).

These equations for α are simple in structure and therefore easy to program, while capturing the key features of the response of α to CO_2 concentration and temperature. It should be noted that the

coefficient σ_α in eqn (3.30) is also taken to be dependent on C by Cannell & Thornley (1998), although this influence was found to be quite negligible during the development of PlantMod, with the influence of C being dominated by the $f_C(C)$ function in eqn (3.28).

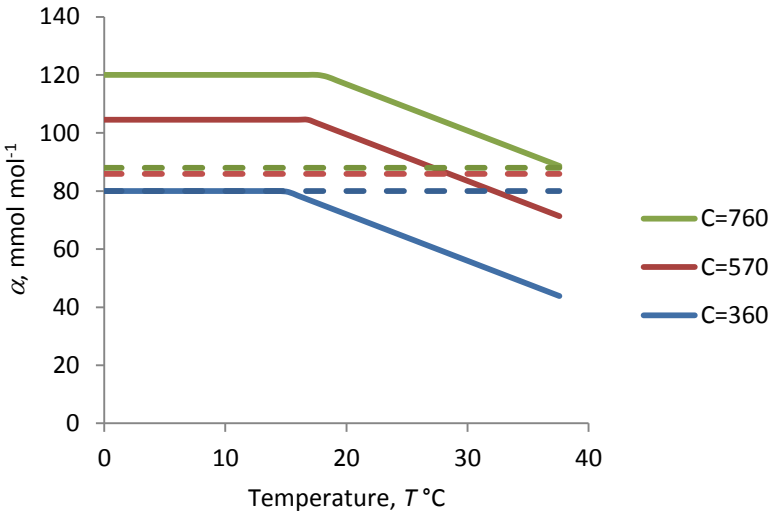

Figure 3.8: Leaf photosynthetic efficiency, α, as a function of temperature for CO_2 concentrations of 380 (current ambient), 570 (50% increase) and 760 (doubling) μmol mol^{-1} as indicated. The solid lines are for C_3 plants and the broken lines for C_4 plants.

3.3 Leaf respiration

The approach for leaf respiration is fairly simple, with a more complete treatment given for canopy photosynthesis. It is assumed that the rate of leaf respiration is

$$R_\ell = R_{\ell,ref} f_{R\ell,T}(T) \frac{f_p}{f_{p,ref}} \tag{3.36}$$

where $R_{\ell,ref}$ is the leaf respiration rate at the reference temperature and enzyme concentration, the function $f_{R\ell,T}(T)$ defines the temperature response for respiration, and f_p, $f_{p,ref}$ are the leaf enzyme concentration and reference concentration respectively, as defined earlier. According to this definition, respiration is proportional to the enzyme concentration. The default value for $R_{\ell,ref}$ is taken to be

$$R_{\ell,ref} = 2\ \mu\text{mol CO}_2\ (\text{m}^{-2}\ \text{leaf})\ \text{s}^{-1} \tag{3.37}$$

Respiration in leaves tends to continue to increase with increasing temperature, although if photosynthesis is severely restricted then respiration may decline due to limited substrate. The approach here is to use the simple Q_{10} approach, which was discussed in Section 1.3.5 in Chapter 1, and is given by

$$f_{R\ell,T}(T) = Q_{10}^{(T-T_{ref})/10} \tag{3.38}$$

where Q_{10} is a dimensionless parameter and T_{ref} is the reference temperature with

$$f_{R\ell,T}(T = T_{ref}) = 1 \tag{3.39}$$

For any 10°C increase in temperature, the function increases by a factor of Q_{10}, that is

$$\frac{f_{R\ell,T}(T+10)}{f_{R\ell,T}(T)} = Q_{10} \tag{3.40}$$

The default value used here is

$$Q_{10} = 1.5 \tag{3.41}$$

which corresponds to a 50% increase in respiration for every 10°C increase in temperature.

The more complex Arrhenius equation is sometimes used to describe this type of temperature response. However, as discussed in Section 1.3.5 in Chapter 1, the two approaches have virtually identical behaviour, and there is little theoretical justification for using the Arrhenius equation to describe the sequence of reactions involved in respiration. The Q_{10} approach is preferred since it is much easier to parameterize.

3.4 Illustrations

The equations discussed above give a complete description of the rate of single leaf gross photosynthesis and respiration in response to environmental conditions as well as leaf photosynthetic enzyme concentration. The behaviour of the individual parameters in the leaf photosynthetic response function – that is the light-saturated rate of leaf gross photosynthesis, P_m, and the leaf photosynthetic efficiency, α – can be explored in PlantMod, as well as the rates of leaf gross and net photosynthesis and leaf respiration.

The rates of single leaf gross, net photosynthesis, and respiration are shown as functions of I_ℓ (the PPF incident on the leaves) and T in Fig. 3.9 for the PlantMod default environmental conditions, and the default C_3 and C_4 species parameters (see Tables 3.1 and 3.3). These graphs have been produced by copying directly from PlantMod. These figures display the expected characteristics for C_3 and C_4 species although varying the physiological and environmental parameters will generate a range of responses.

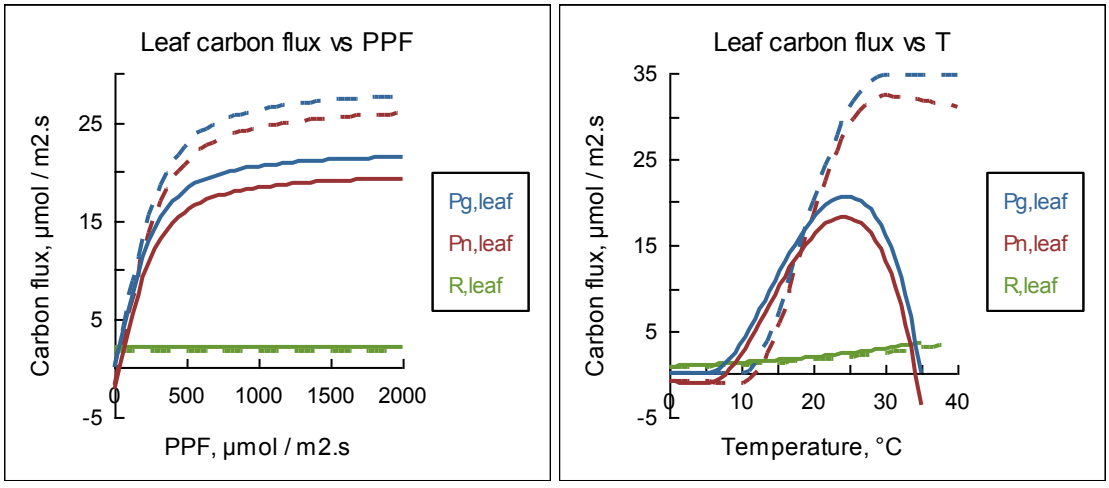

Figure 3.9: Rates of single leaf gross photosynthesis (Pg,leaf), net photosynthesis (Pn,leaf), and respiration (R,leaf) as functions of PPF (left), and temperature (right). The solid lines are C_3 and broken lines are C_4. Environmental and physiological parameters are the PlantMod defaults as given in Tables 3.1, 3.3.
Note the different scales on the y-axes. From PlantMod.

The influence of CO_2 on the rate of leaf net photosynthesis, $P_{\ell,n}$, is shown in Fig. 3.10, again for the default C_3 and C_4 parameter sets. In these illustrations, $P_{\ell,n}$ is presented for ambient CO_2 and a 50% increase in CO_2 concentration. Some points to note are the greater response to CO_2 for C_3 than C_4, and the increase in temperature optimum for the C_3 graph of $P_{\ell,n}$ as a function of T.

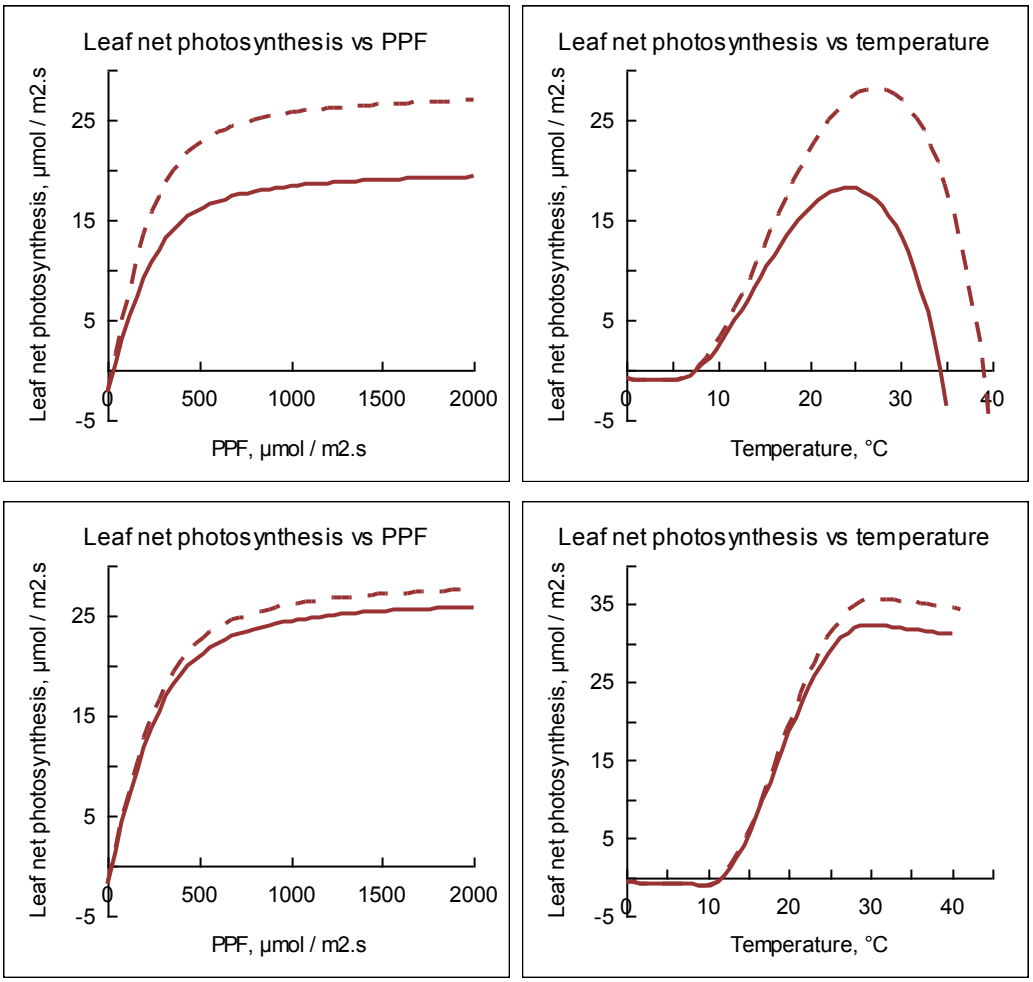

Figure 3.10: The rate of single leaf net photosynthesis as a function of PPF (left) and temperature (right) for the default C_3 plants (top) and C_4 plants (bottom). The solid lines are ambient CO_2, 380 μmol mol^{-1}, and the broken lines are for a 50% increase in CO_2, 570 μmol mol^{-1}. Note the different scale on the y-axis for the C_4 temperature response. From PlantMod.

The illustrations shown here are typical of experimental observations, although it must be emphasised that the values can vary substantially between different species and growing conditions. The parameters in PlantMod are simple to adjust to capture the general characteristics of most photosynthetic responses.

3.5 Final comments

The model of leaf photosynthesis described here incorporates the response to light (PPF), temperature, CO_2 and leaf photosynthetic enzyme content. A simple description of respiration is also presented although the canopy photosynthesis model in the next Chapter includes a more thorough treatment of respiration. The leaf photosynthesis model is designed to be simple to use, with easily defined parameters that have clear physiological interpretations. For example, the temperature response for the light-saturated rate of leaf gross photosynthesis (P_m) is defined in

terms of the minimum, optimum and maximum temperatures, along with a single curvature coefficient.

The model is ideally suited for analysis of carbon exchange in leaves and for incorporation in canopy photosynthesis models: canopy photosynthesis is considered in the next Chapter. Although more complex models of leaf photosynthesis are often used, the objective here has been to describe leaf photosynthesis at a level that is appropriate for practical application in canopy photosynthesis models, as easily defined and interpreted parameters, and is based at a similar level of physiological detail as the description of respiration which is considered in the next Chapter.

3.6 Variables and parameters

Table 3.1: Environmental variables.
These values are used in illustrations unless stated otherwise.

Variable	Definition	Units
C, C_{amb}	Actual and current ambient atmospheric CO_2 concentration	380 μ mol CO_2 (mol air) $^{-1}$
I_ℓ	Photosynthetic photon flux (PPF) incident on the leaf.	750 μmol photons m^{-2} s^{-1}
T	Temperature	22℃

Table 3.2: Model variables, definitions, and units.
PPF is photosynthetic photon flux, μmol m^{-2} s^{-1}. Environmental variables and model parameters are defined in Tables 3.1 and 3.3 respectively.

Variable	Definition	Units
$P_{\ell,g}$	Leaf rate of gross photosynthesis	μmol CO_2 (m^{-2} leaf) s^{-1}.
$P_{\ell,n}$	Leaf rate of net photosynthesis	μmol CO_2 (m^{-2} leaf) s^{-1}.
P_m	$P_{\ell,g}$ at saturating PPF	μmol CO_2 (m^{-2} leaf) s^{-1}.
R_ℓ	Leaf respiration rate	μmol CO_2 (m^{-2} leaf) s^{-1}.
$T_{opt,Pm}(C)$	Optimum temperature for P_m as a function of C	°C
$T_{opt,\alpha}(C)$	Temperature at which α starts to fall	°C
α	Leaf photosynthetic efficiency	mol CO_2 (mol photons)$^{-1}$

Table 3.3: Model parameters, definitions, units, and default values.
Environmental parameters and model variables are defined in Tables 3.1 and 3.2 respectively.

Parameter	Definition	Default value
$f_{C,m}$	$P_m/P_{m,ref}$ at T_{ref}, $f_{p,ref}$, saturating C	C_3: 2.0; C_4: 1.15
$P_{m,ref}$	P_m at C_{amb}, T_{ref}, $f_{p,ref}$	C_3: 20; C_4: 30 μmol CO_2 (m^{-2} leaf) s^{-1}
$f_{p,ref}$	Reference f_p value for leaves	C_3: 0.20; C_4: 0.15 mol protein C (mol leaf C)$^{-1}$
$f_{p,mx}$	Maximum f_p value for $P_{\ell,g}$	C_3: 0.30; C_4: 0.25 mol protein C (mol leaf C)$^{-1}$
q	Curvature parameter for $P_m(T)$	2
$R_{\ell,ref}$	R_ℓ at C_{amb}, T_{ref}, $f_{p,ref}$	C_3: 2; C_4: 1.6 μmol CO_2 (m^{-2} leaf) s^{-1}
T_{mn}	Minimum temperature for P_m	C_3: 5 °C; C_4: 10 °C

$T_{opt,Pm,amb}$	Optimum temperature for P_m at C_{amb}	C_3: 20 °C; C_4: 25 °C
T_{ref}	Reference temperature for P_m and R_ℓ	C_3: 20 °C; C_4: 25 °C
$\alpha_{amb,15}$	α at C_{amb} and 15 °C	80 mmol CO_2 (mol photons)$^{-1}$
γ_α	$T_{opt,\alpha}(C)$ parameter	6 °C
γ_{Pm}	$T_{opt,Pm}$ parameter	10 °C
θ	$P_{\ell,g}$ curvature parameter	0.8
λ	$P_m/P_{m,ref}$ at T_{ref}, $f_{p,ref}$, $2 \times C_{amb}$	C_3: 1.5; C_4: 1.1
σ_α	Temperature parameter for the optimum temperature for α	0.02 °C^{-1}

3.7 References

Allen LH Jr (1989). Plant responses to rising carbon dioxide and potential interaction with air pollutants. *Journal of Environmental Quality*, **19)1),** 15-34.

Anten NPR, Schieving F & Werger MJA (1995). Patterns of light and nitrogen distribution in relation to whole canopy carbon gain in C_3 and C_4 mono- and dicotyledonous species. *Oecologia*, **101,** 504-513.

Anten NPR (1997). Modelling canopy photosynthesis using parameters determined from simple non-destructive measurements. *Ecological Research,* **12,** 77-88.

Boote KJ & Loomis RS (1991). *Modelling crop photosynthesis – from biochemistry to canopy*. CSSA Special Publication No 19, Madison.

Boote KJ & Loomis RS (1991). The prediction of canopy assimilation. In: *Modelling crop photosynthesis – from biochemistry to canopy*, *Chapter 7*. Eds: KJ Boote & RS Loomis. CSSA Special Publication No 19, Madison.

Cannell MGR & Thornley JHM (1998). Temperature and CO2 responses of leaf and canopy photosynthesis: a clarification using the non-rectangular hyperbola model of photosynthesis. *Annals of Botany,* **82,** 883-892.

Collatz CJ, Ball JT, Grivet C & Berry JA (1991). Physiological and environmental regulation of stomatal conductance, photosynthesis, and transpiration: a model that includes a laminar boundary layer. *Agricultural and Forest Meteorology,* **54,** 107-136.

Ehleringer JR & Björkman (1977). Quantum yields for CO_2 uptake in $C_3$and C_4 plants: dependence on temperature, C_2 and O_2 concentration. *Plant Physiology,* **59,** 86-90.

Ethier GJ & Livingston NJ (2000). On the need to incorporate sensitivity to CO_2 transfer conductance into the Farquhar- von Caemmerer – Berry leaf photosynthesis model.

Evans JR & Farquhar GD (1991). Modelling canopy photosynthesis from the biochemistry of the C_3 chloroplast. In: *Modelling crop photosynthesis – from biochemistry to canopy*, *Chapter 1*. Eds: KJ Boote & RS Loomis. CSSA Special Publication No 19, Madison.

Farquhar GD, von Caemmerer S & Berry JA (1980). A biochemical model of photosynthetic CO2 assimilation in leaves of C3 species. *Planta,* **149,** 78-90.

Gifford RM (1992). Interaction of carbon dioxide with growth limiting environmental factors in vegetation productivity: implications for the global carbon cycle. *Advances in Bioclimatolgy,* **1,** 24-58.

Grace J & Zhang R (2006). Predicting the effect of climate change on global plant productivity and the carbon cycle. In: *Plant growth and climate change*. Eds JIL Morison & MD Morecroft, Blackwell Publishing, Oxford, UK

Gutschick VP (1991). Modelling photosynthesis and water use efficiency of canopies as affected by leaf and canopy traits. In: *Modelling crop photosynthesis – from biochemistry to canopy*, *Chapter 4*. Eds: KJ Boote & RS Loomis. CSSA Special Publication No 19, Madison.

Johnson IR, Chapman DF, Snow VO, Eckard RJ, Parsons AJ, Lambert MG, Cullen BR (2008). DairyMod and EcoMod: biophysical pasture-simulation models for Australia and New Zealand. *Australian Journal of Experimental Agriculture,* **48,** 421-631.

Long SP and Drake PG (1991). Effect of the long-term elevation of CO_2 concentration in the filed on the quantum yield of photosynthesis of the C_3 sedge, *Scirpus olneyi. Plant Physiology*, **96,** 221-226.

Norman JM & Arkebauer TJ (1991). Predicting canopy photosynthesis and light use efficiency from leaf characteristics. In: *Modelling crop photosynthesis – from biochemistry to canopy*, *Chapter 7*. Eds: KJ Boote & RS Loomis. CSSA Special Publication No 19, Madison.

Reyenga PJ, Howden SM, Meinke H, McKeon GM (1999). Modelling global change impacts on wheat cropping in south-east Queensland, Australia. *Environmental Modelling & Software.* **14,** 297-306.

Sands PJ (1995). Modelling canopy production. I. Optimal distribution of photosynthetic resources, *Australian Journal of Plant Physiology*, **22,** 593-601.

Thornley JHM (1976). *Mathematical models in plant physiology*. Academic Press, London, UK.

Thornley JHM (1998). Grassland dynamics: an ecosystem simulation model. CAB International, Wallingford, UK.

Thornley JHM and France J (2007). *Mathematical models in agriculture*. CAB International, Wallingford, UK.

Thornley JHM & Johnson IR (2000). *Plant and crop modelling*. Blackburn Press, Caldwell, New Jersey, USA.

von Caemmerer S (2000). *Biochemical models of leaf photosynthesis*. CSIRO Publishing, Collingwood, Australia.

Ziska LH and Bunce JA (2007). Predicting the impact of changing CO2 on crop yields: some thoughts on food. *New Phytologist,* **175,** 607-618.

4 Canopy photosynthesis

4.1 Introduction

In this Chapter the instantaneous and daily rates of both canopy gross and net photosynthesis are considered. The rate of instantaneous canopy gross photosynthesis is calculated by summing the leaf photosynthetic rate over all leaves in the canopy. This is done by combining the treatment of light interception and attenuation in Chapter 2 with that for leaf photosynthesis in Chapter 3, which defines the rate of leaf gross photosynthesis as a function of photosynthetic photon flux, PPF (μmol photons m^{-2} s^{-1}) , incident on the leaves. This approach to calculating canopy photosynthesis is well established. Early models were developed by Thornley (1976), and the basic concept has been widely applied, with greater detail being incorporated into the descriptions of leaf photosynthesis and light interception. The daily gross photosynthesis is then evaluated by summing the instantaneous canopy gross photosynthesis throughout the day taking into account variation in irradiance and temperature. Canopy respiration, including growth and maintenance components, is then calculated which, combined with the canopy gross photosynthesis, gives the rate of canopy net photosynthesis. This is then used to estimate the daily canopy growth rate. Some background to the development of canopy photosynthesis models can be found in Johnson *et al*. (1989), Johnson *et al.* (1995), Anten *et al.* (1995), Anten (1997), Cannell and Thornley (1998), Thornley and Johnson (2000), Thornley (2002), Thornley and France (2007). The general scheme for calculating canopy photosynthesis is illustrated in Fig. 4.1:

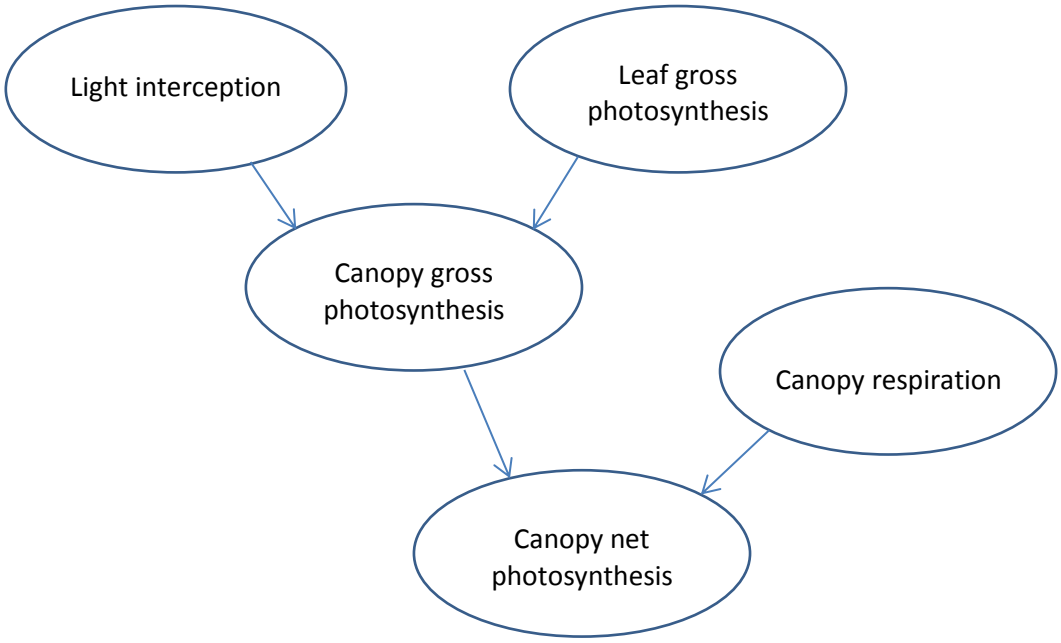

Figure 4.1: Schematic representation for calculating canopy photosynthesis. Canopy light interception and leaf gross photosynthesis are combined to calculate canopy gross photosynthesis. This is then combined with the growth and maintenance components of respiration to estimate canopy net photosynthesis.

It is well established that the leaf photosynthetic potential varies throughout the canopy due to acclimation to the growth environment, which is the physiological adjustment of the plant to environmental conditions (eg Kull, 2002). As discussed in Chapter 3, the light-saturated rate of leaf photosynthesis is related to the leaf photosynthetic enzyme concentration. However, the maintenance respiration rate is also related to the enzyme, or protein, concentration, since a primary source of maintenance costs is the resynthesis of degraded proteins. It therefore follows that for leaves in low light, an increase in leaf enzymes will result in relatively small increases in photosynthesis, while maintenance costs may increase significantly. Consequently, the observed decline in leaf enzyme content and therefore light-saturated rate of photosynthesis through the depth of the canopy is a physiologically plausible acclimation strategy by the plant. Apart from responding to the light intensity, photosynthetic enzyme concentration also varies in relation to the other key climatic factors of temperature and atmospheric CO_2. Acclimation can occur over periods of around 2 to 8 days (Thornley, 2004). This acclimatory response, which is discussed in Johnson *et al.* (2010), will be examined here.

Since both canopy gross photosynthesis and canopy respiration depend on the distribution of photosynthetic enzymes through the canopy, which can be directly related to leaf nitrogen content, this distribution is first considered, followed by the calculations of the canopy photosynthesis components, and also canopy growth rate. All model environmental variables are listed in Table 4.1, model variables in Table 4.2 and parameters in Table 4.3. The leaf photosynthesis variables and parameters are given in Tables 3.2, 3.3 in the previous Chapter. Some illustrations of the behaviour of the models are presented here, but you are encouraged to explore the models by using PlantMod.

In the following discussion, the term 'substrate' is used to refer either to carbohydrate or nitrogen components that are available for plant structural synthesis. Carbon substrate is sugars while nitrogen substrate is either nitrate or amino acids.

4.2 Photosynthetic enzyme distribution through the canopy

To incorporate the decline in leaf photosynthetic potential through the canopy, Charles-Edwards (1981, p. 70) assumed that the rate of leaf gross photosynthesis at saturating PPF, P_m in eqn (3.5), is proportional to the growth PPF, so that

$$P_m = P_{m,0} e^{-k\ell} \tag{4.1}$$

where $P_{m,0}$ is the value at the top of the canopy ($\ell = 0$). This approach has been widely used (eg Thornley, 2004), and is simple to implement.

Since it is assumed that P_m is proportional to the photosynthetic enzyme concentration, eqns (3.17) and (3.18), using eqn (4.1) for P_m implies that

$$f_p(\ell) = f_{p,0} e^{-k\ell} \tag{4.2}$$

where $f_{p,0} = f_p(\ell = 0)$ is the value of f_p for leaves in full sunlight at the top of the canopy. Note that in Chapter 2 the P_m response to f_p was assumed to have a maximum value at $f_p = f_{p,mx}$. For simplicity, this is not included in the present discussion, although it will included in the full analysis of canopy photosynthesis that follows.

Equation (4.2) can be generalized as

$$f_p(\ell) = (f_{p,0} - f_{p,b}) e^{-k\ell} + f_{p,b} \tag{4.3}$$

where $f_{p,b}$ is a basal enzyme concentration that is not involved in photosynthesis. When $f_{p,b} = 0$ this is identical to eqn (4.2). Note that eqn (4.3) is often written in terms of leaf nitrogen rather than enzyme – the latter is used here for convenience to allow plant material to comprise the components of cell wall, protein and substrate that were discussed in Section 1.4 in Chapter 1.

Equations of the form of (4.2) or (4.3) have been derived by several authors. For example, Sands (1995) and Anten *et al.* (1995) separately showed that for a given amount of photosynthetic enzymes (or N), then the rate of canopy photosynthesis is maximized when eqn (4.3) applies. Thornley (2004) has derived eqn (4.2) from a simple model of leaf photosynthetic acclimation to light that incorporates the synthesis and degradation of the photosynthetic enzyme. It should be noted that Thornley's model assumes that synthesis of photosynthetic N from non-photosynthetic N is proportional to PPF and if this is relaxed then other relationships for enzyme distribution will be derived. The approach of eqns (4.1) and (4.2) has been widely applied in canopy photosynthesis models: see, for example, Anten *et al.* (1995), Johnson *et al.* (1995), Kull and Jarvis (1995), Dewar (1996) (de Pury and Farquhar (1997), Anten (1997), Thornley and Johnson (2000) and, for more discussion and references, see Thornley and France (2007).

In spite of the appeal of either eqn (4.2) or (4.3), plant enzyme distribution rarely follows this pattern of exponential decline. Indeed, in an excellent review of the subject, Kull (2002) makes the point that the nitrogen gradient through the canopy is never proportional to the light gradient. Rather, the distribution is fairly linear in the upper canopy and then curves at depth through the canopy. Examples of such observations can be found in Yin *et al.* (2003). Kull (2002) further argues optimization models that lead to eqn (4.2) or (4.3) fail to treat acclimation as a whole plant phenomenon.

All of the optimization approaches are derived from light interception and attenuation models that treat the light in the canopy as homogeneous rather than incorporating the direct and diffuse components (see Section 2.6 in Chapter 2). However, as discussed by Johnson *et al* (1995), de Pury and Farquhar (1997), and others, the role of direct and diffuse PPF indicates that leaves within the canopy may experience intensities of PPF that are greater than the mean at that intensity. For example, at a depth equivalent to an LAI of 1 with the extinction coefficient equal to 0.5 and 70% of the PPF in the direct beam, approximately 80% of the leaves will be in direct sunlight and their incident PFD will have only fallen by 12%. However, according to eqn (4.1), P_m would decline by 40% which seems excessive. This was highlighted by Yin *et al* (2003) in their discussion of experimental observations of nitrogen distribution through canopies. There are other possible limitations to the optimization schemes mentioned here and these are considered in Section 4.8 below.

In order to capture the general pattern of enzyme distribution through canopies, eqn (4.3) can be generalized as

$$f_p(\ell) = f_{p,0} - \left(f_{p,0} - f_{p,b}\right)\left(1 - e^{-k\ell}\right)^{\gamma_p} \tag{4.4}$$

where $\gamma_p \geq 0$ is an empirical coefficient. With $\gamma_p = 0$ eqn (4.4) simplifies to a constant enzyme distribution defined by $f_{p,b}$, with $\gamma_p = 1$ it becomes eqn (4.3), and when $\gamma_p = 1$, $f_{p,b} = 0$, it becomes eqn (4.2). In the present analysis, the starting values $f_{p,0} = 0.25$, $f_{p,b} = 0.05$, $\gamma_p = 3$ are used, although variation in $f_{p,0}$ and γ_p is considered later. Equation (4.4) is illustrated in Fig. 4.2, and is a versatile equation for describing the possible enzyme decline through the canopy. It should be noted that although eqn (4.4) is defined in terms of cumulative LAI, ℓ, this is really a surrogate for

the PPF within the canopy relative to that at the top as given by eqn (2.7) in Chapter 2, so that the enzyme distribution is responding to variation in light within the canopy.

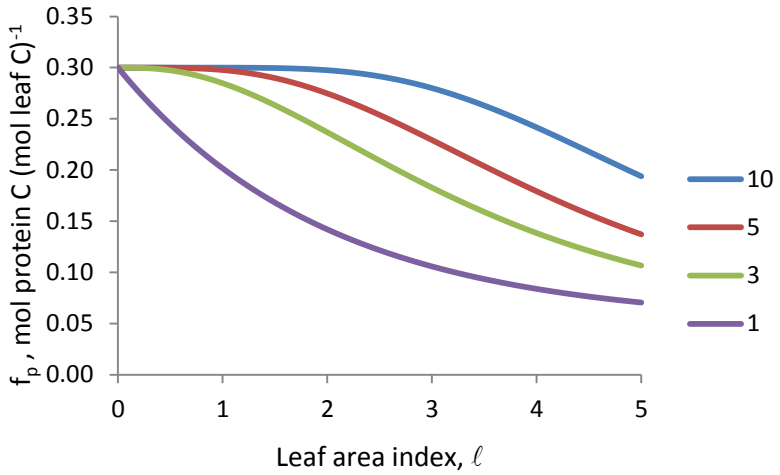

Figure 4.2: Decline in photosynthetic enzyme concentration through the depth of the canopy as defined by eqn (4.4). The extinction coefficient is $k = 0.5$, and values for $f_{p,0}$ and $f_{p,b}$.are 25 and 0.05 mol protein C (mol leaf C)$^{-1}$ respectively. Values for γ_p (0.5, 1, 2,3) are indicated in the figure.

The mean enzyme concentration in the canopy is

$$\bar{f}_p(L) = \frac{1}{L}\int_{\ell=0}^{L} f_p(\ell)\,\mathrm{d}\ell \tag{4.5}$$

which can be integrated analytically with eqn (4.4), provided γ_p is a rational number (that is, the ratio of two integers). However, it is straightforward to solve numerically.

$$\bar{f}_p(L) = \frac{1}{L}\sum_{i=1}^{i=n} f_p(\ell_i)\Delta\ell \tag{4.6}$$

where

$$\ell_i = (i-1)\Delta\ell + \frac{\Delta\ell}{2} = (2i-1)\frac{\Delta\ell}{2}, \quad i = 1 \text{ to } n \tag{4.7}$$

and

$$n = \frac{L}{\Delta\ell} \tag{4.8}$$

According to this scheme, the canopy is divided into layers of depth $\Delta\ell$ and $f_p(L)$ is evaluated at the mid-point of each layer and the total enzyme content of the layer is this value multiplied by the layer depth. This is a common scheme for numerical integration and, while more elaborate numerical techniques can be applied, it works well for the present purposes. The value

$$\Delta\ell = 0.1 \tag{4.9}$$

is used throughout and L is restricted to intervals of 0.1 (which could be relaxed).

4.3 Instantaneous canopy gross photosynthesis

The rate of instantaneous canopy gross photosynthesis, P_g μmol CO_2 (m^{-2} ground) s^{-1}, is calculated by summing the leaf photosynthetic rate over all leaves in the canopy, and is given by

$$P_g = \int_0^L P_{\ell,g}\left(I_\ell\right)\mathrm{d}\ell \tag{4.10}$$

where $P_{\ell,g}$ μmol CO_2 (m^{-2} leaf) s^{-1}, is the rate of leaf gross photosynthesis (Chapter 3) and I_ℓ μmol photons (m^2 leaf)$^{-1}$ s^{-1}, is the photosynthetic photon flux (PPF) incident on the leaf (Chapter 2), L (m^2 leaf) (m^{-2} ground) is the total canopy leaf area index, and ℓ is a dummy variable defining the cumulative leaf area index through the depth of the canopy. All model variables are presented in Table 4.2 and parameters in Table 4.3.

Separating the leaves in direct and diffuse PPF, eqn (4.10) can be written

$$P_g = \int_0^{L_s} P_{\ell,g}\left(I_{\ell,s}\right)\mathrm{d}\ell_s + \int_0^{L_d} P_{\ell,g}\left(I_{\ell,d}\right)\mathrm{d}\ell_d \tag{4.11}$$

which, using eqns (2.17) and (2.18) for ℓ_s and ℓ_d, becomes

$$P_g = \int_0^L P_{\ell,g}\left(I_{\ell,s}\right)e^{-k\ell}\mathrm{d}\ell + \int_0^L P_{\ell,g}\left(I_{\ell,d}\right)\left(1-e^{-k\ell}\right)\mathrm{d}\ell \tag{4.12}$$

Equation (4.12) is the key equation for calculating the rate of canopy gross photosynthesis which, combined with the previous theory, incorporates the effects of PPF, temperature, leaf nitrogen, atmospheric CO_2 concentration and total leaf area index.

The integrals in eqn (4.12) have been solved analytically (Thornley, 2002), when eqn (4.1) applies, although the analysis is quite complex. However, for the present analysis, since the more general equation given by (4.4) is being used here, eqn (4.12) is solved numerically. This is quite straightforward to compute and, analogous to the calculation of $\bar{f}_p(L)$ in the previous section, P_g is evaluated as

$$P_g = \sum_{i=1}^{i=n}\left[P_{\ell,g}\left(I_{\ell_i,s}\right)e^{-k\ell_i} + P_{\ell,g}\left(I_{\ell_i,d}\right)\left(1-e^{-k\ell_i}\right)\right]\Delta\ell \tag{4.13}$$

where the summation scheme in eqns (4.7) and (4.9) again applies.

P_g, as given by eqn (4.13), is illustrated in response to PPF incident on the canopy, I_0, and temperature, T, in Fig. 4.3 for a C_3 canopy with the default climate values as defined in Table 4.3, leaf photosynthetic parameter values (see Chapter 3, Table 3.3), default canopy extinction coefficient $k = 0.5$ (Table 4.2), and with $L = 2$ and 4. These graphs have been produced by copying directly from PlantMod. It can be seen that P_g increases in response to L as expected. P_g can be explored in further detail in PlantMod.

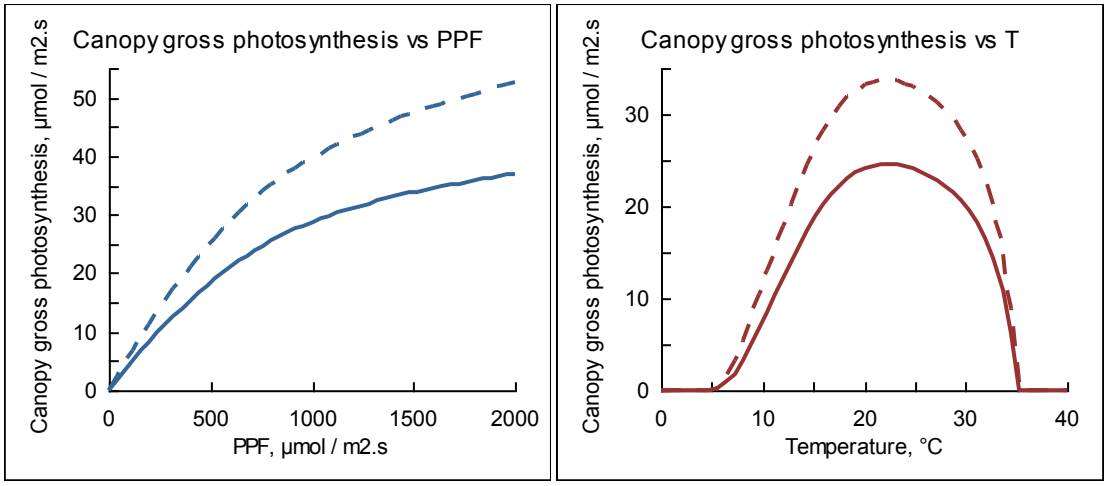

Figure 4.3: Instantaneous canopy gross photosynthesis, P_c, in response to PPF (left) and temperature (right). The solid lines are $L = 2$ and the broken lines are $L = 4$. Note the different scales on the vertical axes. Default values are used for all other parameters (Tables 4.1, 4.3; Table 3.3, Chapter 3). From PlantMod.

4.4 Daily canopy gross photosynthesis

The daily canopy gross photosynthesis, $P_{g,day}$ mol CO_2 (m^{-2} ground) d^{-1} is given by the integral of P_g throughout the day:

$$P_{g,day} = 10^{-6} \int_0^{\tau} P_g \mathrm{d}t \tag{4.14}$$

where t is time (s), τ (s) is the daylight period in seconds and the factor 10^{-6} converts from μmol CO_2 to mol CO_2. This equation can be applied with any daily distribution of PPF and temperature. For constant PPF, I_0, and temperature, T, it is

$$P_{g,day} = 10^{-6} \tau P_g \left(I_0, T \right) \tag{4.15}$$

whereas, if I_0 and T vary, it is evaluated as

$$P_{g,day} = 10^{-6} \sum_{i=1}^{i=n} P_g \left[I_0 \left(t_i \right), T \left(t_i \right) \right] \Delta t \tag{4.16}$$

where Δt is a small time-step,

$$t_i = \left(i - 1 \right) \Delta t + \frac{\Delta t}{2} = \left(2i - 1 \right) \frac{\Delta t}{2}, \quad i = 1 \text{ to } n \tag{4.17}$$

and

$$n = \frac{\tau}{\Delta t} \tag{4.18}$$

Essentially, this scheme sums P_g as evaluated at regular intervals throughout the day. The accuracy of the numerical scheme will increase as the time step (Δt) gets smaller, or the number of time steps (n) gets larger, although the computation will take longer. However, continuing to decrease Δt to very small values can cause numerical errors to increase and the scheme actually becomes less accurate. A general strategy is to start with a relatively small value for n and with Δt calculated from

eqn (4.18), gradually increase n until the estimate of $P_{g,day}$ in eqn (4.16) is reached. In PlantMod the mean daytime PPF and temperature values are used.

4.5 Canopy structure and carbon partitioning

In order to calculate canopy net photosynthesis, it is necessary to evaluate canopy respiration. This, in turn, requires values for leaf area index as a function of plant mass and the carbon allocation between the shoot and root.

Defining the shoot mass as W mol C (m^{-2} ground) it follows that

$$L = \sigma\rho\frac{W}{\varsigma} \tag{4.19}$$

where σ, m^2 leaf (kg leaf d.wt)$^{-1}$ is the specific leaf area, ρ is the leaf fraction of the shoot d.wt., and ς converts from d.wt to mole units and is taken to be 37 mol C (kg d.wt)$^{-1}$ which corresponds to 45% plant carbon content(see Section 1.4 in Chapter 1). While σ could be defined with mole units and the need for the γ_p coefficient avoided, d.wt. units are used to be consistent with the common definition of specific leaf area.

It is also observed that σ and ρ generally decline as the CO_2 concentration increases, corresponding to thicker leaves and a smaller leaf fraction in the shoot. It should be noted that there is some variation in these responses, and a discussion can be found, for example, in Pritchard and Amthor (2005). It is therefore assumed that

$$\sigma = \frac{\sigma_{amb}}{\sqrt{f_C(C)}} \text{ and } \rho = \frac{\rho_{amb}}{\sqrt{f_C(C)}} \tag{4.20}$$

where $f_C(C)$ is the CO_2 response function as defined in Section 3.2.2 in Chapter 3 and in more detail in Section 1.3.4 in Chapter 1. σ_{amb} and ρ_{amb} are the values of σ and ρ at ambient CO_2. The square root term is introduced to moderate the response. For example, with the parameter values in Table 3.3 in Chapter 3, $1/\sqrt{f_C(C)}$ takes the values 0.87 and 0.82 at 50% increase and doubling of CO_2 respectively. These values are consistent with general observations in the literature – for a further discussion of these responses, see Hikosaka *et al.* (2005). Equation (4.19) now becomes

$$L = \frac{\sigma_{amb}\rho_{amb}}{f_C(C)}\frac{W}{\varsigma} \tag{4.21}$$

and this is the equation that is used to relate leaf area index and plant mass. The default values for σ_{amb} and ρ_{amb} are taken to be 15 m^2 leaf (kg d.wt)$^{-1}$ and 0.7 kg leaf d.wt (kg shoot d.wt)$^{-1}$ respectively.

The carbon partitioned to the root is also required for the analysis that follows. There has been much work done in relation to shoot:root partitioning, from the transport-resistance model of Thornley (1972) to simpler schemes based on the functional hypotheses of White (1937), Brouwer (1962) and Davidson (1969) that assume that the carbon allocation between the shoot and root is such that the acquisition of resources from those organs is in some form of equilibrium. There is considerable variation in the observed carbon allocation between the shoot and root as CO_2 increases, although the general trend is for a shift towards root growth (Rogers *et al.*, 1996), which is consistent with the functional hypothesis. We therefore adopt the same approach as for σ and ρ, by assuming that the fraction of gross photosynthesis that is allocated for shoot processes, η, is

$$\eta = \frac{\eta_{amb}}{\sqrt{f_C(C)}} \tag{4.22}$$

which again incorporates a moderate decline in η as CO_2 increases. The default value $\eta_{amb} = 0.9$ is used. Although, a range of factors will influence shoot:root partitioning, eqn (4.22) allows for the influence of atmospheric CO_2 which will be relatively stable as the plant grows.

While this treatment of specific leaf area, σ, and leaf fraction, ρ, and carbon partitioning to the root, η, gives a relatively simple description of the likely response to atmospheric CO_2 concentration, it must be remembered that, in practice, these quantities respond to internal plant variables, particularly carbohydrate and possibly substrate nitrogen (nitrate or amino acids). There are other observed responses, such as thinner leaves at higher temperatures, lower light and higher nitrogen nutrition. However, while these factors are likely to vary during plant growth, the ambient CO_2 will remain relatively stable. Thus, short-term variation in σ, ρ and η should be captured through the parameters σ_{amb}, ρ_{amb} and η_{amb}.

4.6 Daily canopy respiration rate

It is now necessary to calculate the daily respiration rate. Respiration, excluding photorespiration (which is incorporated directly into the calculation of gross photosynthesis, as discussed in Chapter 3) is calculated using the McCree (1970) approach, that has been further developed by Thornley (1970), Johnson (1990), and is widely used. This identifies the growth and maintenance components of respiration. These components are helpful in understanding the respiratory demand by the plants, although the actual underlying respiratory process whereby ATP is produced from sugars with a respiratory efflux of CO_2 (eqn (3.2) in Chapter 3) is common to both growth and maintenance respiration. Growth respiration is the respiration associated with the synthesis of new plant material, while maintenance is the respiration required primarily to provide energy for the re-synthesis of degraded proteins. Consequently, growth respiration is related to the growth rate of the plant, or daily carbon assimilation, whereas maintenance respiration is proportional to the plant dry weight or, more specifically, the actual protein content which may vary in response to plant nutrient status, particularly nitrogen. For a background on this treatment of respiration, see Johnson (1990) or Thornley and Johnson (2000). One point to note here is that canopy respiration is not solely the sum of all the leaf respiration since growth respiration occurs in meristems which may not be included in measurements of respiration if only a section of a mature leaf is used in the experiment.

In its standard form, the McCree-Thornley equation can be written:

$$R_{day} = \left(\frac{1-Y}{Y}\right)\frac{dW}{dt} + mW \tag{4.23}$$

where R_{day} (mol C m^{-2} d^{-1}) is the daily dark respiration rate, W (mol C m^{-2}) is plant mass as discussed in the previous section, dW/dt (mol C m^{-2} d^{-1}) is the growth rate which is discussed later, Y (dimensionless) is the growth efficiency, so that for 1 mole of C utilized for growth, there are Y moles of structural C produced and $(1-Y)$ respired (see below), and m (d^{-1}) is the maintenance coefficient, with maintenance costs being a fraction m of plant mass. Variables and parameters are defined in Tables 4.2 and 4.3. The terms on the right-hand-side of eqn (4.23) are the growth and maintenance components of respiration respectively, denoted by $R_{g,day}$ and $R_{m,day}$, so that

$$R_{day} = R_{g,day} + R_{m,day} \tag{4.24}$$

These components are now considered in turn.

4.6.1 Growth respiration

According to the definition of the growth efficiency Y, one unit of substrate that is utilised for growth results in Y units of plant structural material and $(1-Y)$ units of respiration. Thus, for 1 unit of growth, this can be represented by the scheme in Fig. 4.4:

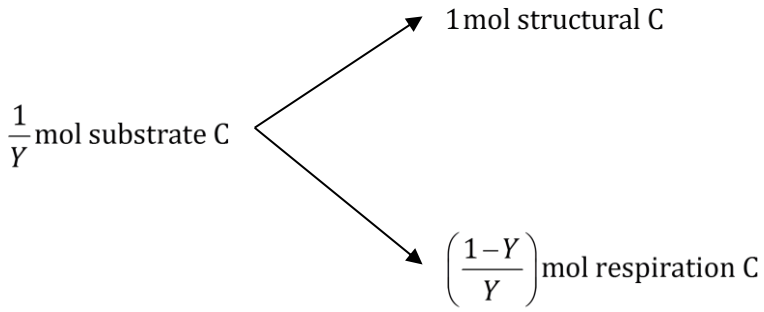

Figure 4.4: Schematic representation of growth respiration.

Hence, in terms of the growth rate, where now the structural C produced is $\mathrm{d}W/\mathrm{d}t$, the growth respiration is

$$R_{g,day} = \left(\frac{1-Y}{Y}\right)\frac{\mathrm{d}W}{\mathrm{d}t} \tag{4.25}$$

which is the first term in eqn (4.23). The respiratory costs for cell wall and protein synthesis are different, with the costs of the more complex protein molecules being greater – a detailed discussion can be found in Thornley and Johnson (2000). The plant composition components discussed in Section 1.4 in Chapter 1, are used, so that the plant structure comprises cell wall, protein and sugars, with molar concentrations f_w, f_p and f_s respectively, and where

$$f_w + f_p + f_s = 1 \tag{4.26}$$

It is readily shown that, if the growth efficiencies for cell wall and protein are Y_w, and Y_p, then these are related to the overall growth efficiency, Y, by

$$\left(\frac{1-Y}{Y}\right) = \left(\frac{1-Y_w}{Y_w}\right)f_w + \left(\frac{1-Y_p}{Y_p}\right)f_p \tag{4.27}$$

from which

$$Y = \frac{1}{1+\left(\frac{1-Y_w}{Y_w}\right)f_w + \left(\frac{1-Y_p}{Y_p}\right)f_p} \tag{4.28}$$

This allows for the direct influence of plant structure on the overall growth efficiency directly. The model defaults are:

$$Y_w = 0.9;\ \ Y_p = 0.55 \tag{4.29}$$

so that, for example, with 20% sugars, 25% protein and 55% cell wall (on a mole basis), $Y = 0.81$, whereas, if the protein content is reduced to 20% and the cell wall increased to 60%, this becomes $Y = 0.83$. Values for Y that are observed experimentally are generally in the range 0.75 to 0.85. For more discussion, see Johnson (1990), Thornley and Johnson (2000), Thornley and France (2007).

4.6.2 Maintenance respiration

Maintenance respiration is generally regarded to be related to the plant live dry weight as in eqn (4.23). However, maintenance respiration is primarily related to the resynthesis of degraded proteins. There are other maintenance costs, such as the energy required for phloem loading, but these are not considered explicitly, so that it is assumed that the enzyme concentration is an indicator of overall maintenance costs. In addition, as a rate process, it is strongly temperature dependent. Incorporating these features, the maintenance respiration is assumed to be given by

$$R_{m,day} = m_{ref} f_m(T) W \frac{\bar{f}_p}{f_{p,ref}} \tag{4.30}$$

where $f_m(T)$ is a maintenance temperature response function which takes the value unity at the reference temperature T_{ref}, W (mol C m^{-2}) is shoot mass which is related to L by eqn (4.21), $\bar{f}_p$ is the mean canopy protein concentration as given by eqn (4.5) or (4.6), and $f_{p,ref}$ is the reference protein composition, and m_{ref} (d^{-1}) is the maintenance coefficient at the reference temperature and enzyme content, with default value

$$m_{ref} = 0.03 \text{ d}^{-1} \tag{4.31}$$

The maintenance coefficient in eqn (4.23) is now

$$m = m_{ref} f_m(T) \frac{\bar{f}_p}{f_{p,ref}} \tag{4.32}$$

The maintenance temperature response function, $f_m(T)$, is defined to take the value unity at the reference temperature T_{ref}, so that

$$f_m\left(T = T_{ref}\right) = 1 \tag{4.33}$$

Common equations that are used for the temperature response function are either the Arrhenius equation or simpler Q_{10}. These can be shown to give virtually identical behaviour (as discussed in Section 1.3.5 in Chapter 1) and so the latter is used as it is simpler to work with. According to the Q_{10} approach, the temperature function is defined by

$$f_m(T) = Q_{10}^{\left(T - T_{ref}\right)/10} \tag{4.34}$$

which is unity at $T = T_{ref}$, and so satisfies eqn (4.33). More detail can be found in Section 1.3.5, Chapter 1. Note that different day and night temperatures are required to calculate $f_m(T)$ and, denoting these with obvious subscripts,

$$f_m(T) = f_m\left(T_{day}\right) f_d + f_m\left(T_{night}\right)\left(1 - f_d\right) \tag{4.35}$$

where f_d is the daytime fraction of the 24 hour period. For more discussion about calculating the daylength, see Section 2.7 in Chapter 2. For variable temperature distributions throughout the day

and night, a scheme similar to eqns (4.16) to (4.18) could be used, although there is very little penalty to using mean temperature values.

Using eqn (4.21), eqn (4.30) can now be written

$$R_{m,day} = m_{ref} f_m(T) \frac{\varsigma f(C) L}{\sigma_{amb} \rho_{amb}} \frac{\bar{f}_p}{f_{p,ref}} \tag{4.36}$$

which completely defines the canopy maintenance respiration rate, as a function of L, in response to temperature, ambient CO_2, canopy structure, and enzyme distribution through the canopy. According to this equation, when $R_{m,day}$ is related to leaf area index, L, it increases in response to C through the function $f(C)$. However, it should be noted that this is due to the influence of ambient CO_2 on the relationship between L and W due to the effect on the specific leaf area and proportion of carbon allocated directly to leaves. There will also be a response to the plant enzyme concentration and, as will be seen below, this may decline in response to C. Furthermore, a decline in the enzyme concentration will result in a decline in the maintenance coefficient, m, in eqn (4.32).

4.7 Daily growth rate and net canopy photosynthesis

The final part of the analysis is to calculate the daily net and gross canopy photosynthesis rates, and the daily growth rate. The approach here allows for carbon being partitioned to the root but then focuses on the shoot which is consistent with most practical applications. Consequently, the estimates of canopy net photosynthesis and growth rate will be for the shoot, after allowing for carbon to be partitioned to the root.

Daily shoot net canopy photosynthesis is

$$P_{n,day} = P_{g,day} - R_{day} \tag{4.37}$$

and the shoot growth rate is

$$\frac{\mathrm{d}W}{\mathrm{d}t} = \eta P_{g,day} - R_{day} \tag{4.38}$$

where $P_{g,day}$ is given by eqn (4.15) or (4.16), η by eqn (4.22), and the growth and maintenance components of R_{day} as defined above. Combining eqn (4.38) with (4.24) and (4.25) leads to

$$R_{day} = (1-Y)\eta P_{g,day} + Y R_{m,day} \tag{4.39}$$

which can be used in eqns (4.37) and (4.38) to calculate $P_{n,day}$ and $\mathrm{d}W/\mathrm{d}t$. Note that $\mathrm{d}W/\mathrm{d}t$ is also readily derived as

$$\frac{\mathrm{d}W}{\mathrm{d}t} = P_{n,day} - P_{g,day}(1-\eta) \tag{4.40}$$

which is consistent with the definitions of the growth rate and net and gross photosynthetic rates – that is, the growth rate is the daily net shoot carbon assimilation less the carbon partitioned to the roots.

This completely defines the shoot growth rate, net and gross canopy photosynthetic rates, along with the growth and maintenance respiration rates

Two derived variables of interest are the *carbon use efficiency* and the *canopy quantum yield*. The carbon use efficiency is defined as the ratio of the shoot photosynthesis to the rate of gross photosynthesis, so that

$$CUE = \frac{P_{n,day}}{P_{g,day}} \tag{4.41}$$

The canopy quantum yield is the ratio of moles of carbon fixed per moles of photons per unit ground area absorbed by the canopy, and is defined by

$$CQY = \frac{P_{n,day}}{PPF_{day,abs}} \tag{4.42}$$

where $PPF_{day,abs}$, mol photons m^{-2} day^{-1} is the total PPF for the day that is absorbed by the canopy. Again, it must be emphasized that CQY as defined here relates the net carbon fixed by the shoot – that is total carbon fixed minus the shoot respiration – to the daily PPF.

The model behaviour is illustrated in Fig. 4.5, which shows $\mathrm{d}W/\mathrm{d}t$ $P_{g,day}$, $P_{n,day}$, R_{day}, $R_{g,day}$, $R_{m,day}$ as functions of PPF and temperature for the default environmental and physiological parameters (Tables 4.1, 4.3, Table 3.3, Chapter 3). The mean temperature is defined as the mean of the day and night temperatures, and the difference in day and night temperatures is 10°C for the illustration. These responses are entirely consistent with general observations and demonstrate that the model has the expected behaviour.

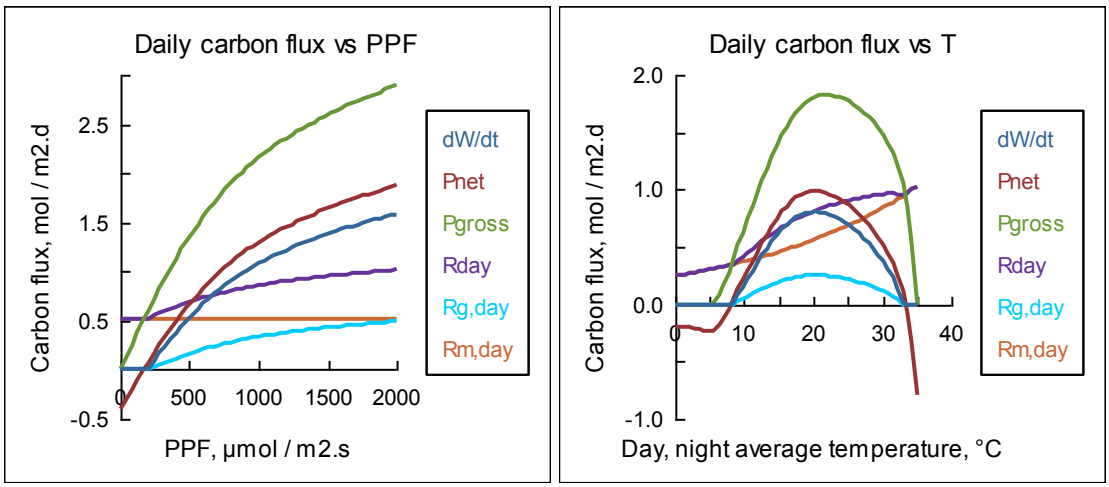

Figure 4.5: $\mathrm{d}W/\mathrm{d}t$, $P_{g,day}$, $P_{n,day}$, R_{day}, $R_{g,day}$, $R_{m,day}$ for the default environmental and physiological parameters (Tables 4.2, 4.3; Table 3.3 in Chapter 3).
Left: PPF response. Right response to the average of the day and night temperature.
Note the different vertical scales for the graphs. From PlantMod.

4.8 Optimized plant enzyme content

The analysis presented so far defines daily growth rate as well as photosynthesis and respiration components in response to plant and canopy characteristics, the environmental conditions, and also enzyme distribution through the canopy as given by eqn (4.4), which relates the enzyme concentration to the value at the top of the canopy, $f_{p,0}$, and light attenuation through the canopy. Just as the enzyme concentration within the canopy will depend on irradiance, so will $f_{p,0}$. Enzyme

concentration and distribution will also vary in response to other factors such as temperature, as is explored later.

Optimum, or goal-seeking teleonomic models, have considerable appeal in the plant sciences. They allow exploration of possible optimum system characteristics in response to a wide variety of environmental conditions. Teleonomic models in biology have been discussed at length by Monod (1972). An example of teleonomic modelling is the partitioning of growth between shoots and roots. As discussed earlier, the functional hypothesis that defines partitioning in relation to resource acquisition, can be viewed as goal-seeking, and Johnson and Thornley (1987) developed this concept to describe partitioning in such a way as to maximize the specific growth rate. Sands (1995) and Anten *et al.* (1995) have derived exponential patterns of nitrogen distribution through the canopy by optimizing the distribution of a given amount of nitrogen for canopies growing in homogeneous light conditions.

While goal seeking models are attractive, they must be applied with caution. Any such model is subject to the actual goal that may be defined. For example, optimum shoot:root partitioning under good growth conditions may result in plants that have shallow root systems that are less resilient to dry periods than deeper rooting species that may appear not to have 'optimum' growth. Similarly, for nitrogen, or enzyme, distribution through the canopy, the underlying assumptions in the model, as well as the choice of optimum behaviour, will influence the outcome.

Clearly, plant canopies do not always necessarily behave in an optimum manner. The definition of optimum behaviour is unlikely to account for all acclimatory requirements and is subject to the limitations of the model. Also, it may be possible to define different equally plausible optimization criteria. Nevertheless, there is value in exploring possible optimum enzyme distributions since it allows comparison across different environments and plant types. For example, if the optimum enzyme concentration or distribution differs in different growth conditions this may point to a general trend, such as lowered enzyme concentration in elevated CO_2 conditions. Once these optimum responses have been considered we can investigate variation with non-optimum growth.

The optimization criterion applied here is simply to maximize the daily net photosynthesis, eqn (4.37), for specified growth conditions by varying both the absolute amount and distribution of enzymes through the canopy. This accounts for the effects on both carbon assimilation and respiratory losses from increasing the enzymes. This differs from other approaches where it is generally assumed either that there is a fixed total canopy enzyme (or N) amount, or that the value at the top of the canopy is prescribed and the subsequent decay is estimated. By looking at both the amount and distribution, it is possible to examine acclimatory responses to factors such as elevated CO_2. It should be noted that Dewar (1996) calculated the optimum N concentration in the canopy by balancing photosynthesis and respiration, and this analysis gave insight into the notion that net primary production is often proportional to total light intercepted. However, Dewar's analysis include several simplifications in the description of canopy photosynthesis and also used the exponential distribution of N through the canopy, similar to eqn (4.1), which, as discussed earlier, does not agree with general observations.

The parameters to be varied are the enzyme concentration at the top of the canopy, $f_{p,0}$, and the coefficient γ_p in eqn (4.4). Recall that $\gamma_p = 1$ corresponds to simple exponential decline. The basal enzyme concentration, $f_{p,b}$, is kept fixed at the value 0.05 mol protein C (mol C)$^{-1}$. The optimum parameters are calculated using a simple search procedure.

The optimum enzyme distribution through the canopy, f_p, is shown in Fig. 4.6 for the default environment and parameters (Tables 4.1, 4.3; Table 3.3, Chapter 3), but with $L = 5$ to highlight the likely variation in f_p. The derived values for $f_{p,0}$ and γ_p are:

$$f_{p,0} = 29.8 \text{ mol protein C (mol leaf C)}^{-1} \text{ and } \gamma_p = 5.18 \quad (4.43)$$

It can be seen that f_p is fairly uniform with a slight decline near the top of the canopy, but with a greater decline as the depth through the canopy increases (as indicated by increasing LAI). This general response is quite typical of general observations (Kull, 2002). Further examples of possible distributions for f_p are considered below.

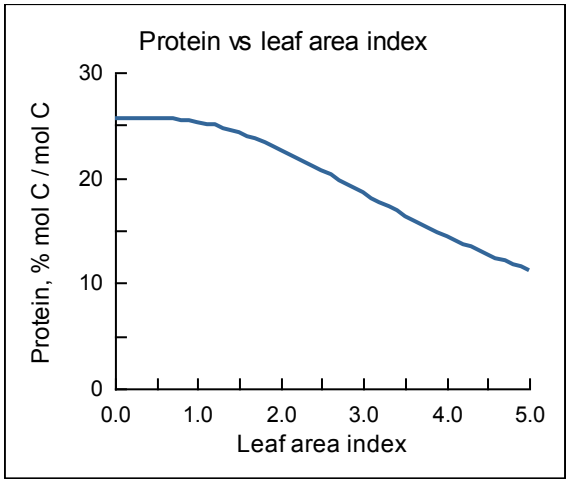

Figure 4.6: Enzyme distribution through the canopy that optimizes daily net photosynthesis. The derived parameters are shown in eqn (4.43). Default values are used for all other parameters (Tables 4.1, 4.3; Table 3.3, Chapter 3). From PlantMod.

The illustration in Fig. 4.6 is for plants growing in a PPF of I_0 =750 μmol photons m^{-2} s^{-1}, which is fairly representative of daily average values for temperate pastures and crops. However, the light environment is subject to considerable variation and the corresponding optimized f_p distributions are shown in Fig. 4.7 for I_0 =500 and 1000 μmol photons m^{-2} s^{-1} and it can be seen that the response is quite substantial, with the overall mean enzyme concentration being 17.3 and 26.8 mol protein C (mol C)$^{-1}$. Although the optimized f_p can be seen to be quite variable in relation to the growth PPF environment, in practice this has much less influence on photosynthesis, as apparent in Fig. 4.7 where the daily gross and net photosynthesis rates, $P_{g,day}$ and $P_{n,day}$, are shown along with the daily respiration rate, R_{day}. The effect of increasing f_p is to increase both $P_{g,day}$ and R_{day}, particularly at high I_0. The effect on $P_{n,day}$ is relatively small at low values of I_0, although the advantage of the greater f_p is apparent at high I_0,. This relative lack of sensitivity to f_p may help explain the wide range of f_p values and distributions that are reported in the literature. However, while the response of $P_{n,day}$ to variation in f_p may be relatively modest, f_p is a direct reflection of pasture quality, and may also be an indicator of likely grain yield in crops.

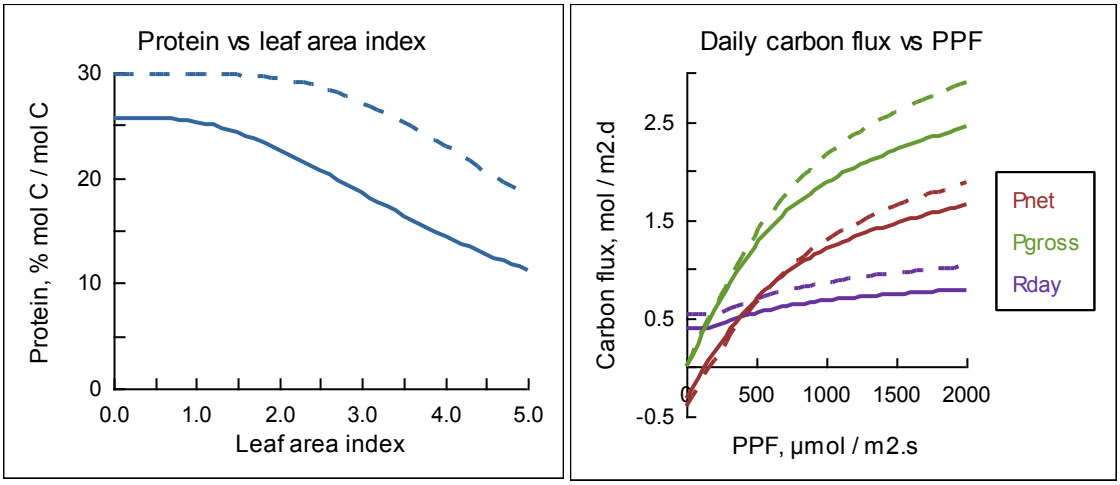

Figure 4.7: Enzyme distribution through the canopy (left) that optimizes daily net photosynthesis, for plants growing in 500 (solid line) or 1,000 (dashed line) μmol photons m^{-2} s^{-1}. This can be compared with Fig. 4.6 where the growth PPF is 750 μmol photons m^{-2} s^{-1}. The corresponding $P_{n,day}$, $P_{g,day}$ and R_{day} are also shown (right). Default values are used for all other parameters (Tables 4.1, 4.3; Table 3.3, Chapter 3).

Turning to the effect of temperature and atmospheric CO_2, Fig. 4.8 shows the optimum f_p distributions for the default environmental and physiological parameters, and either double ambient CO_2 or the day and night temperatures increased or decreased by 5°C from the default values of 22 and 12°C respectively. It can be seen that there is virtually no response to CO_2. Although slight reductions in nitrogen (and therefore f_p) as CO_2 increases are reported in the literature, these may well be due to a dilution effect due to elevated sugars (Pritchard and Amthor, 2005), or variation in plant nitrate.

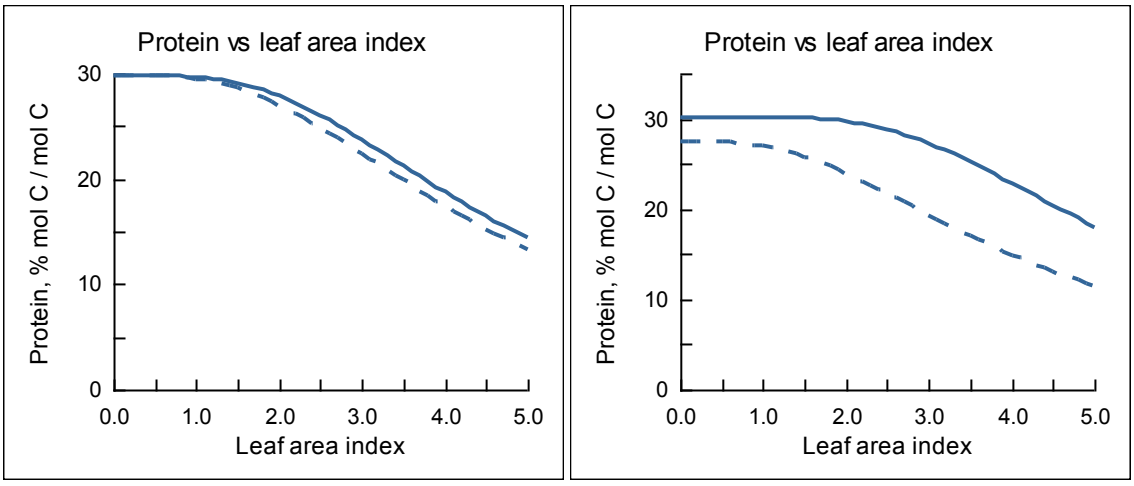

Figure 4.8: Enzyme distribution through the canopy that optimizes daily net photosynthesis. Left: ambient (solid line) and double (dashed line) atmospheric CO_2. Right: day/night temperatures 17/7°C (solid line) and 27/17°C (dashed line). Default values are used for all other parameters (Tables 4.1, 4.3; Table 3.3, Chapter 3). From PlantMod.

These illustrations suggest that the main factors affecting both the overall amount and actual distribution through the canopy of photosynthetic enzymes are the PPF and temperature.

Before proceeding, consider the exponential type decline as in eqn (4.3), which is equivalent to the general form for f_p being used here, eqn (4.4), but with the curvature coefficient $\gamma_p = 1$. In Fig. 4.9 the optimized f_p distribution as well as the daily gross and net photosynthesis rates, $P_{g,day}$ and $P_{n,day}$, and the daily respiration rate, R_{day} are shown for eqn (4.4), so that both $f_{p,0}$ and γ_p are optimized, and the exponential distribution, which is eqn (4.3) with $\gamma_p = 1$ so that only $f_{p,0}$ is optimized. It can be seen that the f_p distribution is quite different, while the respiration terms deviate as the PPF increases. The difference in $P_{g,day}$ at high PPF is because the photosynthetic capacity of leaves near the top of the canopy is reduced quite substantially with the exponential distribution, even though they are at PPFs that could benefit from greater f_p. The total canopy enzyme concentration in these two optimized distributions is different, being 29% for the full model and 22% for the exponential model, so that the assumption of exponential distribution of enzymes may result in lower estimations of total plant protein which could have significant implications in other calculations such as pasture quality.

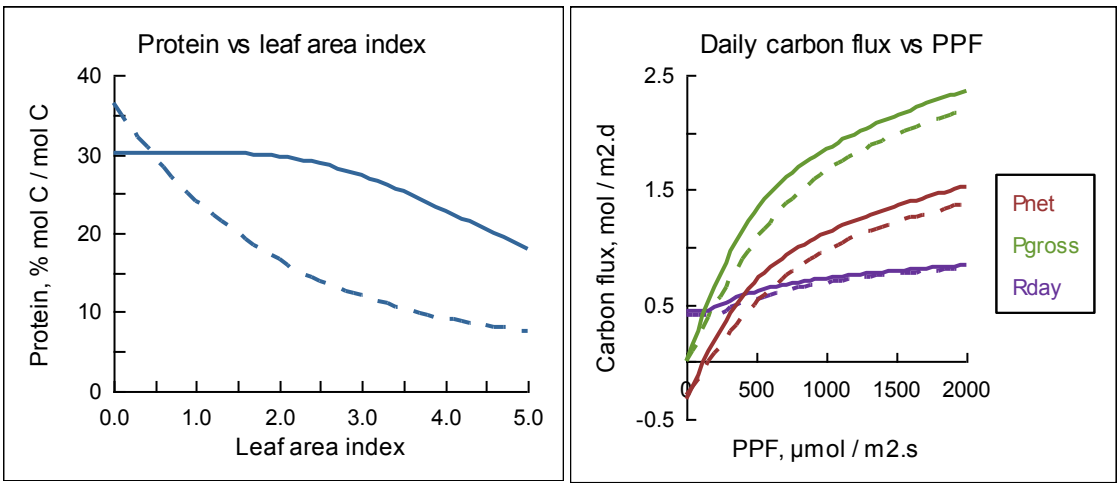

Figure 4.9: Optimum f_p distribution through the canopy (left) and growth rate as a function of PPF (right) for ambient CO_2. The solid lines correspond to the enzyme distribution through the canopy described by eqn (4.4) with both $f_{p,0}$ and γ_p being varied while the broken line is for the exponential distribution, corresponding to eqn(4.3), in which case $\gamma_p = 1$, and only $f_{p,0}$ is adjusted. Default values are used for all other parameters (Tables 4.1, 4.3; Table 3.3, Chapter 3). From PlantMod.

The enzyme distribution given by eqn (4.4) is implemented in PlantMod, although the option to use the exponential decline is also available on the interface. The default parameter values are

$$f_{p,0} = 30 \text{ mol protein C (mol leaf C)}^{-1} \text{ and } \gamma_p = 5 \tag{4.44}$$

which are virtually identical to the optimized values derived in the above example. However, it must be noted that different optimized values will be derived for variation in either the environmental or physiological parameters. This is considered further in the illustrations below.

4.9 Non-optimum plant enzyme distribution

Since it is by no means certain that plants will acclimate in an optimized fashion, it is instructive to look at the model variation under different enzyme concentratons and distributions. In Fig. 4.10 the f_p distribution through the canopy and PPF response for the canopy daily gross and net photosynthesis, $P_{g,day}$ and $P_{n,day}$, and the daily respiration rate, R_{day} are shown with the default

parameters (Tables 4.1, 4.3), and for $f_{p,0}$ reduced from 30 to 25 mol protein C (mol leaf C)$^{-1}$. It can be seen that a substantial reduction in f_p results in a modest change to $P_{n,day}$. While reducing f_p does cause $P_{g,day}$ to fall, it also results in a reduction in maintenance respiration, and so the influence on $P_{n,day}$ is moderated. This suggests that net carbon assimilation is relatively insensitive to variation over a fairly wide range of enzyme contents.

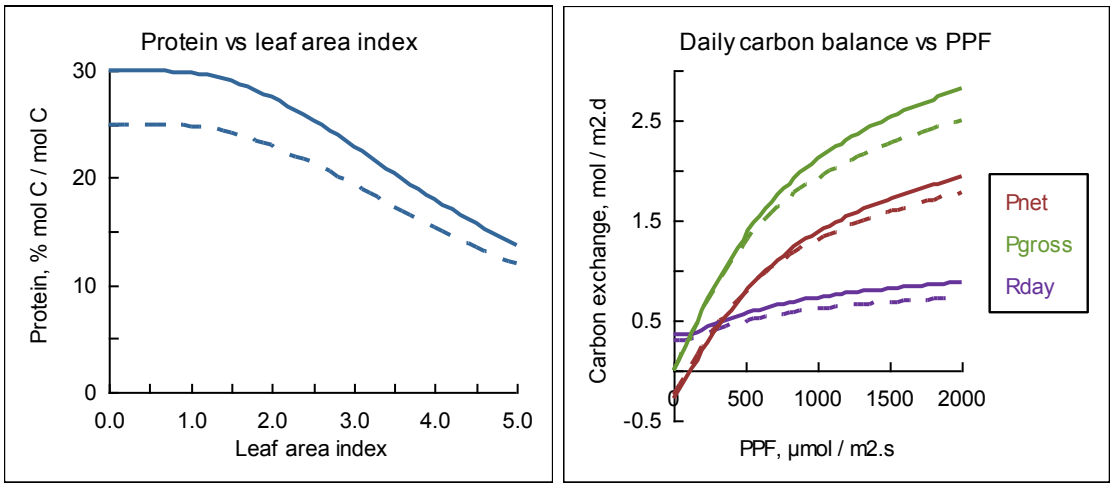

Figure 4.10: Photosynthetic enzyme distribution through the canopy, f_p, (left) for the default parameter values (Tables 4.1, 4.3; Table 3.3, Chapter 3), solid line, and $f_{p,0}$ reduced from 30 to 25 mol protein C (mol leaf C)$^{-1}$, dashed line. The graph on the right shows the corresponding daily net (red) and gross (green) photosynthetic rates. From PlantMod.

4.10 Further illustrations

The PlantMod program allows you to explore a wide range of canopy photosynthesis responses in relation to plant physiological characteristics and environmental conditions, and it is not possible to cover all of these here. Some simulations have been discussed above, particularly the general model behaviour and also the acclimation of photosynthetic enzymes through the depth of the canopy in response to environmental conditions. It is instructive to look at a few further examples. In these examples, all model environmental and physiological parameters take the default values (Tables 4.1, 4.3; Table 3.3, Chapter 3) unless indicated otherwise. As for Fig. 4.5, the mean temperature is defined as the mean of the day and night temperatures, and the difference in day and night temperatures is 10°C for the illustrations.

4.10.1 General model behaviour

The daily carbon balance was shown in Fig. 4.5 above as a function of PPF and temperature for the default model parameters. The corresponding graphs as functions of atmospheric CO_2, C, and leaf area index, L, are illustrated in Fig. 4.11. These graphs show the expected behaviour. In particular, note that both $P_{n,day}$ and $\mathrm{d}W/\mathrm{d}t$ reach a maximum at around $L = 5$, although there is little decline for greater values of L.

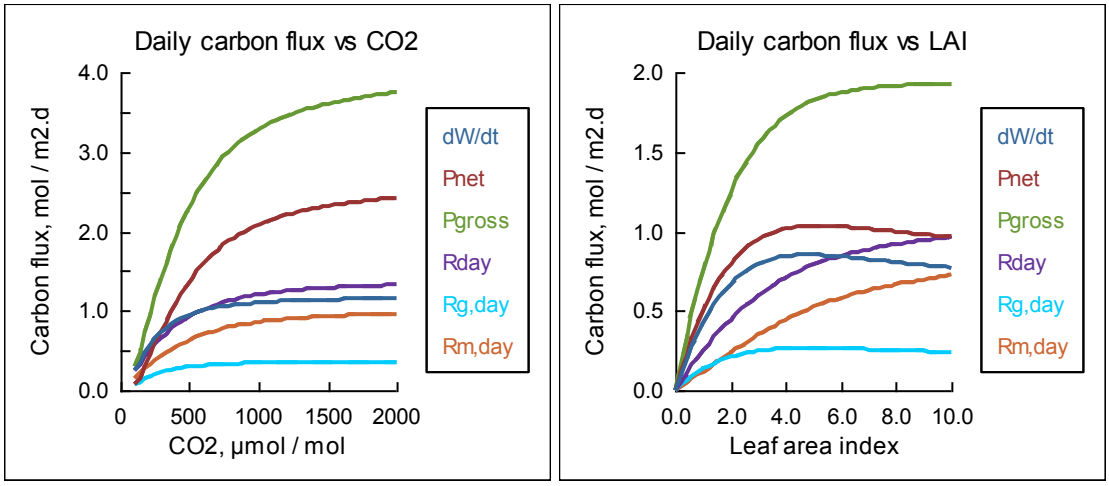

Figure 4.11: $\mathrm{d}W/\mathrm{d}t$, $P_{g,day}$, $P_{n,day}$, R_{day}, $R_{g,day}$, $R_{m,day}$ for the default environmental and physiological parameters. Left: CO_2 response. Right LAI response. Note the different vertical scales for the graphs.

The carbon use efficiency, CUE eqn (4.41), and canopy quantum yield, CQY eqn (4.42), are illustrated in Figs 4.12 and 4.13 as functions of PPF and temperature. Mean temperature denotes the average of day and night temperature with a 10°C difference. These curves are consistent with general observations reported in the literature.

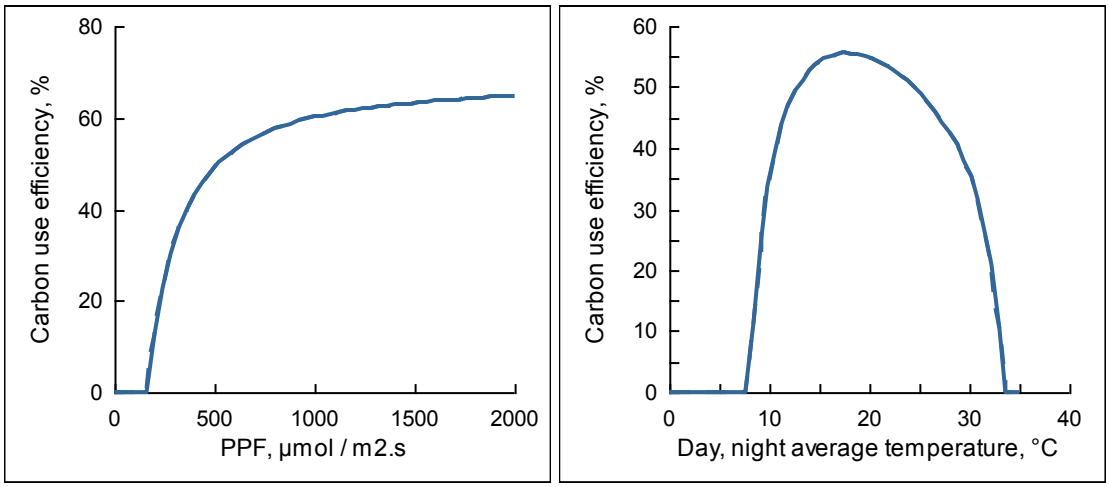

Figure 4.12: CUE for the default environmental and physiological parameters. Left: PPF response. Right temperature response. Mean temperature denotes the average of day and night temperature with a 10°C difference. From PlantMod.

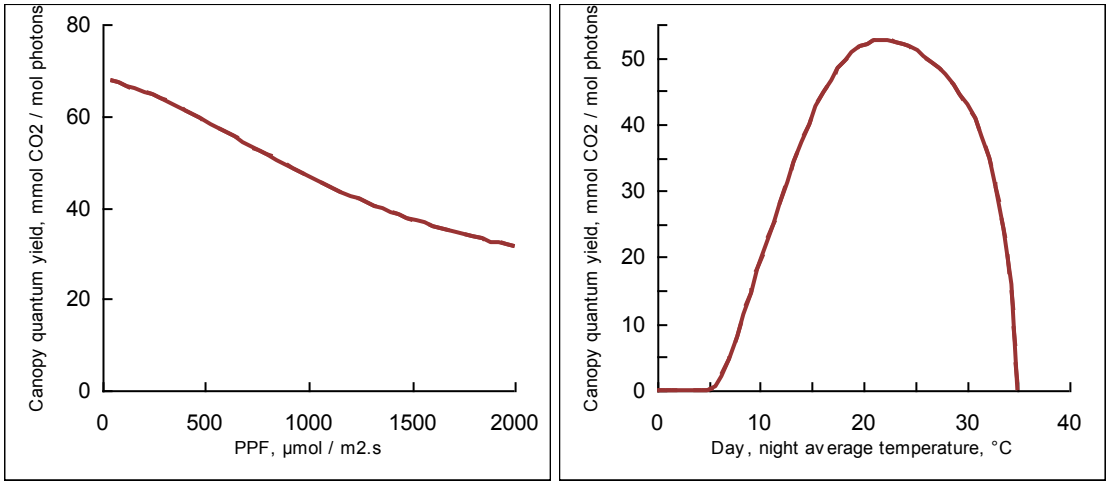

Figure 4.13: CQY for the default environmental and physiological parameters. Left: PPF response. Right temperature response. Mean temperature denotes the average of day and night temperature with a 10°C difference. From PlantMod.

The CUE and CQY are also illustrated as functions of C in Fig. 4.14 where it can be seen that both of these quantities approach asymptotic values at high C. Note that the maximum value the CQY can reach is the leaf photosynthetic efficiency, α eqn (3.4) in Chapter 3. This occurs at low PPF values when all of the leaves are on the initial part of the PPF response curve, as illustrated in Fig. 3.3 in Chapter 3.

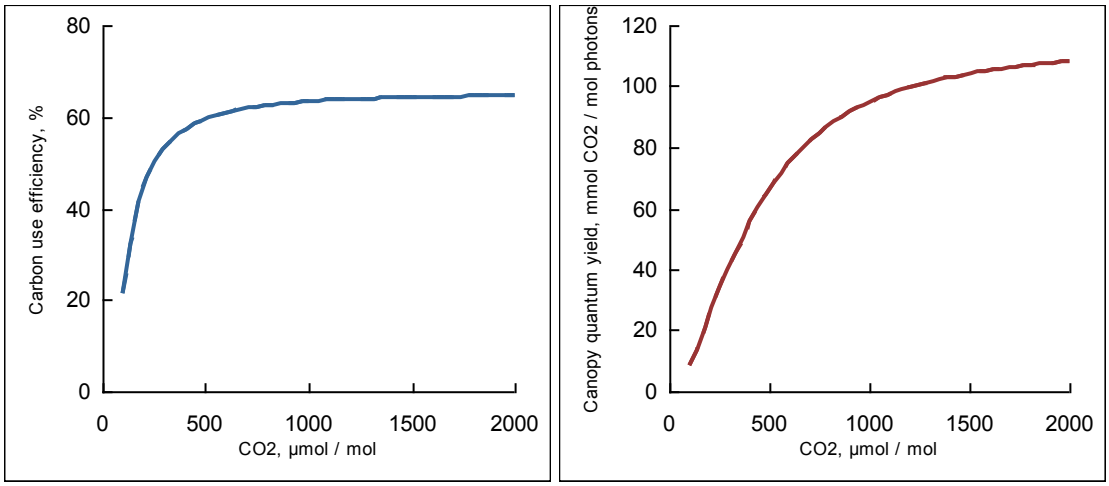

Figure 4.14: CUE (left) and CQY (right) in response to atmospheric CO_2 concentration for the default environmental and physiological parameters. From PlantMod.

The maintenance coefficient, m eqn (4.32), is shown in response to temperature in Fig. 4.15, which demonstrates the expected response. Note that m ranges from around 2 to 3% at typical temperatures, which is consistent with general observations.

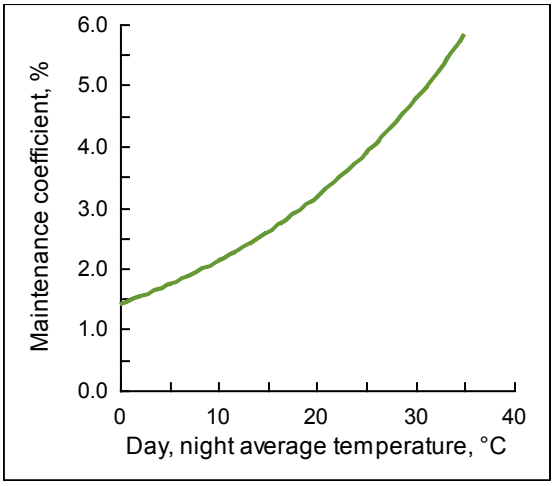

Figure 4.15: Maintenance coefficient, m, eqn (4.32), in response to temperature for the default environmental and physiological parameters. Mean temperature denotes the average of day and night temperature with a 10°C difference.

The growth efficiency, Y (4.28), is not illustrated graphically since it depends only on the prescribed plant composition. For the default simulation its value is

$$Y = 76.2\% \tag{4.45}$$

although this will vary in response to the enzyme content, f_p.

4.10.2 C_4 canopies

So far the illustrations have focused on C_3 canopies – C_4 canopies are now briefly considered. The optimum enzyme distribution for the default C_3 and C_4 canopies, is illustrated in Fig. 4.16, but with the day and night temperatures increased for the C_4 canopy by 5°C from 22/12°C to 27/17°C to reflect the generally higher temperatures that suit C_4 plants. It can be seen that the optimum enzyme distribution for C_4 species is considerably lower than for C_3, which is consistent with generally lower nitrogen contents in C_4 plants, which is reflected in their lower digestibility (eg Lazenby, 1988).

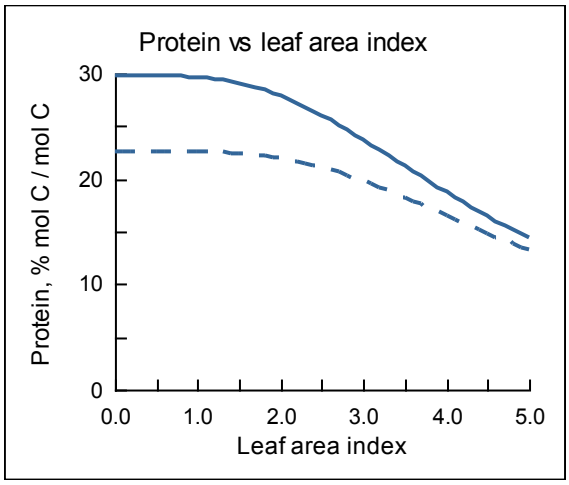

Figure 4.16: Optimum enzyme distribution through the canopy, f_p eqn (4.4), for the C_3 (solid line) and C_4 (dashed line) canopies. Default values are used for all parameters (Tables 4.1, 4.3; Table 3.3, Chapter 3), with the exception of the day and night temperatures for the C_4 canopy which are both increased by 5°C. From PlantMod.

The canopy daily gross and net photosynthesis, $P_{g,day}$ and $P_{n,day}$, and the daily respiration rate, R_{day}, are presented in Fig. 4.17 as functions of PPF and temperature. These responses are as expected with the C_4 canopies having greater rates of carbon assimilation.

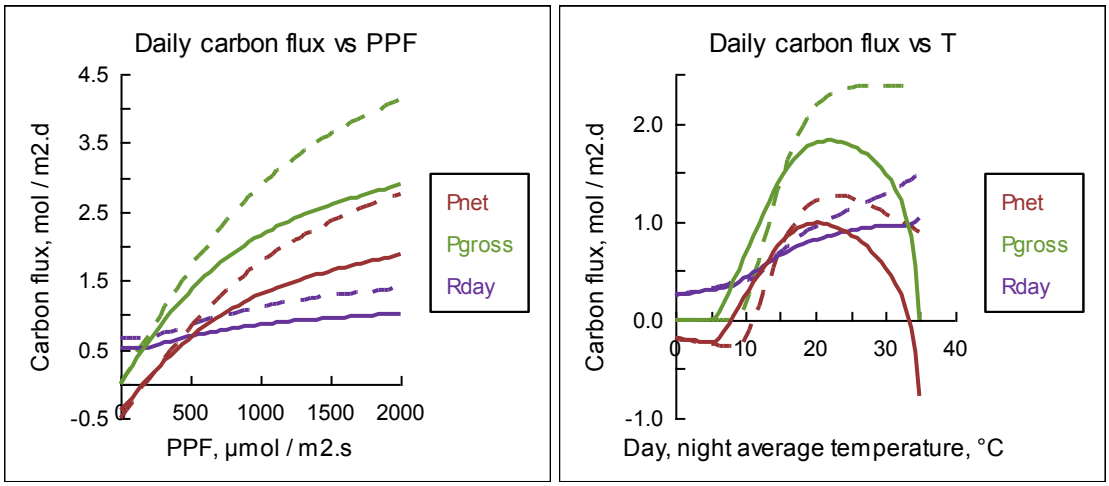

Figure 4.17: $P_{n,day}$, $P_{g,day}$ and R_{day} as functions of PPF (left) and temperature (right) for the default C_3 (solid lines) and C_4 (broken lines). Default values are used for all parameters (Tables 4.1, 4.3; Table 3.3, Chapter 3), with the exception of the day/night temperatures for the C_4 canopy, which are increased by 5°C to 27/22°C. From PlantMod.

4.11 Final comments

The theory presented in this Chapter has combined the treatment of light attenuation and interception in Chapter 2 and that for leaf photosynthesis in Chapter 3 to produce a versatile model of canopy photosynthesis that includes instantaneous and daily descriptions of canopy photosynthesis. Gross photosynthesis, net photosynthesis and respiration are considered as well as the growth and maintenance components of respiration and the derived quantities of carbon use efficiency and canopy quantum yield. The distribution of photosynthetic enzymes through the canopy has been considered and this can be seen to be important in the description of canopy photosynthesis through its influence on photosynthesis and respiration. The optimum distribution of photosynthetic enzymes has also been described. C_3 and C_4 canopies are included.

The model is structured in terms of parameters that have simple physiological interpretations and it is quite straightforward to define different characteristics such as cool or warm temperature species. PlantMod allows for an extensive exploration of the model and a large number of simulations can be explored.

4.12 Variables and parameters

Table 4.1: Environmental variables.
These values are used in illustrations unless stated otherwise.

Variable	Definition	Units
C, C_{amb}	Actual and current ambient atmospheric CO_2 concentration	380 μ mol CO_2 (mol air) $^{-1}$
f_s	Direct solar fraction of PPF	0.7
I	Photosynthetic photon flux, PPF	750 μmol photons m^{-2} s^{-1}
T	Temperature	22℃
T_d, T_n	Day and night temperature	22, 12℃
τ	Daylength	14×3600 secs (14 hours)

Table 4.2: Model variables, definitions, and units. PPF is photon flux density, μmol m^{-2} s^{-1}. Environmental parameters and model parameters are defined in Tables 4.1 and 4.3 respectively. Symbols are grouped for the canopy structure, light attenuation and interception, and canopy photosynthesis.

Variable	Definition	Units
	Canopy structure	
ℓ, ℓ_s, ℓ_d	Total cumulative leaf area index (LAI) within the canopy, and the components in direct (sun) and diffuse PPF	m^2 leaf (m^{-2} ground)
η	Fraction of gross photosynthesis allocated to shoot processes	-
ρ	Leaf fraction of shoot mass	-
σ	Specific leaf area	m^2 leaf (kg d.wt)$^{-1}$
	Light attenuation and interception	
f_p	Leaf enzyme, or protein, concentration. For canopy calculations, f_p is a function of ℓ	mol protein C (mol leaf C)$^{-1}$
$\bar{f_p}$	Mean enzyme concentration in the canopy	mol protein C (mol canopy C)$^{-1}$
$I(\ell)$, $I_s(\ell)$, $I_d(\ell)$	Total, direct and diffuse components of PPF within the canopy	μmol photons (m^{-2} ground) s^{-1}
$I_\ell(\ell)$, $I_{\ell,s}(\ell)$, $I_{\ell,d}(\ell)$	Total, direct and diffuse components of PPF incident on leaves within the canopy	μmol photons (m^{-2} leaf) s^{-1}
	Canopy photosynthesis	
CQY	Canopy quantum yield	mol CO_2 (mol photons)$^{-1}$
CUE	Carbon use efficiency	-
m	Maintenance respiration coefficient	day^{-1}
P_g	Instantaneous rate of canopy gross photosynthesis	μmol CO_2 (m^{-2} ground) s^{-1}
$P_{g,day}$	Daily rate of canopy gross photosynthesis	mol CO_2 (m^{-2} ground) d^{-1}

$P_{n,day}$	Daily rate of canopy net photosynthesis	mol CO_2 (m^{-2} ground) d^{-1}
$PPF_{day,abs}$	PPF for the day absorbed by the canopy	mol photons (m^{-2} ground) d^{-1}.
R_{day}, $R_{g,day}$, $R_{m,day}$	Total respiration, and growth and maintenance components	mol CO_2 (m^{-2} ground) d^{-1}
Y	Growth respiration efficiency	-

Table 4.3: Model parameters, definitions, units, and default values.
Environmental parameters and model variables are defined in Tables 4.1 and 4.2 respectively. Symbols are grouped for canopy respiration, and canopy structure. All leaf photosynthesis parameters are given in Table 3.3 in Chapter 3.

Parameter	Definition	Default value
	Canopy respiration	
m_{ref}	Maintenance respiration coefficient at the reference temperature, T_{ref}.	0.03 day^{-1}
Q_{10}	Q_{10} value for maintenance respiration.	1.5
T_{ref}	Reference temperature for R_m (same as for P_m in Chapter 2)	C_3: 20 °C; C_4: 25 °C
Y_p	Growth efficiency for protein synthesis	0.55
Y_w	Growth efficiency for cell wall synthesis	0.9
	Canopy structure	
$f_{p,0}$	Value of f_p at the top of the canopy	0.3 mol protein C (mol leaf C)$^{-1}$
$f_{p,b}$	Minimum value of f_p for a leaf	0.05 mol protein C (mol leaf C)$^{-1}$
k	Canopy extinction coefficient	0.5 m^2 ground (m^{-2} leaf)
L	Total canopy LAI	5 m^2 leaf (m^{-2} ground)
γ_p	Enzyme variation coefficient	5
η_{amb}	Carbon fraction allocated for shoot growth at C_{amb}	0.9
ρ_{amb}	Leaf fraction of shoot mass at C_{amb}	0.7
σ_{amb}	Specific leaf area at C_{amb}	15 m^2 leaf (kg d.wt)$^{-1}$
ς	Conversion factor for d.wt to mole units	mol C (kg d.wt)$^{-1}$

4.13 References

Anten NPR, Schieving F & Werger MJA (1995). Patterns of light and nitrogen distribution in relation to whole canopy carbon gain in C_3 and C_4 mono- and dicotyledonous species. *Oecologia*, **101,** 504-513.

Anten NPR (1997). Modelling canopy photosynthesis using parameters determined from simple non-destructive measurements. *Ecological Research,* **12,** 77-88.

Brouwer R (1962). Distribution of dry matter in the plant. *Netherlands Journal of Agricultural Science*, **10,** 361-376.

Cannell MGR & Thornley JHM (1998). Temperature and CO2 responses of leaf and canopy photosynthesis: a clarification using the non-rectangular hyperbola model of photosynthesis. *Annals of Botany,* **82,** 883-892.

Charles-Edwards DA (1981). *The mathematics of photosynthesis and productivity*. Academic Press, London, UK.

Davidson RL (1969). Effect of root/leaf temperature differentials on root/shoot ratios in some pasture grasses and clover. *Annals of Botany*, **33,** 561-569.

Dewar RC (1996). The correlation between plant growth and intercepted radiation: an interpretation in terms of optimal plant nitrogen content. *Annals of Botany,* **78,** 125-136.

de Pury DGG & Farquhar GD (1997). Simple scaling of photosynthesis from leaves to canopies without the errors of big-leaf models. *Plant, Cell and Environment,* **20,** 537-557.

Hikosaka K, Onoda Y, Kinugasa T, Nagashima H, Anten NPR & Hirose T (2005). Plant responses to elevated CO_2 concentration at different scales: leaf, whole plant, canopy and population.

Johnson IR (1990). Plant respiration in relation to growth, maintenance, ion uptake and nitrogen assimilation. *Plant, Cell and Environment*, **13,** 319-328.

Johnson IR, Riha SJ & Wilks DS (1995). Modelling daily net canopy photosynthesis and its adaptation to irradiance and atmospheric CO2 concentration. *Agricultural Systems*, **50,** 1-35.

Johnson IR, Parsons AJ & Ludlow MM (1989). Modelling photosynthesis in monocultures and mixtures. *Australian Journal of Plant Physiology,* **16,** 501-516.

Johnson IR, Thornley JHM, Franz J & Bugbee B (2010). Photosynthetic enzyme distribution through canopies and its acclimation to light, temperature and CO_2. *In review*.

Johnson IR & Thornley JHM (1987). A model of shoot:root partitioning with optimal growth. *Annals of Botany*, **60,** 133-142.

Kull O (2002). Acclimation of photosynthesis in canopies: models and limitations. *Oecologia,* **133,** 267-279.

Kull O & Jarvis PG (1995). The role of nitrogen in a simple scheme to scale up photosynthesis from leaf to canopy. *Plant, Cell and Environment*, **18,** 1174-1182.

Lazenby A (1988). The grass crop in perspective: selection, plant performance and animal production. In: *The grass crop – the physiological basis of production.* Eds MB Jones and A Lazenby, Chapman and Hall, London.

McCree KJ (1970). An equation for the respiration of white clover plants grown under controlled conditions. In: *Prediction and measurement of photosynthetic productivity*. Ed. I Setlik, Pudoc, Wageningen, The Netherlands.

Monod J (1972). *Chance and necessity*. Collins, London, UK.

Peri PL, Moot DJ, McNeil DL (2005). Modelling photosynthetic efficiency (α) for the light-response curve of cocksfoot leaves grown under temperate conditions. *European Journal of Agronomy*, **22,** 277-292.

Pritchard SG & Amthor JS (2005). Crops and environmental change. Food Products Press, New York, USA.

Rogers HH, Prior SA, Runion GB & Mitchell RJ (1996). Root to shoot ratio of crops as influenced by CO2, *Plant and Soil*, **187,** 229-248.

Sands PJ (1995). Modelling canopy production. I. Optimal distribution of photosynthetic resources, *Australian Journal of Plant Physiology*, **22,** 593-601.

Thornley JHM (1970). Respiration, growth and maintenance in plants. *Nature*, **227,** 304-305.

Thornley JHM (1972). A balanced quantitative model for root:shoot ratios in vegetative plants. *Annals of Botany,* **36,** 431-441.

Thornley JHM (1976). Mathematical models in plant physiology. Academic Press, London.

Thornley JHM (2002). Instantaneous canopy photosynthesis: analytical expressions for sun and shade leaves based on exponential light decay down the canopy and an acclimatized non-rectangular hyperbola for leaf photosynthesis. *Annals of Botany,* **89,** 451-458.

Thornley JHM (2004) Acclimation of photosynthesis to light and canopy nitrogen distribution: an interpretation. *Annals of Botany*, **93,** 473-475.

Thornley JHM and France J (2007). *Mathematical models in agriculture*. CAB International, Wallingford, UK.

Thornley JHM & Johnson IR (2000). *Plant and crop modelling*. Blackburn Press, Caldwell, New Jersey, USA.

White HL (1937). The interaction of factors in the growth of Lemma XII. The interaction of nitrogen and light intensity in relation to root length. *Annals of Botany*, **1,** 649-654.

Yin X, Lantinga EA, Schapendonk Ad HCM, Zhong X (2003). Some quantitative relationships between leaf area index and canopy nitrogen content and distribution. *Annals of Botany*, **91,** 893-903.

5 Canopy transpiration, temperature and energy budget

5.1 Introduction

The focus of this chapter is the instantaneous and daily transpiration from a canopy, its temperature, and the components of the energy balance. The theory of canopy transpiration has received much attention, and the most widely used model is the Penman-Monteith (PM) equation (Penman (1948) and Monteith (1965)). This approach is based on sound physical principles, and describes the influence of radiation, temperature, vapour deficit, windspeed and canopy structure on water use. As with any theory, there is always scope to incorporate greater complexity, but the PM equation provides an ideal description of canopy water use for most crop and pasture physiological studies, and is widely used in crop and pasture models. For further discussion see Monteith (1973), or the later edition Monteith and Unsworth (2008), Campbell (1977), or the later edition Campbell and Norman (1998), Jones (1992), Allen *et al.* (1998), Thornley and Johnson (2000), Thornley and France (2007). Background definitions for radiation, water vapour and conductance are given in Chapter 1, while the canopy radiation balance was discussed in Chapter 2: this material will be referred to frequently throughout this Chapter. Canopy transpiration is influenced by canopy temperature which, in turn, is affected by the prevailing environmental conditions. A key part of the analysis for canopy transpiration is the elimination of canopy temperature so that transpiration is defined in terms of air temperature and other environmental factors. Instead of eliminating canopy temperature, it is possible to eliminate transpiration in the analysis and derive an expression for canopy temperature as a function of environmental conditions. Once canopy transpiration and temperature are known, the various terms in the canopy energy budget can be evaluated. The analysis here will therefore consider canopy transpiration, followed by the equivalent approach to calculate canopy temperature. The components in the canopy energy balance are then presented.

For daily crop and pasture models that work with standard meteorological data, transpiration is generally required in units of mm d^{-1} to be consistent with rainfall. However, since PlantMod uses mole units for conductance (Section 1.6 in Chapter 1), the analysis here derives transpiration with mole units. The conversion is straightforward with

$$1 \text{ mol water} \equiv 0.018 \text{ kg water} \tag{5.1}$$

and

$$1 \text{ kg water m}^{-2} \equiv 1 \text{ mm water} \tag{5.2}$$

so that

$$1 \text{ mol water m}^{-2} \equiv 0.018 \text{ mm water} \tag{5.3}$$

PlantMod allows transpiration and evaporation to be defined either as moles or mm water.

5.2 Transpiration

Transpiration involves the energy balance for the crop which, in turn, is defined in terms of the shortwave and longwave radiation balance. The analysis is derived using the energy balance for a canopy, as discussed in Chapter 2, and does not explicitly include variation in leaf transpiration

through the canopy, but uses the standard *big-leaf* approach whereby it is assumed that the canopy can be regarded as a single big leaf. While it is common to present the analysis for full ground cover, the approach here is to consider the energy balance of the canopy in terms of actual ground cover. The derivation is presented for the instantaneous canopy transpiration (mol water m^{-2} s^{-1}) which is then applied to give the daily value (mol water m^{-2} d^{-1}).

It must be emphasized here that, while the canopy calculations are expressed as per unit ground area, they do not include the soil energy balance. Thus, they should not be interpreted as being the total ground area energy balance calculations.

5.2.1 Instantaneous transpiration

The net radiation balance for the canopy, J_n (J m^{-2} s^{-1}) , was derived in Section 2.8 in Chapter 2. The energy balance of the canopy affects the following components:

1. the transpiration rate, E (mol water m^{-2} s^{-1});
2. heat transfer between the canopy and the air, H (J m^{-2} s^{-1});
3. heat transfer between the canopy and the soil;
4. heat storage by the canopy;
5. metabolic process of photosynthesis and respiration.

Of these, the last three are generally negligible and so are ignored in the analysis. Note that, while the heat transfer between the canopy and the soil is ignored, the analysis for the net radiation balance of the canopy does account for solar radiation that is transmitted through the canopy to the soil. Thus, neglecting components 3, 4 and 5, the energy balance for the canopy is therefore

$$J_n = H + \lambda E \tag{5.4}$$

where λ (J mol^{-1}) is the latent heat of vaporization of water. While λ does vary with temperature, this variation is small, and a standard value that is widely used is 44.1kJ mol^{-1} which is the value at 20°C (see eqn (1.91) in Chapter 1).

It is quite common to proceed from here to derive the canopy transpiration in terms of the canopy net radiation balance. However, as was seen in Chapter 2, the net outgoing longwave radiation actually involves the canopy temperature, and the aim of the theory is to eliminate canopy temperature to define transpiration solely in terms of atmospheric conditions. The separate terms of the net radiation balance, eqn (2.67) are therefore used.

Combining eqn (5.4) with eqn (2.67) gives

$$f_g\left[J_n' - c_p g_r\left(T_c - T_a\right)\right] = H + \lambda E \tag{5.5}$$

where f_g is the fractional ground cover by the canopy, J_n' (J m^{-2} s^{-1}) is the canopy isothermal net radiation (see Section 2.8.3, Chapter 2), c_p is the specific heat capacity of the air (J mol^{-1} K^{-1}), g_r (mol m^{-2} s^{-1}) is the radiative conductance (eqn (2.52) in Chapter 2), and T_c and T_a are the canopy and bulk air temperatures (K or °C since the difference is the same for both units). The specific heat capacity of the air, c_p, will depend on the atmospheric composition but a good standard value to use is 29.3 J mol^{-1} K^{-1}, which is based on a value of 0.029 kg mol^{-1} for the molar mass of dry air (see eqn (1.69) in Chapter 1). The canopy isothermal net radiation in eqn (5.5) was discussed in Section 2.8.3 in Chapter 2, and is the net radiation balance, including both shortwave (solar) and longwave components, for a canopy with full ground cover under isothermal conditions (that is, $T_c = T_a$). The second term on the left-hand-side of eqn (5.5) accounts for the influence of the difference between

the canopy and air temperatures on the net outgoing longwave radiation. The ground cover was derived in Chapter 2 and is given by

$$f_g = 1 - e^{-kL} \tag{5.6}$$

where k, (m^2 ground) (m^{-2} leaf), is the canopy extinction coefficient and L, (m^2 leaf) (m^{-2} ground), is the leaf area index.

The sensible heat flux between the canopy and the air is defined by Fourier's law of heat transfer, which can be written as

$$H = f_g c_p g_H \left(T_c - T_a\right) \tag{5.7}$$

where g_H is the conductance for heat (mol m^{-2} s^{-1}). Note the presence of the ground cover term, f_g.

Eliminating H from eqns (5.5) and (5.7) gives

$$f_g \left(T_c - T_a\right) c_p \left(g_H + g_r\right) = f_g J_n' - \lambda E \tag{5.8}$$

The transpiration across the boundary layer from the evaporating surface to the bulk air stream, as discussed in Section 1.6 in Chapter 1, is given by

$$E = g_v \frac{e_{v,l} - e_{v,a}}{P} \tag{5.9}$$

where $e_{v,l}$ and $e_{v,a}$ (kPa) are the vapour pressures within the leaf and atmosphere respectively, P (kPa) is the atmospheric pressure, and g_v (mol m^{-2} s^{-1}) is the conductance for water vapour. Again, since the pressure ratios are used, there is no problem using kPa pressure units. This equation for the canopy transpiration rate, E, does not include the fractional ground cover term f_g since the influence of leaf area index is included in the conductance term g_v, as discussed later.

Equation (5.9) for E involves the vapour pressure at the evaporating surface, e_l, which is the sub-stomatal cavity of the leaves. It is readily shown that the vapour pressure (or density) at this evaporating surface is, to a very good approximation, saturated (eg, Thornley and Johnson, 2000, p. 205), so that

$$e_{v,l} \approx e_v'\left(T_c\right) \tag{5.10}$$

where $e_v'(T_c)$ is the saturated vapour pressure at the canopy temperature. For most practical situations this will be more than 99% accurate. $e_v'(T_c)$ can be expanded as a Taylor series and, taking the first two terms, can be written as

$$e_v'\left(T_c\right) = e_v'\left(T_a\right) + sP\left(T_c - T_a\right) \tag{5.11}$$

where

$$s = \frac{1}{P}\frac{\mathrm{d}e_v'}{\mathrm{d}T}\left(T = T_a\right) \tag{5.12}$$

is the of the slope of the saturated vapour density with respect to temperature at the air temperature divided by atmospheric pressure, with units K^{-1} or °C^{-1}. Using the Teten formula, eqn (1.76) in Chapter 1, and normal pressure P = 101.325 kPa, eqn (5.12) can be evaluated as

$$s = \frac{25.4}{\left(T + 241\right)^2} \exp\left(\frac{17.5T}{T + 241}\right) \tag{5.13}$$

Using eqns (5.10) and (5.11), eqn (5.9) can be written

$$E = g_v\left[\Delta e_{v,a}/P + s\left(T_c - T_a\right)\right] \tag{5.14}$$

where

$$\Delta e_{v,a} = e'_v\left(T_a\right) - e_{v,a} \tag{5.15}$$

is the vapour pressure deficit of the air (kPa).

Combining eqns (5.8) and (5.14) to eliminate $(T_c - T_a)$ leads to

$$E = \frac{f_g\left[sJ'_n + \lambda\gamma\left(g_H + g_r\right)\Delta e_{v,a}/P\right]}{\lambda\left[s + \gamma f_g\left(\frac{g_H + g_r}{g_v}\right)\right]} \tag{5.16}$$

where

$$\gamma = \frac{c_p}{\lambda} = 664\times 10^{-6} \text{ mol water (mol air)}^{-1}\text{ K}^{-1} \tag{5.17}$$

Is known as the psychrometric parameter. Note that since λ varies slightly with temperature, γ is not constant but will also vary with temperature. However, this variation has negligible effect on the simulations and so the constant value in eqn (5.17) is used. It can be seen from eqn (5.16) that canopy transpiration is not directly proportional to ground cover, f_g, since this term is in both the numerator and denominator.

It now remains to consider the conductance terms g_H and g_v. First consider the conductance for water vapour, g_v. The water vapour transfer pathway includes movement out of the sub-stomatal cavities from the evaporating surfaces to the leaf surfaces and then from the leaf surfaces across the boundary layer to the bulk air stream. g_v can therefore be partitioned into the components for the transfer across the stomates and then to the bulk air stream. Denoting these by g_c and g_a respectively, it follows that

$$\frac{1}{g_v} = \frac{1}{g_c} + \frac{1}{g_a} \tag{5.18}$$

Note that the reciprocals of conductance are used, which are equivalent to resistances, and these are summed since they are in series (see section 1. in Chapter 1). g_c is termed the canopy conductance, and is related to stomatal conductance, as discussed below. g_a is termed the boundary layer conductance.

For turbulent flow, the transport of both heat and water vapour is dominated by eddy diffusion so that the processes are the same and so the conductances for heat and water vapour from the canopy to the bulk air stream can be taken to be equal (Jones, 1992), that is

$$g_H = g_a \tag{5.19}$$

Equation (5.16) now becomes

$$E = \frac{f_g\left[sJ'_n + \lambda\gamma\left(g_a + g_r\right)\Delta e_{v,a}/P\right]}{\lambda\left[s + \gamma f_g\left(g_a + g_r\right)\left(1/g_c + 1/g_a\right)\right]} \tag{5.20}$$

This is the form of the Penman-Monteith (PM) equation that is widely used, although it is generally derived for full ground cover with $f_g = 1$. Earlier derivations (eg Thornley and Johnson, 2000) did not incorporate the radiative conductance, g_r. The PM equation describes the transpiration rate as a function of the isothermal radiation, J'_n, the vapour pressure deficit, $\Delta e_{v,a}$, the canopy and boundary layer conductances, g_c and g_a, the radiative conductance, g_r, and the physical parameters λ, s and γ, which depend on air temperature, and are readily available from standard tables or functions. J'_n is a function of solar radiation, J_S, and the net isothermal outgoing longwave radiation, $J'_{L,n}$. $J'_{L,n}$ is related to temperature, vapour pressure, and cloud cover according to the analysis in section 2.8.3 in Chapter 2. Leaf area index, L, affects the ground cover term, f_g, through eqn (5.6), and it also influences the canopy and boundary layer conductances through eqns (5.44) and (5.50). Equation (5.20) is attributed to Penman (1948) for his analysis that eliminated canopy temperature, and to Monteith (1965) for the treatment of the canopy and boundary layer conductances.

5.2.2 Daily transpiration

The daily transpiration rate, E_{day} (mol water m^{-2} d^{-1}), is the sum of the instantaneous transpiration rate throughout the day. In order to calculate E_{day}, it is assumed that the stomata close at night so that there is no transpiration during the dark period. Thus, using the notation from Chapter 2 where daily radiation terms are denoted by R, with the same subscripts as for J to describe the individual components, eqn (5.20) can be applied to give

$$E_{day} = \frac{f_g\left[sR'_{n,day} + 86{,}400 f_{day}\lambda\gamma\left(g_a + g_r\right)\Delta e_{v,a}/P\right]}{\lambda\left[s + \gamma f_g\left(g_a + g_r\right)\left(1/g_c + 1/g_a\right)\right]} \tag{5.21}$$

where the temperature and vapour deficit are mean daytime values, $R'_{n,day}$ (J m^{-2} d^{-1}) is the total net isothermal radiation during the daytime period, f_{day} is the daytime fraction (eqn 2.23) and 86,400 is the number of seconds in 24 hours. $R'_{n,day}$, derived from eqn (2.69) in Chapter 2, involves temperature, vapour density, daily solar radiation, latitude and day of year. E_{day} is converted to the more common units of mm water day^{-1} by using eqn (5.3), which gives

$$E_{day,mm} = 0.018 E_{day} \tag{5.22}$$

5.2.3 Summary of climate inputs

The analysis in the previous section has derived the canopy transpiration rate in terms of climatic inputs. These inputs are briefly summarised here.

Instantaneous transpiration

- Incoming solar, or shortwave, radiation, J m^{-2} s^{-1}
- Air temperature (°C)
- Vapour pressure (kPa)
- Windspeed (m s^{-2})
- Fractional cloud cover (0 — 1)

The fractional cloud cover is used in the calculation of the isothermal net radiation, $J'_{L,n}$, eqn (2.63).

Daily transpiration

- Incoming solar, or shortwave, radiation, J m^{-2} d^{-1} (often available as MJ m^{-2} d^{-1})

- Mean daytime air temperature (°C)
- Vapour pressure (kPa)
- Windspeed (m s^{-2})
- Latitude (° which is converted to rad in the calculations)
- Day of year

The latitude and day of year are used in the calculation of potential daily solar radiation which is used to calculate the daily isothermal net radiation, $R'_{L,n,day}$, see Section 2.8.4 in Chapter 2.

Vapour pressure and relative humidity

In the PlantMod program, it is possible to specify atmospheric moisture content either as vapour pressure in kPa units or relative humidity as percent. If relative humidity is used, then the vapour pressure is calculated from temperature and is displayed on the PlantMod interface. On the other hand, if vapour pressure is specified, then the relative humidity is prescribed. For the daily simulations, it is assumed that the vapour pressure is constant for the day and night. In this case, daytime relative humidity can be prescribed and used to calculate vapour pressure which is, in turn, used to calculate nighttime relative humidity from the nighttime temperature.

5.3 Temperature

In the above analysis, eqns (5.8) and (5.14) were combined to eliminate the temperature difference $T_c - T_a$. Eliminating transpiration, E, instead, leads to

$$(T_c - T_a)\left[f_g c_p (g_H + g_r) + \lambda s g_v\right] = f_g J'_n - \lambda g_v \Delta e_{v,a}/P \tag{5.23}$$

so that, using (5.17), (5.18), (5.19), it follows that

$$T_c = T_a + \frac{f_g J'_n (1/g_c + 1/g_a) - \lambda \Delta e_{v,a}/P}{\lambda\left[s + \gamma f_g (g_a + g_r)(1/g_c + 1/g_a)\right]} \tag{5.24}$$

which is the temperature equivalent to the PM equation. As for transpiration, the leaf area index, L, affects the ground cover term, f_g, through eqn (5.6), and the canopy and boundary layer conductances through eqns (5.44) and (5.50).

The mean daytime canopy temperature can be calculated by using the daytime value of J'_n (Section 2.8.3 in Chapter 2), so that

$$T_{c,day} = T_{a,day} + \frac{f_g J'_{n,day} (1/g_c + 1/g_a) - \lambda \Delta e_{v,a}/P}{\lambda\left[s + \gamma f_g (g_a + g_r)(1/g_c + 1/g_a)\right]} \tag{5.25}$$

For the nighttime, there is no solar radiation and the stomata are closed, so that $g_c = 0$, and using eqn (2.66) leads to

$$T_{c,night} = T_{a,night} - \frac{f_g J'_{L,n,night}}{\lambda\gamma (g_a + g_r)} \tag{5.26}$$

where the nighttime isothermal net outgoing radiation is defined by eqn (2.59). It can be seen that if $J'_{L,n,night}$ is positive then the canopy will be cooler than the air at night, whereas if it is negative, the canopy will be warmer.

5.4 Energy components

The analysis deriving canopy transpiration and temperature involves the canopy energy balance, which is defined in terms of the net radiation balance, the latent heat of vaporization and the sensible heat flux of the canopy. The net radiation balance involves the absorbed solar, absorbed longwave, and emitted longwave radiation, with the latter combining to give the net outgoing longwave radiation. Since both canopy transpiration, E, and the canopy temperature, T_c, have been calculated, it is quite straightforward to evaluate these components of the radiation balance and look at how they each respond to the environmental conditions. These energy terms were derived either in Chapter 2 or in this Chapter, and are summarized here.

The environmental inputs for defining the energy components are the incoming solar radiation, J_S, the isothermal net outgoing longwave radiation , $J'_{L,n}$, and the temperature difference between the canopy and air, $T_c - T_a$, as derived in this Chapter. The transpiration rate that is also derived here is used for the latent heat flux. For daily energy calculations, the corresponding daily environmental inputs, temperature difference between the canopy and air, and transpiration rate are used. Note that in PlantMod, for daily illustrations the separate daytime and nighttime energy components can be plotted.

5.4.1 Latent heat flux

The instantaneous latent heat flux, which is the heat lost by the canopy, is

$$\text{Canopy latent heat loss} = \lambda E \quad \text{J m}^{-2}\ \text{s}^{-1} \tag{5.27}$$

and the daily value is

$$\text{Daily canopy latent heat loss} = \lambda E_{day} \quad \text{J m}^{-2}\ \text{d}^{-1} \tag{5.28}$$

5.4.2 Sensible heat flux

The sensible heat flux is the energy flux between the canopy and air as a result of their temperature difference. The instantaneous value is

$$H = f_g c_p g_a \left(T_c - T_a\right) \quad \text{J m}^{-2}\ \text{s}^{-1} \tag{5.29}$$

and for the day it becomes

$$H_{day} = 86,400 f_g c_p g_a \times \left[f_{day}\left(T_{c,day} - T_{a,day}\right) + \left(1 - f_{day}\right)\left(T_{c,night} - T_{a,night}\right) \right] \quad \text{J m}^{-2}\ \text{d}^{-1} \tag{5.30}$$

5.4.3 Absorbed solar radiation

The instantaneous absorbed solar radiation is

$$J_{S,a} = f_g \left(1 - \alpha\right) J_S \quad \text{J m}^{-2}\ \text{s}^{-1} \tag{5.31}$$

while the daily value is

$$R_{S,a} = f_g \left(1 - \alpha\right) R_S \quad \text{J m}^{-2}\ \text{d}^{-1} \tag{5.32}$$

5.4.4 Absorbed longwave radiation

The instantaneous absorbed longwave radiation is given by

$$J_{L,a} = f_g \left[\varepsilon \sigma T_{K,a}^4 - J'_{L,n} \right] \quad \text{J m}^{-2}\ \text{s}^{-1} \tag{5.33}$$

and for the whole day it is

$$R_{L,a} = f_g \left[86,400 f_{day} \varepsilon \sigma T_{K,a,day}^4 + 86,400 \left(1 - f_{day}\right) \varepsilon \sigma T_{K,a,night}^4 - R'_{L,n} \right] \quad \text{J m}^{-2}\ \text{d}^{-1} \tag{5.34}$$

5.4.5 Emitted longwave radiation

The instantaneous emitted longwave radiation is

$$J_{L,e} = f_g \varepsilon \sigma T_{K,c}^4 \quad \text{J m}^{-2}\ \text{s}^{-1} \tag{5.35}$$

The corresponding daily value is

$$R_{L,e} = 86,400 f_g \varepsilon \sigma \left[f_{day} T_{K,c,day}^4 + \left(1 - f_{day}\right) T_{K,c,night}^4 \right] \quad \text{J m}^{-2}\ \text{d}^{-1} \tag{5.36}$$

5.4.6 Net outgoing longwave radiation

The instantaneous net outgoing longwave radiation is

$$J_{L,n} = f_g \left[J'_{L,n} + c_p g_r \left(T_c - T_a \right) \right] \quad \text{J m}^{-2}\ \text{s}^{-1} \tag{5.37}$$

$J_{L,n}$ is also given by

$$\begin{aligned} J_{L,n} &= J_{L,e} - J_{L,a} \\ &= f_g \left[J'_{L,n} + \varepsilon \sigma \left(T_{K,c}^4 - T_{K,a}^4 \right) \right] \end{aligned} \tag{5.38}$$

and it can be shown that eqns (5.37) and (5.38) are equivalent by using eqns (2.51) and (2.53) in Chapter 2.

The daily net outgoing longwave radiation is

$$\begin{aligned} R_{L,n} &= f_g R'_{L,n} + \\ & f_g 86,400 c_p g_r \left[f_{day} \left(T_{c,day} - T_{a,day} \right) + \left(1 - f_{day}\right) \left(T_{c,night} - T_{a,night} \right) \right] \end{aligned} \quad \text{J m}^{-2}\ \text{d}^{-1} \tag{5.39}$$

5.4.7 Net radiation balance

The overall instantaneous net radiation balance for the canopy is now

$$J_n = J_{S,a} - J_{L,n} \tag{5.40}$$

where eqns (5.31) and (5.37) are used.

Similarly, the daily net radiation balance is

$$R_n = R_{S,a} - R_{L,n} \tag{5.41}$$

which uses eqns (5.32) and (5.39).

5.5 Canopy conductances

The canopy and boundary layer conductances need to be specified in the PM equation and associated calculations for canopy temperature. The canopy height is first defined as a function of leaf area index, as this is required in the calculation for boundary layer conductance.

5.5.1 Canopy height

In order to evaluate canopy conductance as defined above, it is necessary to prescribe the canopy height. The usual strategy is to relate canopy height to LAI. Allen *et al.* (1998) assume a linear relationship but a more general curvilinear form is used here, as given by

$$h = h_{mx}\left(1 - e^{-0.69L/L_h}\right) \tag{5.42}$$

where h_{mx} (m) is the maximum canopy height attained as leaf area index, L, increases, 0.69 =ln(2), and L_h is the LAI at which the height is half maximal, so that $h = h_{mx}/2$ when $L = L_h$. The default values

$$L_h = 1, \quad h_{mx} = 1 \text{ m} \tag{5.43}$$

are used in PlantMod.

While eqn (5.42) is quite flexible for the relationship between canopy height and LAI, in practice this may change during crop development. For example, following anthesis in cereals and pastures, stem elongation occurs with little change in LAI. Equation (5.42) is illustrated in Fig. 5.1.

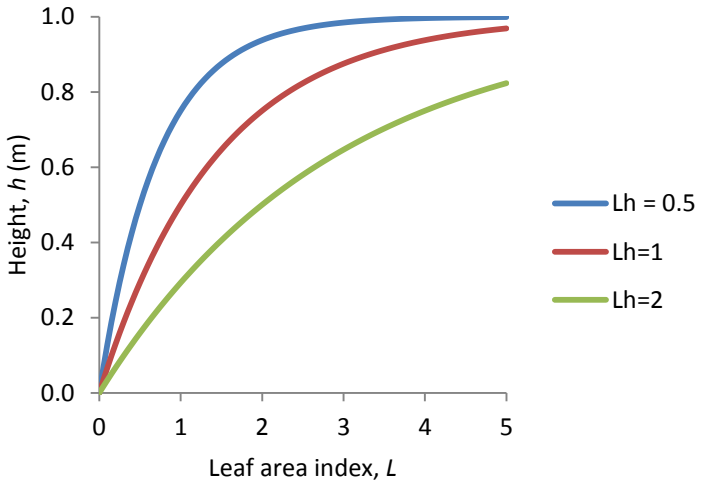

Figure 5.1: Relationship between canopy height, h (m), and LAI, L, using eqn (5.42) with $h_{mx} = 1$ and different values for L_h as indicated.

The illustration in Fig. 5.1 is most applicable to a crop. Many applications of the canopy energy balance focus on turf grass which may be maintained at around 5 to 15 cm. In this case, it is necessary to set $h_{mx} = 1$ to an appropriate value.

5.5.2 Canopy conductance

For canopy conductance, it is assumed that

$$g_c = L_{live} g_\ell \tag{5.44}$$

where, L_{live} is the canopy live leaf area index and g_ℓ, mol m^{-2} s^{-1}, is the mean stomatal conductance for the leaves, and must account for both sides of the leaves. It is assumed that the live component of the leaf area index, L, is

$$L_{live} = f_{L,live} L \tag{5.45}$$

where the default value

$$f_{L,live} = 0.8 \tag{5.46}$$

is used.

The possible dependence of stomatal conductance on environmental conditions must be considered. With traditional units of m s^{-1} for stomatal conductance it is possible to apply the basic physics of diffusion to derive the direct temperature and pressure effects, and this was discussed in Section 1.6 in Chapter 1. Converting to mol m^{-2} s^{-1}, the conductance depends on temperature alone and is given by eqn (1.91), although for practical temperatures this variation is quite small and can be ignored. As discussed in Section 1.6.4 in Chapter 1, responses to environment are observed that are a direct result of climatic conditions on stomatal aperture. A simple empirical approach was introduced to capture these effects and is very similar to the widely used equation proposed by Ball *et al* (1987). It is therefore assumed that the influence of the environmental conditions on g_ℓ is defined by

$$g_\ell = g_{\ell,ref} f_{g,J}(J) f_{g,h_r}(h_r) f_{g,C}(C) \tag{5.47}$$

where the three f functions capture the stomatal conductance response to irradiance or photosynthetic photon flux, J (Chapter 2), relative humidity, h_r (Section 1.5.2), and atmospheric CO_2 concentration, C (Section 1.5.1), and $g_{s,ref}$ is a reference value of g_ℓ, so that

$$g_\ell\left(J_S = J_{S,ref}, h = h_{r,ref}, C = C_{amb}\right) = g_{\ell,ref} \tag{5.48}$$

with the default value

$$g_{\ell,ref} = 0.2 \text{ mol m}^{-2}\text{ s}^{-1} \tag{5.49}$$

The remainder of the default parameters are given in Section 1.6.4 in Chapter 1, where the response functions are illustrated. These functions define the response to irradiance as increasing to an asymptote as irradiance increase, increasing from a non-zero level as relative humidity increases, and decreasing as atmospheric CO_2 increases. This approach is applied directly for the instantaneous calculations and, for daily values, the mean daytime environmental conditions are used.

5.5.3 Boundary layer conductance

Various slightly different expressions have been used for the boundary layer conductance, and for references see Thornley and France (2007). A discussion is also given by Blonquist *et al.* (2009). Allen *et al.* (1998, eqn(4)) define the boundary layer conductance, g_a mol m^{-2} s^{-1}, by

$$g_a = \frac{41.6\kappa^2 u_z}{\ln\left(\frac{z-d}{\zeta_m}\right)\ln\left(\frac{z-d}{\zeta_{Hv}}\right)} \tag{5.50}$$

where $\kappa = 0.41$ (dimensionless) is von Karman's constant, u_z (m s^{-1}) is the windspeed measured at height z (m), d (m) is the *zero plane displacement*, which is the projected height at which the windspeed is zero, ζ_m (m) is the roughness length governing momentum transfer, ζ_{Hv} is the roughness length governing the transfer of heat and water vapour, and 41.6 mol m^{-3} is the molar density of air and converts conductance from m s^{-1} to mol m^{-2} s^{-1} (see Section 1.6 in Chapter 1). The reference height is taken to be

$$z = 2 \text{ m} \tag{5.51}$$

A similar equation, derived by Campbell (1977), is

$$g_a = \frac{41.6\kappa^2 u_z}{\ln\left(\frac{z+\varsigma_m-d}{\varsigma_m}\right)\ln\left(\frac{z+\varsigma_{Hv}-d}{\varsigma_{Hv}}\right)} \tag{5.52}$$

A derivation of this equation is also presented in Thornley and Johnson (2000).

According to Blonquist *et al.* (2009), a more general equation based on the Monin-Obukov Similarity Theory (MOST) (Monin & Obukhov, 1954) is

$$g_a = \frac{41.6\kappa^2 u_z}{\left[\ln\left(\frac{z-d}{\varsigma_m}\right)-\psi_m\right]\left[\ln\left(\frac{z-d}{\varsigma_{Hv}}\right)-\psi_{Hv}\right]} \tag{5.53}$$

where ψ_m and ψ_{Hv} are stability terms. These stability terms are difficult to calculate for practical applications as is apparent from the discussion by Blonquist *et al.* (2009).

Regardless of which of these equations are used, the parameters d, ζ_m and ζ_{Hv} are generally assumed to be proportional to the canopy height and Blonquist *et al.* (2009) give these responses as

$$\begin{aligned} d &= 0.65h \\ \varsigma_m &= 0.14h \\ \varsigma_{Hv} &= 0.028h \end{aligned} \tag{5.54}$$

There are practical problems with each of these equations for g_a with (5.54) since g_a approaches zero as either the windspeed, u_z, approaches zero or the canopy height, h, approaches zero. In addition, the stability parameters ψ_m and ψ_{Hv} are difficult to define (see Blonquist *et al.*, 2009). If g_a is zero, or close to zero, the canopy temperature which was discussed earlier, becomes very large – possibly in excess of 50°C above air temperature – which is inconsistent with general experimental observations (Bruce Bugbee, *pers. comm.*). These problems arise since the theory does not adequately deal with low windspeeds or canopy height. With regard to windspeed, when u_z is at, or close to, zero, buoyancy effects for vapour transport will be significant and the theory does not adequately deal with this. For low h, the linear relationships in eqn (5.54) are unlikely to be valid.

These limitations are important since the aim of PlantMod is to be able to deal with all practical conditions, which will include very low windspeeds and canopy heights. For example, many studies of canopy transpiration and temperature focus on turfgrass which may be maintained at heights of around 5 cm.

Rather than attempt to add greater complexity to the theory, a much simpler approach is used in PlantMod that captures the general characteristics of the expected behaviour for canopy conductance. g_a is assumed to be given by

$$g_a = g_{a,0} + \left(g_{a,ref} - g_{a,0}\right)\frac{u}{u_{ref}}\left(\frac{h}{h_{ref}}\right)^{0.5} \tag{5.55}$$

where $g_{a,ref}$ is the value of g_a at the reference windspeed u_{ref} and canopy height h_{ref}. The reference values for windspeed and canopy height are taken to be

$$u_{ref} = 2 \text{ m s}^{-1}$$
$$h_{ref} = 0.3 \text{ m} \tag{5.56}$$

and the default conductance parameters are

$$g_{a,0} = 0.3 \text{ mol m}^{-2} \text{ s}^{-1}$$
$$g_{a,ref} = 0.8 \text{ mol m}^{-2} \text{ s}^{-1} \tag{5.57}$$

The values in (5.57) have been derived by fitting to the data in Blonquist *et al.* (2009), and I am grateful to Mark Blonquist for his comments and for deriving these parameter values.

According to this approach, g_a is non-zero when windspeed is zero or canopy height close to zero; it varies linearly with windspeed and is proportional to the canopy height raised to the power 0.5 (square root). The reason for not assuming that g_a is proportional to height is that it to reduce the sensitivity of g_a to h as h gets quite large.

Equation (5.55) for g_a, with eqns (5.56) and (5.57) is illustrated in Fig. 5.2 as a function of LAI, L, for canopies with maximum height 0.1 m and 1 m: the relationship between L and h is given in Section 5.5.1 above. It can be seen that g_a is relatively insensitive to L at the low h, but is subject to more variation in response to increases in L for taller canopies. This behaviour is realistic.

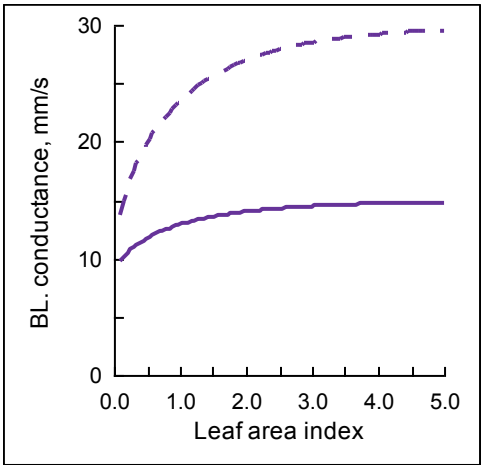

Figure 5.2: Boundary layer conductance, g_a, eqn (5.55), with (5.56) and (5.57), as a function of leaf area index, L. Canopy height, h, is given by .(5.42), $L_h = 1$ m and the curves are $h_{mx} = 0.1$ m (solid line) and 1 m (broken line). From PlantMod.

These various approaches for defining g_a have been explored extensively during the development of PlantMod and eqn (5.55) has been found to be robust and to give realistic results for a wide range of conditions. This is a subject that requires further exploration.

5.6 Illustrations

In PlantMod, instantaneous and daily transpiration, temperature and components of the energy budget can be explored in relation to both the canopy parameters and the climatic conditions. Some illustrations of the behaviour of the models discussed here are now presented. All of the graphs are copied directly from the PlantMod interface, and you are encouraged to explore some of the many other possible simulations.

In Fig. 5.3, the instantaneous transpiration is shown as a function of windspeed for two different temperatures. It can be seen that transpiration increases as both windspeed and temperature increase.

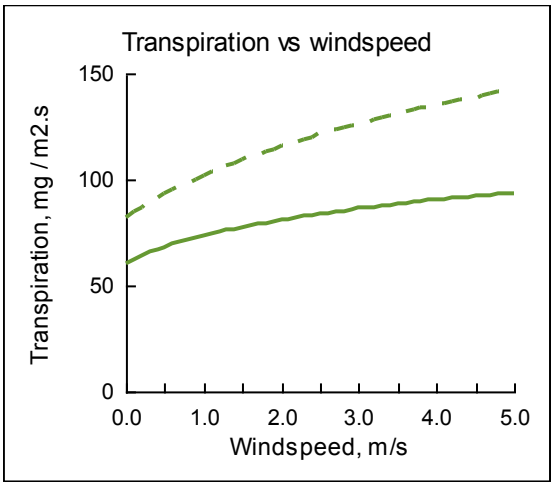

Figure 5.3: Instantaneous transpiration rate, E, as a function of windspeed. The environmental parameters are the PlantMod defaults, apart from $T_a = 15$°C (solid line) and 25°C (broken line). From PlantMod.

An interesting scenario to consider is the influence of atmospheric vapour pressure, P, on the daily transpiration rate. While variation in P is generally negligible at a specific location, it does vary quite substantially with latitude, falling by around 10 to 11% for every 1000m increase in elevation. For example, at Mexico City where the altitude is 2,240 m P will be approximately 77kPa compared with the standard sea level value of 101.3 kPa. Atmospheric pressure can be varied in PlantMod. In Fig. 5.4 the daily transpiration rate with default parameters is illustrated for sea level, $P = 101.3$ kpa, and an elevation of 2,000m with $P = 80$ kPa. It is clear that pressure has a noticeable effect on the daily transpiration rate. This is consistent with observations (Gale, 2004; Bruce Bugbee, *pers comm.*)

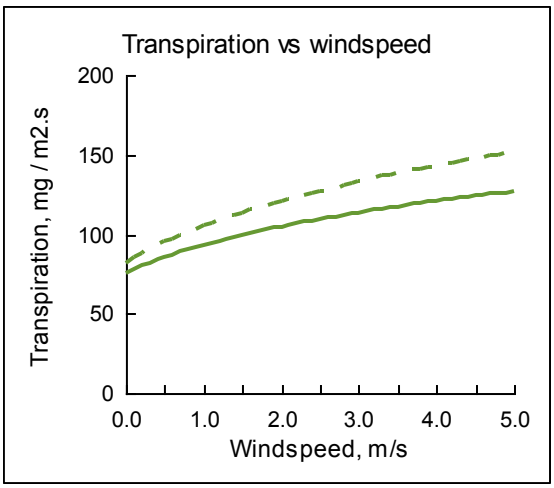

Figure 5.4: Influence of atmospheric pressure on transpiration. The solid line is for standard pressure, $P = 101.3$ kPa, and the broken line is $P = 80$ kPa which corresponds to around 2km altitude. From PlantMod.

In Fig. 5.5 the day and night canopy temperatures are illustrated as functions of windspeed – both the absolute temperature and the difference between the canopy and air temperature are

illustrated (these options are both available in PlantMod). Here it can be see that as windspeed increases the daytime canopy temperature declines and falls below the air temperature, which is due to the cooling effect of transpiration which increases with windspeed, as well as the greater conductive transfer of heat from the canopy. However, the nighttime canopy temperature increases slightly with windspeed, although it is lower than the air temperature. This is explained by looking at eqns (5.4) and (5.7) which show that when there is no transpiration (which occurs at night with the stomata closed), the net radiation is balanced entirely by sensible heat loss. As discussed earlier, the conductance for heat loss, g_H, is the same as the boundary layer conductance, g_a, (eqn (5.19)) and, since g_a is proportional to wind speed, eqn (5.50), it follows that any increase in windspeed will result in a reduction in the difference between canopy and air temperature, that is the term $(T_c - T_a)$ in eqn (5.7). Thus, the greater the windspeed, the greater the conductive heat transfer between the canopy and air, and the closer the canopy and air temperatures become.

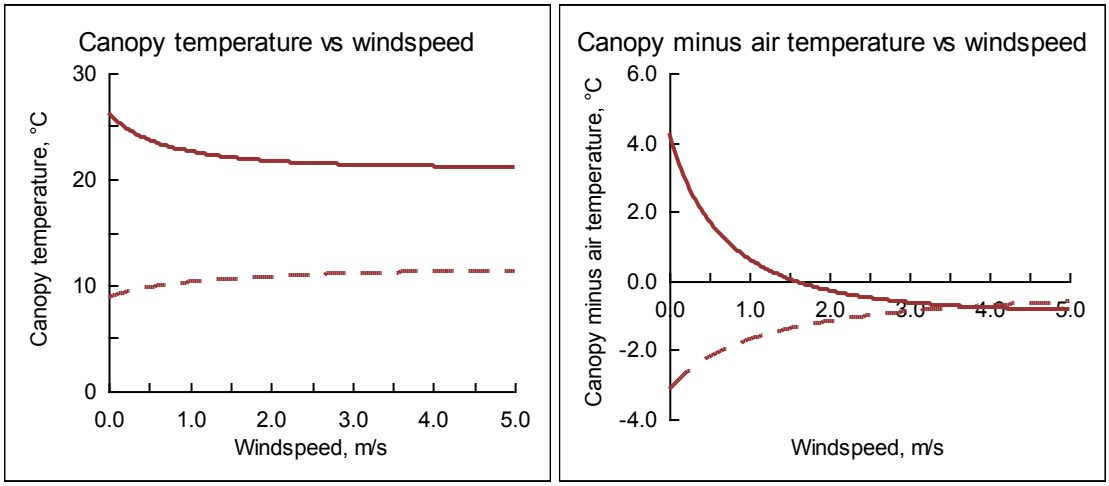

Figure 5.5: Daytime (solid) and nighttime (dashed) canopy temperature as a function of windspeed for the default PlantMod parameter values. The day and night air temperatures are 22°C and 12°C respectively. From PlantMod.

The day and night sensible heat and latent heat transfers, along with the canopy net radiation balance, are shown in Fig. 5.6, again as functions of windspeed. Note that the latent heat transfer at night is zero because there is no transpiration, and so the net radiation balance and the sensible heat flux are identical. It can be seen that, during the day the latent heat increases with windspeed corresponding to the increase in transpiration. However, the sensible heat declines due to the combination of the increase in latent heat and the greater convective heat transfer. Negative sensible heat corresponds to the canopy being cooler than the air.

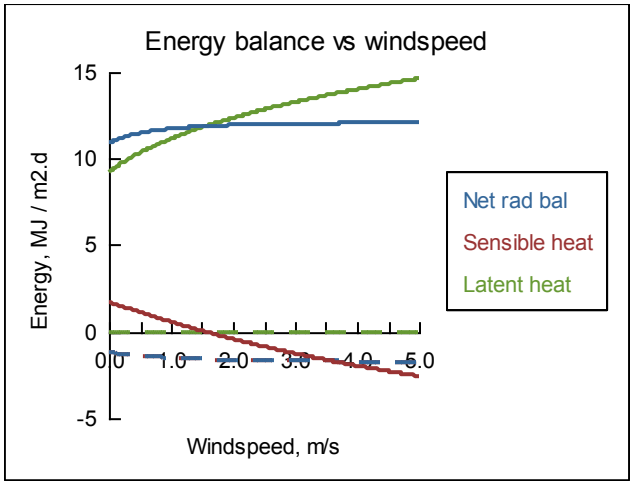

Figure 5.6: Daytime (solid) and nighttime (dashed) canopy energy balance components as a function of windspeed with PlantMod defaults. The day and night air temperatures are 22°C and 12°C respectively. The net radiation balance, sensible heat flux and latent heat transfer are indicated. Note that the latent heat flux is zero at night (since there is no transpiration) and so the net radiation balance is equal to the sensible heat flux. From PlantMod.

As a final illustration, the difference between specifying vapour pressure, e_v, or relative humidity, h_r, is considered. The temperature responses for $\Delta e_{v,a}$ (the vapour pressure deficit) and h_r were discussed in Section 1.5.2 in Chapter 1, and illustrated in Fig. 1.11. Figure 5.7 shows the transpiration rate as a function of temperature with either e_v or h_r being specified. It can be seen that the responses are different. If h_r is fixed then, as temperature increases so does e_v since h_r is the ratio $e_v/e_{v,sat}$. Thus, at low temperatures, $\Delta e_{v,a}$ is greater at fixed h_r while, at high temperatures, it is greater with fixed e_v. The values for e_v and h_r used in Fig. 5.7 are such that the atmospheric vapour content is the same at 20°C.

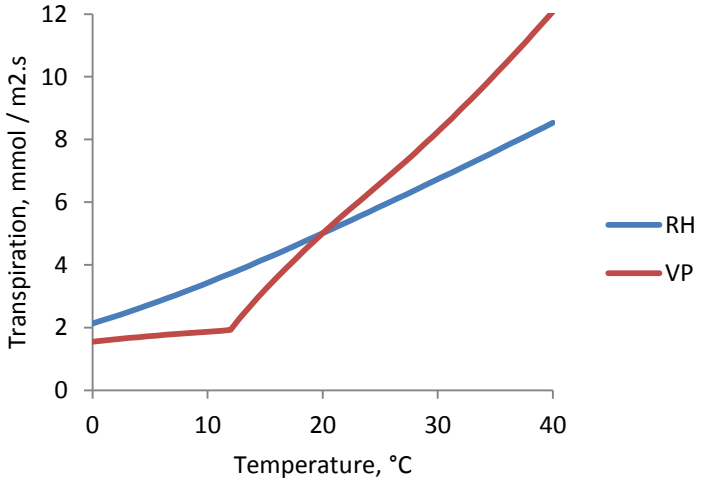

Figure 5.7: Transpiration rate as a function of temperature with either a fixed vapour pressure (red), with $e_v = 1.4$ kPa, or fixed relative humidity (blue), with $h_r = 60\%$. These values give the same atmospheric water vapour content at 20°C.

5.7 Final comments

The models presented here define the canopy transpiration, canopy temperature and energy balance components in terms of canopy physical parameters and environmental conditions. A key part of this analysis is in the description of the net radiation balance for the canopy which was discussed in Chapter 2 and is incorporated here. This includes the treatment for the longwave radiation which is related to canopy temperature and is defined in terms of the isothermal net longwave radiation, and is an improvement on defining a fixed net longwave radiation balance that is independent of temperature. The analysis for instantaneous transpiration, temperature and energy requires an estimate of cloud cover, which is used in the radiation calculations, while for the daily model calculations, the data and latitude are used, along with the ratio of actual to potential solar radiation. The analysis also relies on estimates of both the canopy conductance and boundary layer conductance. Canopy conductance is calculated in relation to leaf stomatal conductance and canopy leaf area index, with the leaf stomatal conductance being related to the atmospheric conditions as discussed in Section 5.5.2, and boundary layer conductance related to windspeed and canopy height. Both of these relationships are empirical, but they are at similar levels of complexity, are quite robust, and are ideally suited to practical analyses at the canopy level.

The underlying physics for defining the energy balance for crops, and therefore the transpiration and temperature in response to climatic conditions, is well established. However, there are a number of parameters relating to canopy physiology and structure that need to be prescribed and that can lead to a wide range of possible responses to environmental conditions. The simulations in PlantMod allow many aspects of these topics to be explored.

5.8 Variables and parameters

Table 5.1: Environmental variables and parameters. Radiation components are listed in Table 5.2 below

Variable or parameter	Definition	Units and default value (parameters)
C	Atmospheric CO_2 concentration	μmol mol^{-1}
C_{amb}	Ambient atmospheric CO_2 concentration	380 μmol mol^{-1}
e_v'	Saturated vapour pressure as a function of temperature	kPa
$e_{v,a}$	Vapour pressure in the air	1.4 kPa
$\Delta e_{v,a}$	Vapour pressure deficit in the air	kPa
h_r	Relative humidity	dimensionless
$h_{r,ref}$	Reference relative humidity for leaf stomatal conductance	0.5 (50%)
$J_{S,ref}$	Reference solar radiation for leaf stomatal conductance	400 J m^{-2} s^{-1}
P	Atmospheric pressure	101.3 kPa
T_a	Air temperature	22 °C
$T_{a,day}$	Daytime air temperature	22 °C
$T_{a,night}$	Nighttime air temperature	12 °C
u_z	Windspeed at height z	m s^{-1}
z	Reference height for windspeed	2 m

Table 5.2: Model variables, definitions and units. Model parameters are defined in Table 5.3. Unless stated otherwise, areas refer to ground area. Note that J (m^{-2} ground) s^{-1} ≡ W (m^{-2} ground).

Variable	Definition	Units
d	Zero plane displacement	m
$e_{v,\ell}$	Vapour pressure within the leaf	kPa
E	Canopy transpiration rate	mol water m^{-2} s^{-1}
E_{day}	Daily canopy transpiration rate	mol water m^{-2} d^{-1}
$E_{day,mm}$	Daily canopy transpiration rate in mm	mm water d^{-1}
H	Sensible heat flux between the canopy and air	J m^{-2} s^{-1}
H_{day}	Daily sensible heat flux between the canopy and air	J m^{-2} d^{-1}
f_{day}	Daylength as a fraction of 24 hours	dimensionless
f_g	Fractional ground cover by the canopy	dimensionless
g_ℓ	Leaf stomatal conductance for water vapour	mol m^{-2} s^{-1}
g_a	Boundary layer conductance	mol m^{-2} s^{-1}
g_c	Canopy conductance	mol m^{-2} s^{-1}
g_H	Conductance for heat	mol m^{-2} s^{-1}
g_r	Radiative conductance	mol m^{-2} s^{-1}
g_v	Conductance for water vapour	mol m^{-2} s^{-1}
H	Sensible heat flux between the canopy and air	J m^{-2} s^{-1}
H_{day}	Daily sensible heat flux between the canopy and air	J m^{-2} d^{-1}
L_{live}	Live leaf area index	(m^2 leaf)(m^{-2} ground)
T_c	Canopy temperature	°C
$T_{K,c}$	Canopy temperature	K
	Instantaneous radiation	
J_n	Canopy net radiation balance (shortwave and longwave)	J m^{-2} s^{-1}
J'_n	Canopy isothermal net radiation balance (shortwave and longwave)	J m^{-2} s^{-1}
$J'_{n,day}$	Canopy isothermal net radiation balance during the day	J m^{-2} s^{-1}
$J'_{L,n,day}$	Canopy outgoing isothermal net longwave radiation balance during the night	J m^{-2} s^{-1}
$J_{L,n}$	Net outgoing longwave canopy radiation balance	J m^{-2} s^{-1}
$J_{L,a}$, $J_{L,e}$	Canopy absorbed and emitted longwave radiation	J m^{-2} s^{-1}
J_S	Incoming solar radiation	J m^{-2} s^{-1}
$J_{S,a}$	Canopy absorbed solar radiation	J m^{-2} s^{-1}
	Daily radiation	
R_n	Daily canopy net radiation balance (shortwave and longwave	J m^{-2} d^{-1}
$R'_{n,day}$	Daily canopy isothermal net radiation balance (shortwave and longwave)	J m^{-2} d^{-1}
$R_{S,a}$	Daily solar radiation absorbed by the canopy	J m^{-2} d^{-1}

$R_{L,n}$	Daily net outgoing longwave canopy radiation balance	J m^{-2} d^{-1}
$R_{L,a}$, $R_{L,e}$	Daily absorbed and emitted longwave radiation	J m^{-2} d^{-1}

Table 5.3: Model parameters, definitions, units, and default values. Model variables are defined in Table 5.2. Unless stated otherwise, areas refer to ground area. Note that J (m^{-2} ground) s^{-1} ≡ W (m^{-2} ground).

Parameter	Definition	Default value
c_p	Specific heat capacity of air	29.3 J mol^{-1} K^{-1}
$f_{L,live}$	Live fraction of leaf area	0.8
$g_{a,0}$	Basal value for boundary layer conductance	0.3 mol m^{-2} s^{-1}
$g_{a,ref}$	Reference value for boundary layer conductance, at h_{ref} and u_{ref}	0.8 mol m^{-2} s^{-1}
$g_{\ell,ref}$	Leaf stomatal conductance at the reference values in eqn (5.49).	0.2 mol m^{-2} s^{-1}
h_{ref}	Reference height for boundary layer conductance	0.3 m
h_{mx}	Maximum canopy height	1 m
K_J	Solar radiation parameter for stomatal conductance	100 J m^{-2} s^{-1}
k	Canopy extinction coefficient	0.5 m^2 ground (m^{-2} leaf)
L	Leaf area index	5 (m^2 leaf)(m^{-2} ground)
L_h	Leaf area index for half maximal canopy height	1 (m^2 leaf)(m^{-2} ground)
$T_{c,day}$, $T_{c,night}$	Daytime and nighttime canopy temperature	°C
u_{ref}	Reference windspeed for boundary layer conductance	2 m s^{-1}
α	Canopy reflection coefficient, or albedo	0.23 (dimensionless)
ε	Canopy emissivity	0.97 (dimensionless)
κ	von Karman's constant	0.41
γ	Psychrometric parameter	664×10^{-6} mol water (mol air)$^{-1}$ K^{-1}
λ	Latent heat of vaporization	44.1 kJ mol^{-1}
σ	Stefan-Boltzmann constant	5.670×10^{-8} J m^{-2} s^{-1} K^{-4}

5.9 References

Allen RG, Pereira LS, Raes D and Smith M (1998). FAO irrigation and drainage paper no. 56: crop evapotranspiration. www.kimberly.uidaho.edu/ref-et/fao56.pdf.

Ball JT, Woodrow IE & Berry JA (1987). A model predicting stomatal conductance and its contribution to the control of photosynthesis under different environmental conditions. In: *Progress in Photosynthesis Research*, vol IV, ed J Biggens. Martinus Nijhoff / American Society of Agronomy, Dordrecht, the Netherlands / Madison, WI, USA, 221-224.

Campbell GS (1977). *An introduction to environmental biophysics*. Springer-Verlag, New York, USA.

Campbell GS and Norman JM (1998). *An Introduction to environmental biophysics*, second edition. Springer, New York, USA.

Gale J (2004). Plants and altitude – revisited. *Annals of Botany,* **94,** 199.

Jones HG (1992). *Plants and microclimate*. Cambridge University Press, Cambridge, UK.

Monteith JL (1965). Evaporation and environment. *Symposium of the Society for Experimental Biology,* **19,** 205-234.

Monin AS & Obukhov AM (1954). Basic laws of turbulent mixing in the ground layer of the atmosphere. Tr. Geofiz. Inst. Akad. Nauk, SSSR no. 24 (151). In: Goering, H.(Ed.), Sammelband zur Statistischen Theorie der Turulenz (German translation 1958). Akademie Verlag, Berlin, Germany, 163-187. As cited by Blonquist *et al.* (2009).

Monteith JL (1973). *Principles of environmental physic,* third edition. Edward Arnold, London, UK.

Monteith JL & Unsworth MH (2008). *Principles of environmental physic,* third edition. Academic Press, London, UK.

Penman HL (1948). Natural evaporation from open water, bare soil and grass. *Proceedings of the Royal Society of London, Series A*, **193,** 120-145.

Thornley JHM and France J (2007). *Mathematical models in agriculture*. CAB International, Wallingford, UK.

Thornley JHM & Johnson IR (2000). *Plant and crop modelling*. Blackburn Press, Caldwell, New Jersey, USA.